Lipid nanoparticles for topical delivery: solid lipid nanoparticles (SLN) & smartLipids

Inaugural-Dissertation

to obtain the academic degree

Doctor rerum naturalium (Dr. rer. nat.)

submitted to the Department of Biology, Chemistry and Pharmacy

of Freie Universität Berlin

by

Yuan Ding

from Nei Mongol, People's Republic of China

2018

The enclosed doctoral research work was performed from October 2014 to June 2018 under the supervision of Prof. Dr. Rainer H. Müller at the Institute of Pharmacy, Department of Pharmaceutics, Biopharmaceutics & NutriCosmetics, Freie Universität Berlin.

1st Reviewer: Prof. Dr. Rainer H. Müller
2nd Reviewer: Prof. Dr. Cornelia M. Keck

date of defense: 09 July 2018

to my family and friends
with all my love and gratitude

Table of contents

1. Introduction

1.1. Classical lipid nanoparticles — SLN® and NLC®

Following the development of liposomes and polymeric nanoparticles, solid lipid nanoparticles (SLN®) were invented at the beginning of the 1990's for the delivery of active ingredients (Lucks and Müller, 1991). A major advantage of the solid lipid matrix is its ability to protect the incorporated active ingredients against chemical degradation, resulting in significantly enhanced shelf life. However, crystalline lattice structures within the SLN® can lead to drug expulsion and lower drug loading capacities (Mehnert and Mäder, 2001; Müller et al., 2000). In order to tackle these drawbacks, the second generation of lipid nanoparticles – nanostructured lipid carriers (NLC®) – were developed in 2000. The lipid matrix of NLC® is composed of both a solid lipid and a certain amount of a liquid lipid (oil), creating imperfections in the crystal lattice, resulting in improved drug loading capacity as well as physical stability.

The development of SLN® and NLC® formulations with uniform particle size distributions and good physical long-term stability requires careful optimization of the composition across a wide spectrum of stabilizers/surfactants. The type of surfactants used also influences the possible applications of SLN® and NLC® products. For example, in dermal delivery systems, the toxicity of the surfactant is an important consideration. Conventional nonionic polyhydroxy and polyglyceride surfactants exhibiting a good safety profile - for example Plantacare®, Sisterna®, Surfhope® and Plurol Stearique® - are widely used for the stabilization of lipid nanoparticles (von Rybinski and Hill, 1998). Furthermore, the type of surfactant used also influences the particle size and physical stability. The molecular structure of the surfactant also influences the particle size: surfactants with high hydrophilic-lipophilic balance (HLB) values and a lower molecular weight tend to form smaller particles (Kovačević et al., 2014). A relevant investigation of different alkyl polyglycosides (APGs) supports a similar conclusion, showing surfactants with shorter alkyl chains and higher critical micelle concentrations (CMC) lead to a reduced particle size (Keck et al., 2014).

In recent years, the use of lipid nanoparticle systems has become increasingly popular.

However, for each specific drug candidate loaded using SLN$^®$ or NLC$^®$ formulations, a tedious lipid screening procedure is inevitable. Usually, the development of such a system includes screening the miscibility, solubility and partition coefficients of the drug in various lipids, which is a time-consuming and resource-intensive process. Moreover, the drug loading capacity of the SLN$^®$ or NLC$^®$ system could be significantly higher than the solubility of the drug, further complicating the formulation development. A recent study (Göke and Bunjes, 2017) introduced a novel screening approach named passive drug loading, in which different lipid nanoparticles are incubated with the raw drug powder. After removing the undissolved drug by filtration, the exact amount of solubilized drug is determined. Furthermore, this approach can be used to determine the drug localization by relating the specific lipid nanoparticles' surface area to the drug solubility. For SLN$^®$ and NLC$^®$, three different models describe the localization of the active compound in the system: the homogeneous matrix model, drug-enriched shell model and drug-enriched core model. Formulation composition as well as production conditions provide a toolbox to target a specific drug localization in the lipid nanoparticle, and each type of drug localization brings about distinct release properties (Dingler et al., 1997; Müller et al., 2002). The homogeneous matrix facilitates continuous release from 1 day up to weeks, whereas the drug-enriched shell model is suitable for dermal applications, enabling a very fast release as well as enhanced drug penetration. The drug-enriched core model leads to a passive membrane-controlled release. The identification of the drug localization not only reduces formulation development time, but also serves as a reference for development targeting a specific application.

1.2. Lipid-drug-conjugate (LDC)

A major drawback of SLN$^®$ and NLC$^®$ systems is the low loading capacity for hydrophilic drugs as a result of the partitioning effect. This is not a problem for highly potent actives such as follicle-stimulating hormone (FSH) and erythropoietin (EPO), but poses a serious limitation when higher dosages of hydrophilic drugs are required. In order to overcome this obstacle, lipid-drug-conjugate (LDC) systems were developed (Olbrich et al., 2002). This method is based on transforming the hydrophilic drug into a more lipophilic, often

water-insoluble molecule by either covalent linkage or by salt formation (Muchow et al., 2008). The obtained LDC can be incorporated into lipid nanoparticle formulations either with or without other lipids using high-pressure homogenization production techniques. Such LDC nanoparticles demonstrate several advantages including improved oral bioavailability, enhanced tumor targeting and increased drug loading capacity into delivery carrier systems (Irby et al., 2017).

Numerous drugs cannot be utilized for oral application directly, owing to low bioavailability. The first-pass effect as well as other metabolic restrictions limit the uptake of these drugs. Delivering drugs in LDC form avoids these barriers by following lipid metabolism pathways. The main function of the lymphatic system is transporting dietary lipids from the intestines to lymphatic capillaries. In this way, uptake of the drug is enhanced by the avoidance of the first-pass effect (Trevaskis et al., 2015). A further study demonstrated that conjugating cytarabine (1-β-D-arabinofuranosylcytosine, Ara-C) with lauric acid results in an almost 33-fold increase of cytarabine bioavailability by oral administration in rats (Liu et al., 2016). LDC have also been used in conjugation with lipid nanoparticle systems, where the increased lipophilicity of the conjugate improves compatibility with the other components and reduces drug leakage (Li et al., 2016; Shao et al., 2013). One study showed a novel 2′-behenoyl-paclitaxel conjugate nanoparticle formulation for the treatment of breast cancer (Ma et al., 2013). The lipophilic paclitaxel derivative increased drug loading in lipid-based nanoparticles from 10% to 47%. Aside from increased drug loading and stability, LDC nanoparticles can also aid in the delivery of hydrophilic drugs. For example, LDC nanoparticles containing a conjugate of the hydrophilic drug diminazene diaceturate with stearic and oleic acid was developed for potential delivery to the brain (Olbrich et al., 2004). With a drug loading capacity of 33% (w/w), the LDC-based SLN® showed strong potential owing to the combination of increased loading with enhanced delivery. In addition, gene medicines such as siRNA are novel promising therapeutic agents which started attracting worldwide interest in recent years, but their poor stability and negative charge limits clinical application of siRNA agents (Petrova et al., 2011; Urbinati et al., 2016). As LDC can both stabilize as well as increase loading capacity for hydrophilic actives, such systems have also been investigated for gene agent

delivery. A recent study showed that conjugating siRNA to lipophilic palmitic acid increased the loading capacity in nanoparticle formulations (Sarett et al., 2015). This conjugation exhibited 35-fold increased intracellular uptake of the siRNA, and at the same time led to a 3.1-fold increase in intracellular half-life in comparison to unconjugated siRNA. Complexation with cationic lipids - such as DOPAP - also proves to be a useful strategy towards forming lipid nanoparticles for siRNA transfection (Lobovkina et al., 2011).

Medical applications of LDC in lipid nanoparticles have already been demonstrated, showing high drug loading as well as enhanced targeted drug delivery *in vivo*. LDC can be a promising delivery system in cancer therapy, since many tumor cells are fenestrated, and thus can easily be penetrated by nanoparticles (Ferrari, 2005). In one study, the LDC stearoyl gemcitabine was loaded into lipid nanoparticles (GemC18-NPs) for solid tumor therapy (Chung et al., 2012). Combined with soy lecithin, glycerol monostearate and LDC, this lipid nanoparticle formulation was physically stable for 20 days. The results showed GemC18-NPs effectively controlled the growth of gemcitabine resistant tumors *in vivo*.

1.3. smartLipids®

Recently, smartLipids® particles were developed as the new generation of lipid nanoparticles after SLN® and NLC®. The first generation, SLN®, are typically produced from one solid lipid, and the lipid matrix exists as a highly ordered crystalline structure. Because of this, SLN® show limitations in drug loading capacity, and drug expulsion can occur during storage. NLC®, the second generation of lipid nanoparticles, were developed with a mixture of typically a single solid lipid and a single liquid lipid. The addition of liquid lipid introduces imperfections in the lipid matrix, increasing the solubility of the actives and reducing drug expulsion. Following these iterative advancements, smartLipids® were developed in 2014 as the 3rd generation of lipid nanoparticles, consisting of a more complex lipid mixture (Müller et al., 2014). The particle matrix consists in most cases of more than five different lipids, containing mono-, di- and triglycerides with various carbon chain lengths. In contrast to the classical lipid core structure, the complex "chaotic" lipid

mixture provides increased drug loading and better protection for chemically labile molecules.

Owing to the highly optimized matrix structure formed using various lipid molecules, polymorphic transitions during shelf life are minimized or even can be completely avoided (Ruick, 2016). This firm inclusion in the particle matrix is required to protect the loaded drug. As mentioned in 1.1, the development procedure for a new formulation based on classical lipid nanoparticle systems takes considerable effort and time, owing to the screening of numerous potential lipids. Consisting of multiple solid and liquid lipids, smartLipids® possess great potential to incorporate a variety of drugs, and thus the requirement of lipid screening procedures in conventional lipid nanoparticle formulation development can be minimized by pursuing this more universal approach. The complex lipid nanoparticle matrix has a low ordered crystallinity of solid lipids, increasing the amount of imperfections leading to higher drug loading capacity compared to classical SLN® and NLC® delivery system.

As the 3rd generation of lipid nanoparticle systems, they inherit the advantages of SLN® and NLC® systems. These include a nano-range and narrow particle size distribution, prolonged release profile, minimizing side effects of the incorporated drug and the feasibility of scale-up to industrial production scales. In addition, lipid nanoparticles possess adhesive properties when applied to topical and mucosal surfaces (Liu et al., 2011; Pyo et al., 2016). By adhesion to the skin, an occlusive film also protects the skin against exogenous hazards. Combining these advantages, smartLipids® show great potential for dermal application. In a previous work, smartLipids® with a physical stability of at least three months at room temperature were demonstrated (Junmahasathien, 2015). This formulation was further investigated by incorporating it into different dermal bases, such as a Poloxamer 407 hydrogel, cream and lotion (Li, 2016). Nowadays, smartLipids® products are already commercially available (e.g. BergaCare smartLipids® (Olechowski et al., 2016)), underlining strong perspectives for further practical applications.

1.4. Lipid nanoparticles for dermal and mucosal application

Lipid nanoparticles were first introduced into dermal delivery around 2000. In the past 10 years, SLN® and NLC® have drawn much attention for dermal application and shown great advantages such as the good skin compatibility and skin penetration of drugs (Keck et al., 2007; Müller et al., 2011). Since adhesiveness increases with a decreasing particle size, the nano-sized particles are able to adhere strongly to surfaces. In addition, hydrophobic interactions further enhance the adhesiveness of lipid nanoparticles to the skin. The nanoparticles form a dense "invisible patch" onto the bare patches of the skin. This protective lipid film increases the skin hydration, reduces water loss, enhances penetration of actives and restores the living conditions for the skin cells (Keck and Müller, 2010). Furthermore, the lipids making up the nanoparticles bear a resemblance to those making up the skin cell membranes, and show no toxicity (Pardeike et al., 2009).

A review by Müller (Müller et al., 2011) already summarized numerous SLN®-based dermal investigations, but recently several new concepts emerged in this area. Chantaburanan et al. developed SLN® with solid complex triglycerides (Softisan 378) and solid wax (cetyl palmitate) in different ratios for ibuprofen delivery. All the SLN® formulations prepared from different ratios demonstrated an initial burst release followed by sustained release properties. The addition of Softisan 378 into a cetyl palmitate matrix led to slow ibuprofen release owing to the drug-lipid interaction when increasing the amount of Softisan 378, showing sustained release properties can be adjusted depending on the lipid ratio (Chantaburanan et al., 2017). Another group prepared a SLN®-based gel for the dermal delivery of meloxicam. The formulation was produced with cetyl palmitate, Tween® 80 and propylene glycol, and subsequently incorporated into a hydrogel using carbopol 940. The resulting formulation showed controlled release properties as well as the potential of transporting the drug to deeper skin layers, as evidenced by increased penetration of meloxicam into the skin of mice. Furthermore, this delivery system exhibited anti-inflammatory activity as well as good skin tolerability, proving to be an excellent method for the delivery of meloxicam (Khurana et al., 2013). Pyo introduced a new concept by combining nanocrystals into SLN® for the treatment of couperosis. In this

study, vitamin K_1 and A_1 were incorporated into SLN®, and rutin was formulated as a nanocrystal. SLN® prolonged drug release and enhanced penetration in porcine ear skin, and the presence of rutin nanocrystals performed antioxidant activity. The *in vivo* study showed three to six times faster recovery by twice daily application of the new formulation compared to the raw drug as a micro-sized powder (Pyo et al., 2016). Lipid nanoparticles were also used for griseofulvin application. The formulation showed more than 5 folds penetration as well as a controlled drug release (Aggarwal and Goindi, 2013).

Mucosa shares morphological similarities with skin, and thus transmucosal drug delivery is considered as a convenient, mild and safe method. In general, mucosal delivery routes include oral, buccal, ocular, intranasal and vaginal. Owing to their nanoscale size, lipid nanoparticles possess advantageous properties for mucosal application. Shah et al. investigated rivastigmine-loaded SLN® composed of Compritol 888 ATO, Tween® 80 and Poloxamer 188, using a Quality by Design (QbD) approach for intranasal delivery. By identifying the effect of independent variables (drug-to-lipid ratio, surfactant concentration and homogenization time), rivastigmine-loaded SLN® showed high *in-vitro* and *ex-vivo* diffusion. A histopathology study ensured the safety of rivastigmine-loaded SLN® for intranasal administration (Shah et al., 2015).

However, the application of lipid nanoparticle into mucosa is limited by the protective mucus layer, which covers the epithelium and removes foreign particles (Wu et al., 2015). In order to overcome this, several strategies are pursued. One of the major methods is producing positively charged nanoparticles. Because the mucosa carries a negative charge, positively charged lipid nanoparticles can adhere strongly to mucosa. Thus, cetylpyridinium chloride (CPC) was used as positively charged ionic surfactant to form NLC®, and the resulting particles adhered excellently to the mucosa (Hommoss et al., 2017; Müller et al., 2009). A further effective way to overcome this barrier is the so-called modification strategy, such as the production of targeting delivery vehicles. CSKSSDYQC (CSK) was found to be an effective peptide, exhibiting a strong goblet cell targeting property (Jin et al., 2012; Kang et al., 2008). Based on this, Fan et al. designed SLN® formulations modified with CSK or IRQ (IRQRRRR, a cell penetrating peptide) peptides

in order to improve cellular uptake of the drug. The result showed that the two modified SLN® formulations enhanced drug permeation in excised rat duodenum mucosa, and increased the drug bioavailability compared to conventional SLN® (Fan et al., 2014). In a further study, SLN® were successfully incorporated into mucoadhesive sponges for buccal delivery of curcumin (Hazzah et al., 2015).Curcumin was formulated as a SLN® system, and the prepared SLN® suspension was thickened using mucoadhesive polymers. The investigation showed a polycarbophil sponge provided a sustained release for 15 hours in the buccal cavity, exhibiting a steady release of curcumin, indicating a promising method for mucosal delivery.

1.5. References

Aggarwal, N., Goindi, S., 2013. Preparation and in vivo evaluation of solid lipid nanoparticles of griseofulvin for dermal use. Journal of biomedical nanotechnology 9, 564-576.

Chantaburanan, T., Teeranachaideekul, V., Chantasart, D., Jintapattanakit, A., Junyaprasert, V.B., 2017. Effect of binary solid lipid matrix of wax and triglyceride on lipid crystallinity, drug-lipid interaction and drug release of ibuprofen-loaded solid lipid nanoparticles (SLN) for dermal delivery. J Colloid Interf Sci 504, 247-256.

Chung, W.-G., Sandoval, M.A., Sloat, B.R., Lansakara-p, D.S., Cui, Z., 2012. Stearoyl gemcitabine nanoparticles overcome resistance related to the over-expression of ribonucleotide reductase subunit M1. Journal of controlled release 157, 132-140.

Dingler, A., Weyhers, H., zur Mühlen, A., Mehnert, W., 1997. Solid Lipid Nanoparticles (SLN) ein neuartiger Wirkstoff-Carrier für Kosmetika und Pharmazeutika. III. Langzeitstabilität, Gefrier und Sprühtrocknung, Anwendung in Kosmetika und Pharmazeutika. Pharm. Ind.

Fan, T., Chen, C., Guo, H., Xu, J., Zhang, J., Zhu, X., Yang, Y., Zhou, Z., Li, L., Huang, Y., 2014. Design and evaluation of solid lipid nanoparticles modified with peptide ligand for oral delivery of protein drugs. European Journal of Pharmaceutics and Biopharmaceutics 88, 518-528.

Ferrari, M., 2005. Cancer nanotechnology: opportunities and challenges. Nature Reviews

Cancer 5, 161.

Göke, K., Bunjes, H., 2017. Drug solubility in lipid nanocarriers: Influence of lipid matrix and available interfacial area. Int J Pharmaceut 529, 617-628.

Hazzah, H.A., Farid, R.M., Nasra, M.M., EL-Massik, M.A., Abdallah, O.Y., 2015. Lyophilized sponges loaded with curcumin solid lipid nanoparticles for buccal delivery: Development and characterization. Int J Pharmaceut 492, 248-257.

Hommoss, G., Pyo, S.M., Müller, R.H., 2017. Mucoadhesive tetrahydrocannabinol-loaded NLC–Formulation optimization and long-term physicochemical stability. European Journal of Pharmaceutics and Biopharmaceutics 117, 408-417.

Irby, D., Du, C., Li, F., 2017. Lipid–Drug Conjugate for Enhancing Drug Delivery. Molecular pharmaceutics 14, 1325-1338.

Jin, Y., Song, Y., Zhu, X., Zhou, D., Chen, C., Zhang, Z., Huang, Y., 2012. Goblet cell-targeting nanoparticles for oral insulin delivery and the influence of mucus on insulin transport. Biomaterials 33, 1573-1582.

Junmahasathien, T., 2015. Myristyl Nicotinate Loaded Lipid Nanoparticles. Ph.D. thesis, Department of Pharmaceutics, Free University of Berlin.

Kang, S.K., Woo, J.H., Kim, M.K., Woo, S.S., Choi, J.H., Lee, H.G., Lee, N.K., Choi, Y.J., 2008. Identification of a peptide sequence that improves transport of macromolecules across the intestinal mucosal barrier targeting goblet cells. Journal of biotechnology 135, 210-216.

Keck, C., Hommoss, A., Muller, R., 2007. Lipid nanoparticles for encapsulation of actives: dermal & oral formulations. AMERICAN PHARMACEUTICAL REVIEW 10, 78.

Keck, C., Müller, R., 2010. Silber-Lipid-Zwerge–Ein neues Therapiekonzept gegen Neurodermitis. Quantos 1, 6-11.

Keck, C.M., Kovačević, A., Müller, R.H., Savić, S., Vuleta, G., Milić, J., 2014. Formulation of solid lipid nanoparticles (SLN): The value of different alkyl polyglucoside surfactants. Int J Pharmaceut 474, 33-41.

Khurana, S., Bedi, P., Jain, N., 2013. Preparation and evaluation of solid lipid nanoparticles based nanogel for dermal delivery of meloxicam. Chemistry and physics of lipids 175, 65-72.

Kovačević, A.B., Müller, R.H., Savić, S.D., Vuleta, G.M., Keck, C.M., 2014. Solid lipid

nanoparticles (SLN) stabilized with polyhydroxy surfactants: preparation, characterization and physical stability investigation. Colloids and Surfaces A: Physicochemical and Engineering Aspects 444, 15-25.

Li, F., Snow-Davis, C., Du, C., Bondarev, M.L., Saulsbury, M.D., Heyliger, S.O., 2016. Preparation and Characterization of Lipophilic Doxorubicin Pro-drug Micelles. JoVE (Journal of Visualized Experiments), e54338-e54338.

Li, X., 2016. Nanocarriers for Topical Delivery: Nanocrystals, Nanoemulsions Et SmartLipids. Ph.D. thesis, Department of Pharmaceutics, Free University of Berlin.

Liu, J., Zhao, D., Ma, N., Luan, Y., 2016. Highly enhanced leukemia therapy and oral bioavailability from a novel amphiphilic prodrug of cytarabine. RSC Advances 6, 35991-35999.

Liu, Y., Wang, P., Sun, C., Zhao, J., Du, Y., Shi, F., Feng, N., 2011. Bioadhesion and enhanced bioavailability by wheat germ agglutinin-grafted lipid nanoparticles for oral delivery of poorly water-soluble drug bufalin. Int J Pharmaceut 419, 260-265.

Lobovkina, T., Jacobson, G.B., Gonzalez-Gonzalez, E., Hickerson, R.P., Leake, D., Kaspar, R.L., Contag, C.H., Zare, R.N., 2011. In vivo sustained release of siRNA from solid lipid nanoparticles. ACS nano 5, 9977-9983.

Lucks, J.S., Müller, R.H., 1991. Medication vehicles made of solid lipid particles (solid lipid nanospheres SLN), EP0000605497.

Ma, P., Benhabbour, S.R., Feng, L., Mumper, R.J., 2013. 2′-Behenoyl-paclitaxel conjugate containing lipid nanoparticles for the treatment of metastatic breast cancer. Cancer letters 334, 253-262.

Mehnert, W., Mäder, K., 2001. Solid lipid nanoparticles: production, characterization and applications. Advanced drug delivery reviews 47, 165-196.

Muchow, M., Maincent, P., Müller, R.H., 2008. Lipid nanoparticles with a solid matrix (SLN®, NLC®, LDC®) for oral drug delivery. Drug Dev Ind Pharm 34, 1394-1405.

Müller, R., Shegokar, R., Singh, K., 2009. Positively charged nanostructured lipid carriers (NLC) for drug delivery by adhesion, Presentado en Ninth International Symposium on'Advances in Technology and Business Potential of New Drug Delivery Systems, pp. 25-26.

Müller, R.H., Mäder, K., Gohla, S., 2000. Solid lipid nanoparticles (SLN) for controlled

drug delivery–a review of the state of the art. European journal of pharmaceutics and biopharmaceutics 50, 161-177.

Müller, R.H., Radtke, M., Wissing, S.A., 2002. Solid lipid nanoparticles (SLN) and nanostructured lipid carriers (NLC) in cosmetic and dermatological preparations. Advanced drug delivery reviews 54, S131-S155.

Müller, R.H., Ruick, R., Keck, C.M., 2014. smartLipids® - the new generation of lipid nanoparticles after SLN and NLC, AAPS Annual Meeting, San Diego.

Müller, R.H., Shegokar, R., Keck, C., 2011. 20 years of lipid nanoparticles (SLN & NLC): present state of development & industrial applications. Current drug discovery technologies 8, 207-227.

Olbrich, C., Gessner, A., Kayser, O., Müller, R.H., 2002. Lipid-drug-conjugate (LDC) nanoparticles as novel carrier system for the hydrophilic antitrypanosomal drug diminazenediaceturate. J Drug Target 10, 387-396.

Olbrich, C., Gessner, A., Schröder, W., Kayser, O., Müller, R.H., 2004. Lipid–drug conjugate nanoparticles of the hydrophilic drug diminazene—cytotoxicity testing and mouse serum adsorption. Journal of Controlled Release 96, 425-435.

Olechowski, F., Pyo, S.M., Keck, C.M., Müller, R.H., 2016. BergaCare smartLipids®-commercial lipid submicron particle concentrates for cosmetics, consumer care & pharma.

Pardeike, J., Hommoss, A., Müller, R.H., 2009. Lipid nanoparticles (SLN, NLC) in cosmetic and pharmaceutical dermal products. Int J Pharmaceut 366, 170-184.

Petrova, N.S., Chernikov, I.V., Meschaninova, M.I., Dovydenko, I.S., Venyaminova, A.G., Zenkova, M.A., Vlassov, V.V., Chernolovskaya, E.L., 2011. Carrier-free cellular uptake and the gene-silencing activity of the lipophilic siRNAs is strongly affected by the length of the linker between siRNA and lipophilic group. Nucleic acids research 40, 2330-2344.

Pyo, S.M., Meinke, M., Klein, A.F., Fischer, T.C., Müller, R.H., 2016. A novel concept for the treatment of couperosis based on nanocrystals in combination with solid lipid nanoparticles (SLN). Int J Pharmaceut 510, 9-16.

Ruick, R., 2016. smartLipids -die neue Generation der Lipidnanopartikel nach SLN und NLC. Ph.D. thesis, Department of Pharmaceutics, Free University of Berlin.

Sarett, S.M., Kilchrist, K.V., Miteva, M., Duvall, C.L., 2015. Conjugation of palmitic acid improves potency and longevity of siRNA delivered via endosomolytic polymer

nanoparticles. Journal of Biomedical Materials Research Part A 103, 3107-3116.

Shah, B., Khunt, D., Bhatt, H., Misra, M., Padh, H., 2015. Application of quality by design approach for intranasal delivery of rivastigmine loaded solid lipid nanoparticles: effect on formulation and characterization parameters. European Journal of Pharmaceutical Sciences 78, 54-66.

Shao, W., Paul, A., Zhao, B., Lee, C., Rodes, L., Prakash, S., 2013. Carbon nanotube lipid drug approach for targeted delivery of a chemotherapy drug in a human breast cancer xenograft animal model. Biomaterials 34, 10109-10119.

Trevaskis, N.L., Kaminskas, L.M., Porter, C.J., 2015. From sewer to saviour [mdash] targeting the lymphatic system to promote drug exposure and activity. Nature Reviews Drug Discovery 14, 781-803.

Urbinati, G., de Waziers, I., Slamiç, M., Foussignière, T., Ali, H.M., Desmaële, D., Couvreur, P., Massaad-Massade, L., 2016. Knocking Down TMPRSS2-ERG Fusion Oncogene by siRNA Could be an Alternative Treatment to Flutamide. Molecular Therapy-Nucleic Acids 5, e301.

von Rybinski, W., Hill, K., 1998. Alkyl polyglycosides—properties and applications of a new class of surfactants. Angewandte Chemie International Edition 37, 1328-1345.

Wu, L., Liu, M., Zhu, X., Shan, W., Huang, Y., 2015. Modification strategies of lipid-based nanocarriers for mucosal drug delivery. Current pharmaceutical design 21, 5198-5211.

2. Aims of the thesis

The overarching aim of this thesis was developing lipid nanoparticle delivery systems – solid lipid nanoparticles (SLN®) and smartLipids® – for various pharmaceutical actives. These systems should be able to offer significant advantages, such as increased drug loading capability and stability. This goal was subdivided into the following subtopics:

Chapter 3: Nicotine-loaded SLN® were to be developed for suppressing common side effects of conventional nicotine replacement therapy. The main aim was to maximize the encapsulation efficiency of the hydrophilic nicotine, and the strategy pursued involved incorporating lipid drug conjugates (LDC) of nicotine and fatty acids (stearic acid and Kolliwax® S) into SLN®. The formed delivery system should be compared to non-LDC SLN® formulations in order to identify key advantages.

Chapter 4: The dermal application of retinol for anti-skin-aging treatment receives considerable interest, but retinol is susceptible to chemical oxidation. Thus, optimized smartLipids® formulations should be developed offering higher retinol stability. In addition to both chemical and physical stabilities, the possibility of increasing the retinol loading in the novel formulations should be investigated. Working towards practical application, the lipid nanoparticles should be incorporated into a dermal gel base and the stability should also be determined.

Chapter 5: Although smartLipids® are highly promising based on their unique structure of the lipid matrix, their complex composition can make the development of stable formulations cumbersome. Therefore, the influence of relevant parameters - including lipid composition, surfactant, addition of oil and production parameters - on formulation stability should be investigated.

Chapter 6: The powerful antioxidant α-tocopherol can protect the skin against UV-induced oxidative damage, but higher active loading is desirable. For cosmetic products, a concentrate with higher α-tocopherol content is needed. Therefore, the α-tocopherol SLN® formulations with increased loading should be developed, and the stability of the produced formulations should be investigated.

3. Lipid-drug-conjugate (LDC) solid lipid nanoparticles (SLN®) for the delivery of nicotine to the oral cavity – optimization of nicotine loading efficiency

(Ding, Y., Nielsen, K. A., Nielsen, B. P., Bøje, N. W., Müller, R. H., Pyo, S. M., Lipid-drug-conjugate (LDC) solid lipid nanoparticles (SLN) for the delivery of nicotine to the oral cavity–optimization of nicotine loading efficiency. European Journal of Pharmaceutics and Biopharmaceutics, 2018, 128: 10-17.)

4. smartLipids® as third solid lipid nanoparticle generation – stabilization of retinol for dermal application

https://doi.org/10.1691/ph.2017.7016 (page 41-69)

(Ding, Y., Pyo, S. M., Müller, R. H., smartLipids® as third solid lipid nanoparticle generation–stabilization of retinol for dermal application. Die Pharmazie-An International Journal of Pharmaceutical Sciences, 2017, 72(12): 728-735.)

5. The influencing factors of producing stable smartLipids®: lipids, surfactants and production parameters

5.1. Abstract

smartLipids®, which consist of a complex combination of lipids, are used to improve the chemical stability and entrapment efficiency of poorly soluble active pharmaceutical ingredients (APIs). Although the possibility of increased loading for a wide variety of drugs makes a more universal delivery approach possible, mixing multiple lipids makes it challenging to develop smartLipids® formulations with long-time storage stability. Thus, the focus of this study is the development of stable smartLipids®, as well as in-depth investigation of the factors directly influencing physical stability properties. The physical stability was determined by monitoring particle size as well as size distribution by photon correlation spectroscopy (PCS) and laser diffractometry (LD) up to 180 days of storage. The smartLipids® formulations produced with four lipid combinations with different melting ranges, four stabilizing surfactants at two different concentrations, and various homogenization parameters were investigated. The results show that stable smartLipids® formulations can be achieved with low melting range lipid compositions, stabilized with surfactants having relative high hydrophilic-lipophilic balance (HLB) values, and performing one or two homogenization cycles. Furthermore, adding liquid lipid into the lipid matrix improves the physical stability of smartLipids®. In this work, a framework critical for the production of stable smartLipids® is outlined, which can be used for further dermal drug delivery system in cosmetics and pharma.

5.2. Introduction

Lipid nanoparticles – first generation: solid lipid nanoparticles (SLN®) (Lucks and Müller, 1991) and second generation: nanostructured lipid carriers (NLC®) (Müller et al., 2002a) – are amongst the most promising formulation approaches for the delivery of lipid-soluble drugs. As an improvement on nanoemulsion, SLN® are composed of a solid rather than liquid lipid. Due to the solid matrix, this system is superior to nanoemulsions in terms of both chemical protection of actives, as well as occlusion behavior in order to increase biocompatibility and bioavailability (Müller et al., 2000). As the second generation of lipid

nanoparticles, NLC® were developed in 2002 using typically a blend of one solid lipid and one liquid lipid. The addition of the liquid lipid (oil) distorts the ordered crystalline structure of SLN® and increases imperfections in the lipid matrix. In many cases, active pharmaceutical ingredients (APIs) present better solubility behavior in oil compared to solid lipid mixtures. Thus, the entrapment efficiency of NLC® was improved. A pharmaceutical or cosmetic delivery system should be able to have a sufficiently high drug loading, and keep the API chemically stable during the shelf life. For developing a new formulation based on classical lipid nanoparticle systems, the first step is lipid screening, meaning the measurement of solubility for the API in different lipids (Chen et al., 2012). However, the procedure of solubility screening in various lipids is a time and resource intensive process, since there are numerous potential lipids that need to be investigated. Additionally, not each lipid-drug combination showing promising loading capacity also provides long term stability, meaning numerous dead ends will inevitably be pursued. Recently, Bunjes' research group developed a novel screening method named "passive drug loading". After incubating different lipid nanocarrier dispersions with pure drug powder, the exact amount of loaded drug was measured. Using this method, the best formulation with the highest drug loading was determined (Göke and Bunjes, 2017). This method not only established an effective and rational way for drug solubility identification, but could also serve as a direct approach for formulation development. However, this method does not overcome the limitations of conventional SLN® and NLC® systems in terms of drug loading capacity.

smartLipids®, the 3rd generation of lipid nanoparticle delivery system for lipophilic components were developed in 2014 (Müller et al., 2014). The particle matrix consists of typically more than five different lipids, including mono-, di- and triglycerides, fatty acids and fatty alcohols with various carbon chain lengths. In contrast to the classical lipid core structure, the complex "chaotic" lipid mixture gives them special properties such as the increased drug loading as well as the improved physical stability. More importantly, because of the mixing of multiple solid lipids and liquid lipid, smartLipids® are able to incorporate a variety of drugs, significantly reducing the workload of lipid screening by offering a more universal applicability. The complex lipid nanoparticle matrix has a low

ordered crystallinity with an increased amount of imperfections, leading to improved drug loading capability. As demonstrated in Chapter 4, the loaded retinol in smartLipids® could be increased up to 20% (w/w), whereas SLN® and NLC® systems were limited to only 5%. Aside from increasing the drug loading capacity, the physical as well as chemical stability improved, showcasing two major advantages of this delivery method. This was evidenced by the fact that 87% of the enclosed retinol was detected in smartLipids® after 60 days (drug loading was 20%, w/w), whereas in a comparabled literature report using SLN® only 62% was preserved after 1 week (drug loading was 5%, w/w) (Jenning and Gohla, 2001).

For the development of smartLipids® formulations, a complex lipid matrix allowing high drug loading and high physical stability is required. Due to the complexity of the multi-lipid mixture, obtaining stable smartLipids® is more challenging compared to SLN® and NLC®. Such efforts are worth pursuing as evidenced by an optimized SLN® suspension showing at least 3 years of physical stability (Zur Mühlen et al., 1996). However, some formulations tend to aggregate or even form a gel after production or during the storage period (Freitas and Müller, 1999). Several studies show the aggregation and gelation phenomena depend strongly on for example the lipid matrix, composition and concentration of the surfactants, temperature, light and mechanical stress. For example, during crystallization, the increase of polymorphic transitions at the particle surface leads to the incomplete coverage from the surfactant, thus inducing instability in the nanoparticle system (Helgason et al., 2008; Siekmann and Westesen, 1994). However, the mechanism of aggregation and gelation procedure is still unclear and the unpredictability increases the difficulty of developing a stable lipid nanoparticle formulation.

The primary aim of this study was not only the preparation of smartLipids® formulations with long-term physical stability, but also offering insights into key parameters surrounding the development of stable lipid nanoparticle systems. Therefore, the effects of various lipid combinations, surfactants and production parameters on the physical stability of smartLipids® were fully investigated. Lipids with different melting ranges and carbon chain lengths were used to form the lipid matrixes. Additionally, liquid lipid (Miglyol® 812) was added and the influence on the stability was also monitored. Four different surfactants at

two different concentrations (1.5% and 3.0% w/w) were used for smartLipids® production.

5.3. Materials and methods

5.3.1. Materials

The solid lipids Imwitor® 372 P (V), Imwitor® 900 (F) P, Dynasan® 118, Softisan® 142 and Softisan® 154 were gifts from IOI Oleo GmbH (Hamburg, Germany). Compritol® 888 ATO and Precirol® ATO 5 were provided from Gattefossé (Bad Krozingen, Germany). Dynasan® 114, Dynasan® 116, Dynasan® P 60 (F) and Imwitor® 491 were donated from CREMER OLEO GmbH & Co. KG (Hamburg, Germany). Hydrogenated castor oil (Sternoil HCO*), 12-hydroxystearic acid (Sternoil 12-HSA*), behenyl alcohol (Vegarol 2270*), palmitic acid (Palmac 98-16*), palm triple pressed acid (Palmac 55-16*), stearyl alcohol (Vegarol 1898*), cetyl stearyl alcohol (Vegarol 1618 50:50*), cetyl alcohol (Vegarol 1698*), lauric acid (Palmac 99-12*), myristic acid (Palmac 99-14*) were gifts from Berg + Schmidt GmbH & Co. KG (Hamburg, Germany). Miglyol® 812 was bought from Caesar & Loretz GmbH (Hilden, Germany). Decyl glucoside and lauryl glucoside (both from Berg + Schmidt GmbH & Co. KG, Hamburg, Germany), Plantacare® 2000 UP (alkyl polyglycoside, BASF, Ludwigshafen, Germany) and Tween® 80 (Polyoxyethylene sorbitan monooleate, AMRESCO, Solon, USA) were used as surfactants. Ultra-purified water from Milli-Q apparatus (Millipore GmbH, Darmstadt, Germany) was used. All other reagents used in this study are analytical grade quality.
* indicates the name from Berg + Schmidt GmbH & Co. KG.

5.3.2. Production of smartLipids®

All lipids used in smartLipids® formulations are listed in Table 5.1. The compositions of the lipid and water phase contained in the smartLipids® formulations are shown in Table 5.2 and 5.3. The nomenclature used for the of smartLipids® suspensions is illustrated in Fig. 5.1. In brief, smartLipids® nanosuspensions were produced using the

hot high pressure homogenization procedure according to literature (Müller et al., 2000). The lipid phase was mixed and melted at 85 °C, and subsequently dispersed in the water phase at the same temperature. This was performed using an Ultra-Turrax (Janke & Kunkel GmbH, Germany) for one minute at 8,000 rpm. Following this, the obtained pre-emulsion was homogenized using a Micron LAB 40 (APV Deutschland GmbH, Germany) for 3 cycles at 500 bar at 85 °C. 8 mL of the suspension is collected after each cycle for further analysis. Following homogenization, the produced hot nanosuspensions were cooled down to room temperature.

For the production parameter investigation, the pre-emulsion of lipid composition 4 was homogenized for 5 cycles at 300, 400, 500, 600, 700, 800, 900 and 1000 bar, respectively. A 3 mL sample was collected after each cycle for further analysis. The produced hot nanosuspensions were cooled down to room temperature.

Table 5.1. An overview of all solid lipids used for the production of smartLipids® suspensions, classified by their chemical structures (glyceride, fatty acid or fatty alcohol) and sorted by ascending melting ranges.

glyceride				
lipid trade name	melting range [°C]	type	percentage [%]	chain length
Softisan® 142	42.0-44.0	diglyceride	10	C12, C14, C16, C18
		triglyceride	89	
Precirol® ATO 5	50.0-60.0	monoglyceride	8-17	C16, C18
		diglyceride	54	
		triglyceride	30	
Softisan® 154	53.0-58.0	triglyceride	100	C16, C18
Imwitor® 900 (F) P	54.0-66.0	monoglyceride	40-55	C16, C18
		diglyceride	30-45	
		triglyceride	5-15	
Dynasan® 114	55.0-58.0	triglyceride	100	C14
Imwitor® 372 P (V)	56.0-60.0	monoglyceride	10-30	C16, C18
		diglyceride	70-90	
		triglyceride		
Dynasan® P60	58.0-62.0	triglyceride	100	C16, C18
Dynasan® 116	61.0-65.0	triglyceride	100	C16
Compritol® 888 ATO	65.0-77.0	monoglyceride	12-18	C22
		diglyceride	52-54	
		triglyceride	28-32	
Imwitor® 491	66.0-77.0	monoglyceride	100	C16, C18
Dynasan® 118	69.0-73.0	triglyceride	100	C18
hydrogenated castor oil	85.0-88.0	triglyceride	100	C18

Table 5.1. continued

fatty acid				
INCI	**melting range [°C]**	**type**	**percentage [%]**	**chain length**
lauric acid	42.0-44.0			C12
myristic acid	52.0-54.0			C14
palm triple pressed acid	55.0-56.5			C16, C18
palmitic acid	61.0-63.0			C16
12-hydroxystearic acid	72.0-80.0			C18
fatty alcohol				
INCI	**melting range [°C]**	**type**	**percentage [%]**	**chain length**
cetyl alcohol	47.0-50.0			C16
cetyl stearyl alcohol	48.0-52.0			C16, C18
stearyl alcohol	56.0-59.0			C18
behenyl alcohol	62.0-67.0			C18, C20, C22

Table 5.2. The overview of the four lipid compositions (1, 2, 3 and 4) used for smartLipids® production, sorted by their melting range.

solid lipids	melting range [°C]	lipid composition			
		1	2	3	4
lauric acid	42.0-44.0	-	10%	-	-
Softisan® 142	42.0-44.0	-	10%	-	-
cetyl alcohol	47.0-50.0	-	10%	10%	-
cetyl stearyl alcohol	48.0-52.0	-	10%	10%	10%
Precirol® ATO 5	50.0-60.0	-	10%	10%	10%
myristic acid	52.0-54.0	-	10%	-	-
Softisan® 154	53.0-58.0	-	10%	-	-
Imwitor® 900 (F) P	54.0-66.0	10%	-	-	10%
palm triple pressed acid	55.0-56.5	10%	-	10%	10%
Dynasan® 114	55.0-58.0	-	10%	-	-
stearyl alcohol	56.0-59.0	-	10%	10%	10%
Imwitor® 372 P (V)	56.0-60.0	-	10%	-	10%
Dynasan® P60	58.0-62.0	-	-	-	10%
palmitic acid	61.0-63.0	10%	-	10%	-
Dynasan® 116	61.0-65.0	10%	-	-	-
behenyl alcohol	62.0-67.0	10%	-	10%	10%
Compritol® 888 ATO	65.0-77.0	10%	-	10%	10%
Imwitor® 491	66.0-77.0	10%	-	10%	10%
Dynasan® 118	69.0-73.0	10%	-	-	-
12-hydroxystearic acid	72.0-80.0	10%	-	-	-
hydrogenated castor oil	85.0-88.0	10%	-	10%	-

Table 5.3. Compositions of smartLipids® suspensions produced using four different lipid compositions (1-4) and stabilized by various types of surfactants (decyl glucoside, lauryl glucoside, Tween® 80 and Plantacare® 2000 UP) and concentration (1.5 or 3.0%).

formulation code	lipid phase		water phase	
	lipid composition	Miglyol® 812	surfactant	water
LM1-4/0	10%	0%		
LM1-4/10	9%	1%	1.5 / 3.0%	88.5 / 87.0%
LM1-4/20	8%	2%		

smartLipids formulation code

LM ⬛ / 🟠

lipid composition
1, 2, 3 or 4

amount of Miglyol® 812
0, 10 or 20 (%)
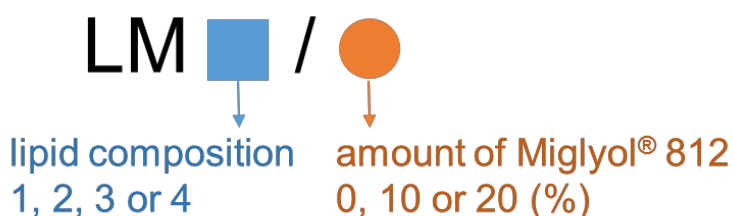
Fig. 5.1. Nomenclature explanation for the lipid phase of smartLipids® suspensions. For example: LM2/10 means that this smartLipids® suspension was produced using lipid composition 2 (c.f. Table 5.2) with additional 10% of Miglyol® 812.

5.3.3. Characterization of the smartLipids®

5.3.3.1. Photon correlation spectroscopy (PCS)

The hydrodynamic diameter (z-ave) of the smartLipids® particles was measured by photon correlation spectroscopy (PCS, Zetasizer Nano ZS, Malvern Instruments, UK). The measuring range of the PCS is around 0.6 nm to 6 µm. PCS also gives the polydispersity index (PDI), providing information about the width of the particle size distribution. All samples were diluted with double distilled water (10 µL into 5 mL) at room temperature and each z-ave and PDI was calculated as the mean of 10 measurements.

5.3.3.2. Laser diffractometry (LD)

For potentially large particles or aggregates, laser diffractometry (LD) with a broad measuring range of 20 nm to 2,000 µm was performed using a Mastersizer 2000 (Malvern Instruments, UK), yielding the volume distribution of the particles. The particles were analyzed using the Mie theory applying 1.456 as the real refractive index (RI) and 0.01 as the imaginary refractive index (IRI). The dispersion medium was distilled water and the stirring speed was 1,750 rpm. The D50 value represents 50% particles are equal to or lower than the given size. The same applies to the diameter D10, D90 and D95. Each value is the mean value of five measurements.

5.3.3.3. Zeta potential (ZP)

The zeta potential is a measurement of the electrostatic charge on the surface of the particles. Measurements were performed using a Zetasizer Nano ZS (Malvern Instruments, UK) in conductivity water (Milli-Q water adjusted to 50 µS/cm with NaCl solution at pH 5.5) and original dispersion medium (water phase of smartLipids® suspension). The electrophoretic mobility was converted into the zeta potential by the Helmholtz–Smoluchowski equation. The zeta potential measurement was conducted after production. All samples were diluted (10 µL into 5 mL) at room temperature and the mean values were calculated from three measurements.

5.3.3.4. Differential scanning calorimetry (DSC) measurements

Differential scanning calorimetry (DSC, Mettler Toledo, Germany) was used to investigate the melting behavior of lipid mixtures. 1-2 mg lipid composition 1-4 without Miglyol® 812, 1.11-2.22 mg lipid composition 1-4 with 10% Miglyol® 812 (equal to 1-2 mg of solid lipid composition) and 1.25-2.50 mg lipid composition 1-4 with 20% Miglyol® 812 (equal to 1-2 mg of solid lipid composition) were weighed into a standard aluminum pan (40 µL, Mettler Toledo, Switzerland) and sealed. The lipid mixtures were measured under nitrogen using an empty pan as reference. The samples were heated from 20 °C to 80 °C

applying a heating rate of 10 K/min. The crystallinity index (CI) was calculated from the heat of fusion according to former literature to determine the degree of crystallinity of smartLipids® (Freitas and Müller, 1999). The CI was calculated relating to the mass of solid lipid in the mixture (not the total lipid mass composed of solid and liquid lipid).

5.3.3.5. Long-term physical stability

To determine the physical stability of smartLipids® in dependence of applied production parameters, each sample was stored at room temperature for 180 days. The physical stability was determined by particle size and size distribution changes, based on PCS and LD data, during the storage period (Vivek et al., 2007).

5.4. Results and discussion

5.4.1. Current benchmarks

The lipid composition is one of the key parameters in controlling the characteristics of lipid nanoparticles (Borgia et al., 2005; Souto and Müller, 2006). Firstly, the number of the lipids influence the degree of distortion in the lipid matrix, and thus the loading capacity for the selected actives. For example, single solid lipid based SLN® limit the loading capacity while NLC® composed by solid-liquid-mixture improve active loading capacity. Secondly, the differences in crystallization behavior between the selected lipid composition and the active determine the structure of lipid nanoparticles during the cooling process (Müller et al., 2002b). Thus, an active-enriched shell or active-enriched core can be formed. Consequently, these different lipid matrix structures determine the release profile of the incorporated active. Thirdly, the recrystallization phenomena in the lipid matrix influence the stability of the lipid nanopartices because of the potentially formed unstable α-modification. During storage, this α-modification could transform into a more stable β-modification. The degree of polymorphic transformations is also influenced by the cooling procedure, playing a significant role in the overall stability of the

system. In smartLipids®, the selected lipid composition is important as well, especially considering the lipid matrix contains more than five different lipids. Since crystallization behavior strongly depends on the cooling rate, the temperature profile of the lipid matrix in the cooling process is a key parameter in the development of lipid nanoparticles. The main consideration in selecting the lipid composition were the different melting ranges of the lipids. According to former studies, high melting range lipids, e.g. Compritol® 888 ATO (melting point 65.0-77.0 °C) (Jenning et al., 2000a), and low melting range lipids, e.g. Softisan® 142 (melting point 42.0-44.0 °C) (Radomska-Soukharev, 2007) were used to form lipid nanoparticles. Therefore, commonly used lipids (Table 5.1) from current publications within the melting range from around 42.0-85.0 °C were selected for smartLipids® preparation. Lipid composition 1 and 2 are combinations of high and low melting range lipids, respectively. Lipid composition 3 is composed by various melting range lipids with a broad range. Lipid composition 4 consists of medium melting point range lipids.

5.4.2. The influence of melting points

The physical stability was studied by monitoring the change in particle size of the smartLipids® during storage. An overview of the physical stabilities of smartLipids® suspensions is listed in Table 5.4. The suspensions produced with LM1/0 and LM3/0 all gelated after production regardless of surfactant or homogenization cycles, whereas the LM2/0 and LM4/0 groups yielded more stable formulations. Fig. 5.2 shows the most stable formulations, which were stable for 180 days of storage at room temperature. It is important to note that all of the 180-day-stable formulations were produced from lipid composition 2 and 4. Considering the melting range differences, the physical stabilities indicate that higher melting range lipids - making up lipid composition 1 and 3 - are more likely to form less stable lipid matrixes compared to lipid composition 2 and 4 formed by lower melting range lipids.

One possible reason is the miscibility of the lipids. In general, a lower melting character represents superior solubility (Yamaoka et al., 1983). This indicates lipid compositions

consisting of low melting point lipids tends to generate a highly homogenous lipid matrix. After the homogenization procedure, the lipid matrix of lipid nanoparticle inherits good solubility and miscibility and is likely to yield a stable lipid suspension system. In addition, the melting range distributions of the four lipid compositions are different. Table 5 shows the melting ranges of the four lipid composition and the corresponding numbers of the stable formulations. Lipid compositions 2 and 4 have narrow melting range distributions. Since lipids with smaller melting point differences tend to possess similar chemical structures, e.g. chain length and functional group, better miscibility can be expected (Greenhalgh et al., 1999). Therefore, lipid mixtures with a narrower melting range spreads, such as lipid composition 2 and 4, are more likely to form homogeneous and stable lipid matrix.

Another possible explanation for the suspension instability relates to recrystallization phenomena, originating from polymorphic transformations of lipids. The polymorphic transformation from α-modification to the more stable β-modification poses a significant threat to the overall stability of the system (Helgason et al., 2008). During the cooling process, the solidification velocity of higher melting point lipids is faster than lower melting point lipids according to the Newton's law of cooling. Jenning's research (Jenning et al., 2000a) found that faster solidification resulted in the formation of α-modification, whereas the β-modification formed predominantly when cooling at a lower rate. For lipid composition 1 and 3 groups, a large amount of α-modification lipids formed a highly instable lipid matrix system, leading to the breakdown of the nanosuspension.

Table 5.4. An overview of the storage stabilities for all produced smartLipids® suspensions as a function of the lipid composition (1, 2, 3 and 4), oil content (0, 10 and 20%), surfactant type (DG: decyl glucoside; LG: lauryl glucoside; T: Tween® 80; P: Plantacare® 2000 UP), surfactant concentration (1.5 and 3.0%) and cycle number (1, 2 and 3). The number of days is specified for the stable formulation (e.g. 30, 60, 90, 120 and 180). No value is listed for formulations which aggregated or gelated one day after production (indicated by "-"). red: 30-60 days; yellow: 90-120 days; green: 180 days

surfactant type	concentration	cycle number	storage stability [day] LM1/0,10 and 20	LM2/0	LM2/10	LM2/20	LM3/0	LM3/10	LM3/20	LM4/0	LM4/10	LM4/20
DG	1.5%	1	-	-	-	30	-	-	-	-	-	-
DG	1.5%	2	-	-	-	60	-	-	-	-	-	-
DG	1.5%	3	-	-	30	60	-	-	-	-	-	-
DG	3.0%	1-3	-	-	-	-	-	-	-	-	-	-
LG	1.5%	1-3	-	-	-	-	-	-	-	-	-	-
LG	3.0%	1-3	-	-	-	-	-	-	-	-	-	-
T	1.5%	1	-	-	180	120	-	-	-	-	-	180
T	1.5%	2	-	-	90	120	-	-	-	-	-	90
T	1.5%	3	-	-	30	30	-	-	-	-	-	-
T	3.0%	1	-	-	180	120	-	30	30	60	180	180
T	3.0%	2	-	-	90	90	-	30	-	180	180	180
T	3.0%	3	-	-	-	90	-	-	-	60	-	-
P	1.5%	1	-	-	60	90	-	-	-	-	-	-
P	1.5%	2	-	-	60	60	-	-	-	-	-	-
P	1.5%	3	-	30	30	60	-	-	-	-	-	-
P	3.0%	1	-	-	90	-	-	-	-	-	-	-
P	3.0%	2	-	-	120	-	-	-	-	-	-	-
P	3.0%	3	-	-	-	-	-	-	-	-	-	-

Fig. 5.2. upper part

LM4/10-3.0%T (1 cycle)

LM4/10-3.0%T (2 cycles)

LM4/20-1.5%T (1 cycle)

Fig. 5.2. continued
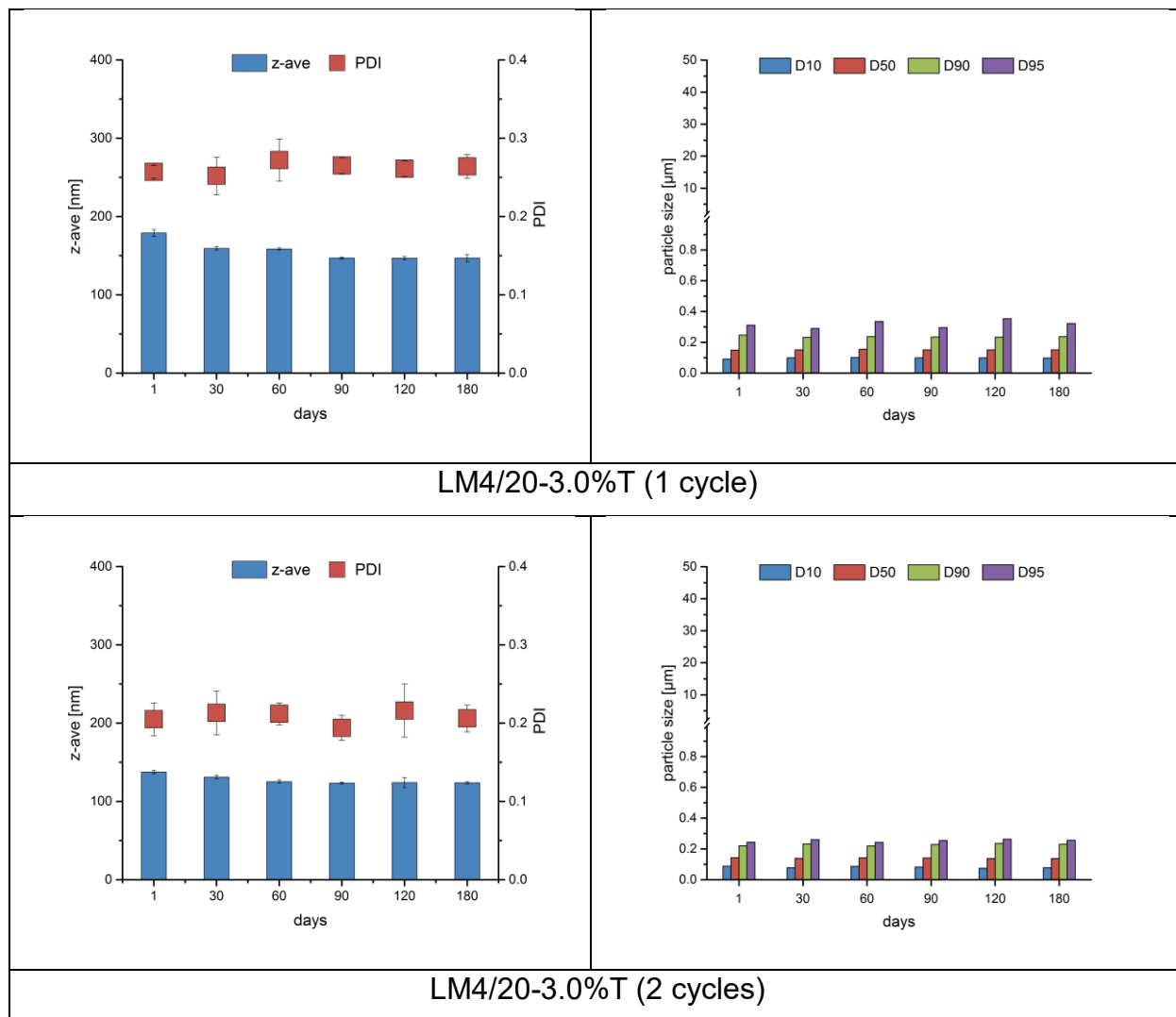
LM4/20-3.0%T (1 cycle)

LM4/20-3.0%T (2 cycles)

Fig. 5.2. The PCS data (z-ave and PDI) and LD data (D10, D50, D90 and D95) of the most stable smartLipids® suspensions up to 180 days. T is the abbreviation of Tween® 80. * the breaks in the y-axis are from 1 to 2 μm, and the scale changes above the break. The rest of the data are listed in the appendix.

Table 5.5. The number of lipids with low (40-60 °C), middle (60-80 °C) and high (> 80 °C) melting ranges in each lipid composition (1, 2, 3 or 4) correlated to their respective storage stabilities grouped in low (30-60 days), middle (90-120 days) and highest (180 days) stability. Stabilities are listed here independent of the cycle number.

	melting range	lipid composition			
		1	2	3	4
number of lipids in specific melting ranges	40-60 °C	2	10	5	7
	60-80 °C	7	-	4	3
	> 80 °C	1	-	1	-
	storage stability				
number of stable formulations	30-60 days	-	12	3	2
	90-120 days	-	10	-	1
	180 days	-	2	-	6

5.4.3. The influence of surfactants

5.4.3.1. The effect of the type of surfactant

Surfactant type plays an important role regarding the particle size and distribution as well as physical stability of lipid nanoparticles (McClements, 2015). A variety of different stabilizers has been used for lipid nanoparticles, including ionic, non-ionic, amphoteric surfactants and polymeric stabilizers (Siekmann, 1994). Non-ionic surfactants, showing low skin sensitization potential and no toxicity, are widely used for stabilizing lipid nanoparticles (Kovacevic et al., 2011; Zhuang et al., 2010). In this study, four nonionic surfactants - decyl glucoside, lauryl glucoside, Plantacare® 2000 UP and Tween® 80 - were used to evaluate the influence on the physical stability.

Plantacare® 2000 UP, which is produced by BASF and consists of decyl glucoside and lauryl glucoside, was used to investigate the influence of a surfactant mixture. smartLipids® prepared from lipid composition 2 stabilized by decyl glucoside, lauryl glucoside and Plantacare® 2000 UP showed very different stabilities (Table 5.6), even though they share similar molecular structures (Table 5.7). The number of stable
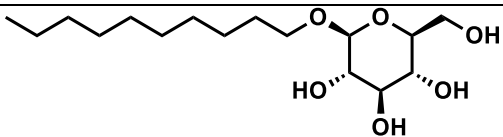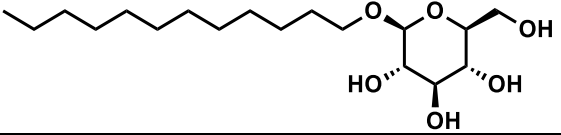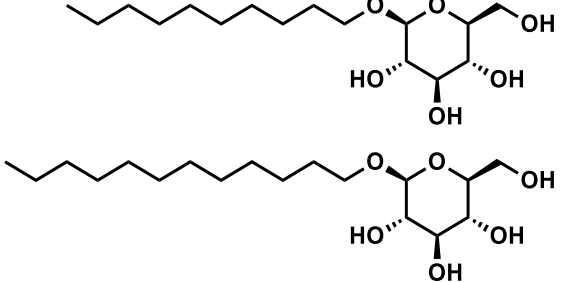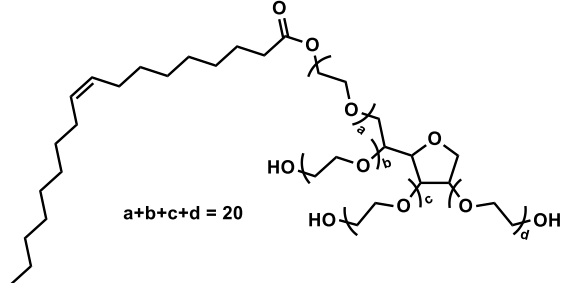
formulations stabilized by Plantacare® 2000 UP were significantly more numerous than those stabilized by decyl glucoside, and were stable for longer periods of time as well. Moreover, all lipid nanoparticles stabilized by lauryl glucoside gelated after production, regardless of the surfactant concentrations or production parameters. The results show Plantacare® 2000 UP performed better stabilizing capability in smartLipids® systems than decyl glucoside and lauryl glucoside, indicating co-surfactants are likely to be more effective in stabilizing smartLipids® nanoparticles than formulations with single surfactant.

Tween - a PEG-containing stabilizer - was used as a reference, because it proved in previous studies effective stabilizer for lipid nanoparticles. Table 5.6 shows that the total number of stable smartLipids® stabilized by Tween® 80 is much higher than those stabilized by decyl glucoside and Plantacare® 2000 UP. More importantly, only formulations stabilized by Tween® 80 showed stability up to 180 days. In addition, only lipid composition 2 could be successfully stabilized by decyl glucoside and Plantacare® 2000 UP. However, formulations prepared from lipid composition 2, 3 and 4 stabilized by Tween® 80 show desirable stability properties. Therefore, Tween® 80 is the most effective surfactant for stabilizing smartLipids® nanoparticles.

Table 5.6. Comparison of number of stable smartLipids® formulations being stabilized by the three surfactants decyl glucoside, Plantacare® 2000 UP and Tween® 80. Lauryl glucoside led to no stable formulations, thus is missing in following. The stabilities were evaluated cycle number independently and grouped in low (30-60 days), middle (90-120 days) and highest (180 days) stability.

lipid composition	decyl glucoside			Plantacare® 2000 UP			Tween® 80		
	number of stable formulations			number of stable formulations			number of stable formulations		
	30-60 days	90-120 days	180 days	30-60 days	90-120 days	180 days	30-60 days	90-120 days	180 days
LM1/0-20	-	-	-	-	-	-	-	-	-
LM2/0	-	-	-	1	-	-	-	-	-
LM2/10	1	-	-	3	2	-	1	2	2
LM2/20	3	-	-	2	1	-	1	5	-
LM3/0	-	-	-	-	-	-	-	-	-
LM3/10	-	-	-	-	-	-	2	-	-
LM3/20							1	-	-
LM4/0	-	-	-	-	-	-	2	-	1
LM4/10	-	-	-	-	-	-	-	-	2
LM4/20	-	-	-	-	-	-	-	1	3

Table 5.7. Overview of surfactants used for the production of smartLipids® suspensions, showing surfactants chemical structure, molecular weight (MW) and HLB values after Davies.

surfactant	chemical structure	chain length	MW (g/mol)	HLB value
decyl glucoside		C10	320	12
lauryl glucoside		C12	348	11
Plantacare® 2000 UP		C10 (30-50%) C12 (20-30%)	340	12
Tween® 80		C18	1310	15

5.4.3.2. The effect of HLB value

HLB theory proposes the HLB value of the surfactant should match the HLB values of the lipids in order to produce physically stable smartLipids® systems. Additionally, the required HLB value decreases with an increasing amount of liquid lipid in the matrix (Kovacevic et al., 2011; Myers, 2005). This was confirmed by lipid composition 2 stabilized by 3% (w/w) Tween® 80. LM2/10-3.0%T with 1 cycle shared the same lipid composition and production parameters with LM2/20-3.0%T with 1 cycle, the only difference being the content of liquid lipid (Miglyol® 812, 10% versus 20%). Table 5.4 indicates LM2/10-3.0%T with 1 cycle and LM2/20-3.0%T with 1 cycle were stable for 180 and 120 days,

respectively. According to the HLB theory, the required HLB value of LM2/20 should be lower than LM2/10. Thus, the stability of LM2/20-3.0%T with 1 cycle decreased.

Table 5.6 shows the most stable smartLipids® suspensions were stable for 180 days. Interestingly, all the 180-day-stable nanosuspensions were stabilized by Tween® 80. Since Tween® 80 possesses the longest carbon chain (C18, Table 5.7) and highest HLB value (15), the HLB values of the four lipid mixtures are likely around or higher than 15. Therefore, the surfactant with high HLB value is more capable of stabilizing the lipid mixture. This is underlined further by the stabilities formulations derived from LM2/10. The most stable (180 days) lipid suspensions of LM2/10 were stabilized by Tween® 80 with the HLB value of 15. With lower HLB value surfactants decyl glucoside (12) and Plantacare® 2000 UP (12), the stability decreased to 60 and 120 days, respectively. With lauryl glucoside, having the lowest HLB value of 11, no stable formulation could be produced.

5.4.3.3. The effect of surfactant concentration

High concentrations of surfactants decrease the surface tension at the water/lipid interface and facilitates particle partition (McClements, 2015). Moreover, insufficient surfactant induces instability as recrystallization processes become more favorable (Weiss et al., 2008). During the cooling process, the α-modification may transfer into the needle-like-structured β-modification with increased surface areas. If the newly formed surface area is not sufficiently covered by surfactant molecules, hydrophobic interactions may lead to flocculation, and thus instability. Formulation LM4/0-1.5%T gelated immediately, whereas increasing the surfactant concentration to 3.0% made the formulation highly stable (180 days). Regarding this stability difference, Helgason (Helgason et al., 2009) offered an explanation. When surfactant concentrations are high, surfactant tail groups are packed tightly at the lipid-water interface. These tightly packed tails result in a solid-like characteristic. Therefore, at high surfactant concentrations, the lipid particles are surrounded by a rigid "shell" formed by sufficient surfactant tail groups. This "shell" acts as a steric constraint and slows down or restricts the particle movement,

resulting in the increased physical stability.

However, higher surfactant concentrations do not always lead to higher stability. smartLipids® nanosuspensions prepared with LM2/10 and LM2/20 as lipid matrix stabilized by 1.5% w/w decyl glucoside were stable up to 60 days. Upon increasing the surfactant concentration to 3.0%, the formulation gelated after production. The results show that in this case, an increased amount of surfactant decreased the stabilities of lipid nanoparticles. According to the production procedure, the lipid mixture formed a nanoemulsion at elevated temperature first, followed by the formation of smartLipids® upon cooling down. The nanoemulsion state significantly affects the state of final smartLipids® nanosuspension. The physical stability of nanoemulsions is influenced by Ostwald ripening (Adams et al., 2007). In Ostwald ripening theory, nanoemulsion tends to generate a single drop and the larger size difference in this nano system exists, the higher rate of Ostwald ripening happens. The Lifshitz–Slesov–Wagner (LSW) theory gives an expression for the Ostwald ripening rate (Capek, 2004; Taylor, 1995):

$$\omega = \frac{dr^3}{dt} = \frac{8}{9}[\frac{C_\infty \gamma V_m D}{\rho RT}]$$

in which r is the average radius of droplets; t is the storage time; C_∞ is the bulk phase solubility; γ is the interfacial tension; V_m is the molar volume; D is the diffusion in the continuous phase; ρ is the density of the oil; R is the gas constant; T is the absolute temperature.

The increasing amount of surfactant decreases the droplet size, which in turn increases the Brownian diffusion, leading to the enhancement of Ostwald ripening rate. With higher surfactant concentrations, lower HLB value (here is decyl glucoside) surfactant molecules may preferentially accumulate at the interface, resulting in reduction of the Gibbs elasticity, inducing the increase of Ostwald ripening rate (Tadros et al., 2004) as well. In the smartLipids® preparation process, this instability of the nanoemulsion results in gelation during cooling.

5.4.4. The melting behavior of lipid compositions

Due to the multiple lipids present in the smartLipids® lipid matrix, the solubility and miscibility of lipids determine the homogeneity of the lipid matrix, and thus influence the stability of the entire lipid suspension system. Experimentally, DSC was employed to investigate the melting behavior of the four lipid compositions and miscibility was predicted.

Fig. 5.3 shows the melting behavior of four lipid compositions. The DSC graph of lipid composition 2 with 0% Miglyol® 812 (Fig. 5.3 upper right) shows there is a broad peak around 30 °C apart from the main peak (around 43 °C). This indicates the lipid mixture without oil was not molecularly dispersed. The immiscibility of the lipid matrix formed by lipid composition 2 might not yield stable smartLipids® nanosuspensions, thus liquid lipid Miglyol® 812 was added into the solid lipid compositions. After adding 10% and 20% Miglyol® 812 (compared to lipid matrix), the 30 °C peak of lipid composition 2 disappeared, indicating more homogeneous lipid matrixes were obtained by addition of liquid lipid.

The detailed DSC results of all lipid compositions are shown in Table 5.8. After adding Miglyol® 812 into the four lipid compositions, all the main melting points shifted to lower temperatures in a concentration dependent manner. For example, the melting points of LM3/0, LM3/10 and LM3/20 were 55.49 °C, 54.07 °C and 53.70 °C, respectively. This depression also occurred in enthalpy values as well as crystallinity indices (CI). This phenomenon aligns with other studies (Jenning et al., 2000a; Kovacevic et al., 2011), indicating the addition of a liquid lipid distorts the structure of the matrix.

Triglycerides are known to exist in multiple modifications (Hernqvist, 1988; Saupe et al., 2005), for example in α-modification (thermodynamic instable modification) and β-modification (thermodynamic stable modification). As it was mentioned in section 5.4.1., the polymorphic transition is one of the main sources of instability in the lipid matrix. The DSC results show no new peak emerging after adding Miglyol® 812 into the four lipid compositions. Therefore, the addition Miglyol® 812 did not induce polymorphic transitions, making it a suitable stabilization tool in smartLipids® production. In addition, the

thermograms of lipid combination 4 show a peak shoulder at higher temperatures (around 63 °C), which becomes more pronounced with higher amounts of Miglyol® 812. This also occurred in another study (Jenning et al., 2000a), and a possible reason is the solubility of Miglyol® 812 in different modifications of lipids is not identical. This inconsistency induced different extend of melting point shift, leading to an obvious separation of the two peaks.

Nevertheless, the DSC measurements show all the lipid mixtures' melting points were higher than 42 °C, except for lipid composition 2 with 0% Miglyol® 812. This is especially important for dermal application, as the skin temperature of humans is 32 °C (Saupe et al., 2005), and the lipid nanoparticles should remain in solid state during dermal application.
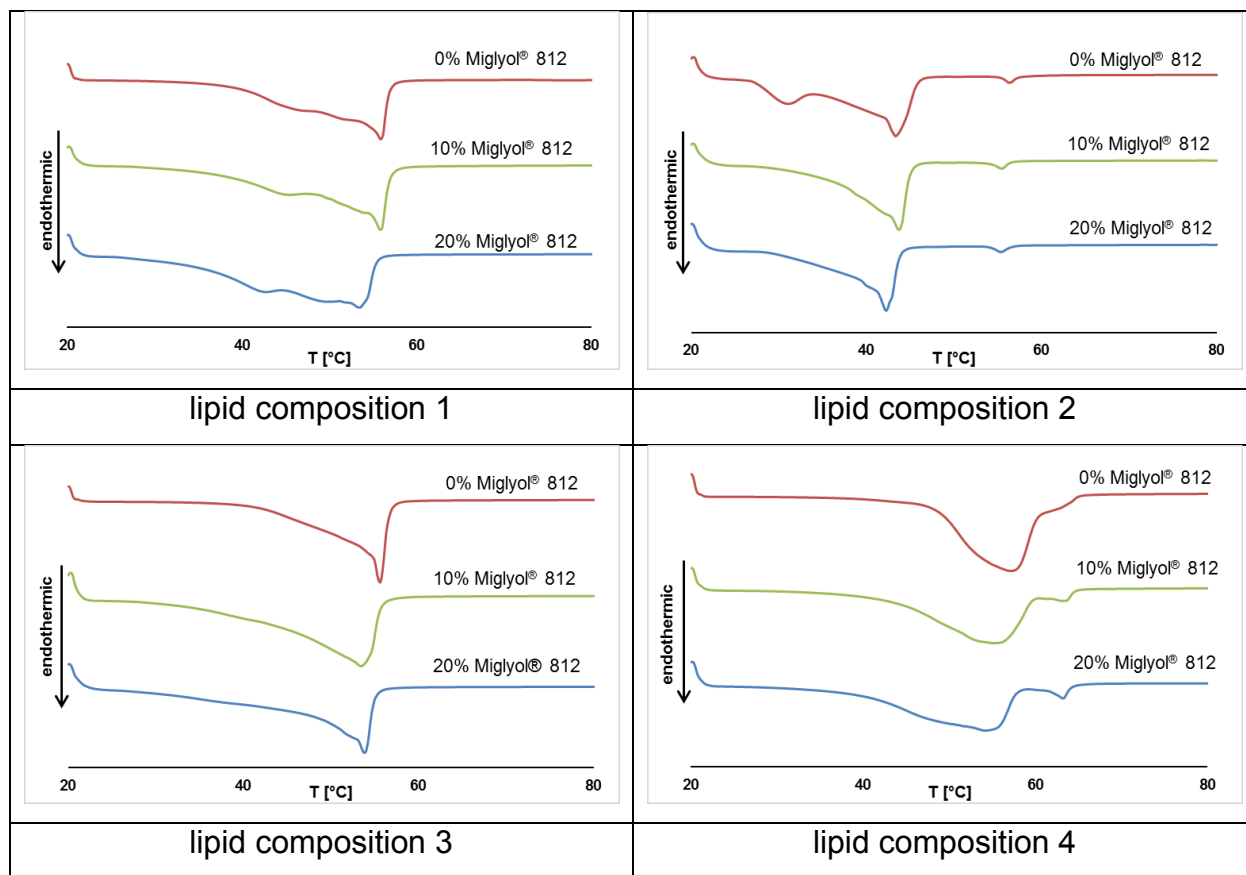
Fig. 5.3. Differential scanning calorimetry thermograms (20-80°C) of all four lipid compositions (1, 2, 3 and 4) with increasing amount of Miglyol® 812 from 0, 10 to 20% measured at a heating rate of 10 K/min.

Table 5.8. Melting peaks, enthalpy and crystallinity index (CI) for each lipid composition as measured by DSC.

lipid composition	peak 1 [°C]	peak 2 [°C]	peak 3 [°C]	enthalpy [J/g]	CI [%]
LM1/0	47.17	55.80	-	-107.47	100
LM1/10	45.83	55.70	-	-97.10	90.3
LM1/20	42.24	53.38	-	-68.00	63.3
LM2/0	30.76	43.59	56.29	-66.78	100
LM2/10	-	43.58	55.45	-52.85	79.1
LM2/20	-	42.19	55.29	-45.76	68.5
LM3/0	55.49	-	-	-84.82	100
LM3/10	54.07	-	-	-72.22	85.1
LM3/20	53.70	-	-	-58.75	69.3
LM4/0	57.02	63.50	-	-76.43	100
LM4/10	56.00	63.16	-	-59.87	78.3
LM4/20	54.23	63.11	-	-55.73	72.9

5.4.5. The influence of the addition of Miglyol® 812 on physical stability

Lipid composition 1-4 with and without the addition of Miglyol® 812 were all used for smartLipids® preparation, and the physical stabilities of the suspensions were investigated. An overview of the physical stabilities is listed in Table 5.4. It is obvious that following the addition of Miglyol® 812, the physical stability of all mixtures improved. For example, Formulation LM2/0 stabilized by 1.5% w/w decyl glucoside gelated regardless of the number of homogenization cycles, but after adding 10% and 20% Miglyol® 812 remained stable for 30 and 60 days respectively. This improved physical stability also occurred for lipid composition 3 (stabilized by 1.5% w/w Tween® 80) and 4 (stabilized by 1.5% w/w Tween® 80). The proposed cause for this is that the addition of liquid lipid causes a decrease in size of the lipid nanoparticles, since a lower viscosity lipid phase can be dispersed more easily (Jenning et al., 2000b). For example, the mean particle size (z-ave) of LM4/0-3.0%T after 1 homogenization cycle was 269 nm, and that of LM4/10-3.0%T after 1 cycle was 180 nm (Fig. 5.4). These two suspensions were stable for 60 and 180 days, respectively, indicating the addition of liquid lipid reduces the particle size and increases the physical stability.

However, indefinitely increasing the amount of liquid lipid does not always yield more stable formulations. LM2/20-1.5%T undergoing 1 homogenization cycle were less stable (120 days) compared to LM2/10-1.5%T after 1 cycle (180 days), even though LM2/20-1.5%T with 1 cycle contained more Miglyol® 812 (Fig. 5.4). Additionally, LM1/0, LM1/10, and LM/1/20 yielded no stable formulation. Following the surfactant influence discussed in section 5.4.3., the addition of liquid lipid may change the optimal HLB value of surfactant, making the previously optimal surfactant type and concentration less suitable. Therefore, adding liquid lipid enhances the general physical stability but constant addition may not further improve the stability.
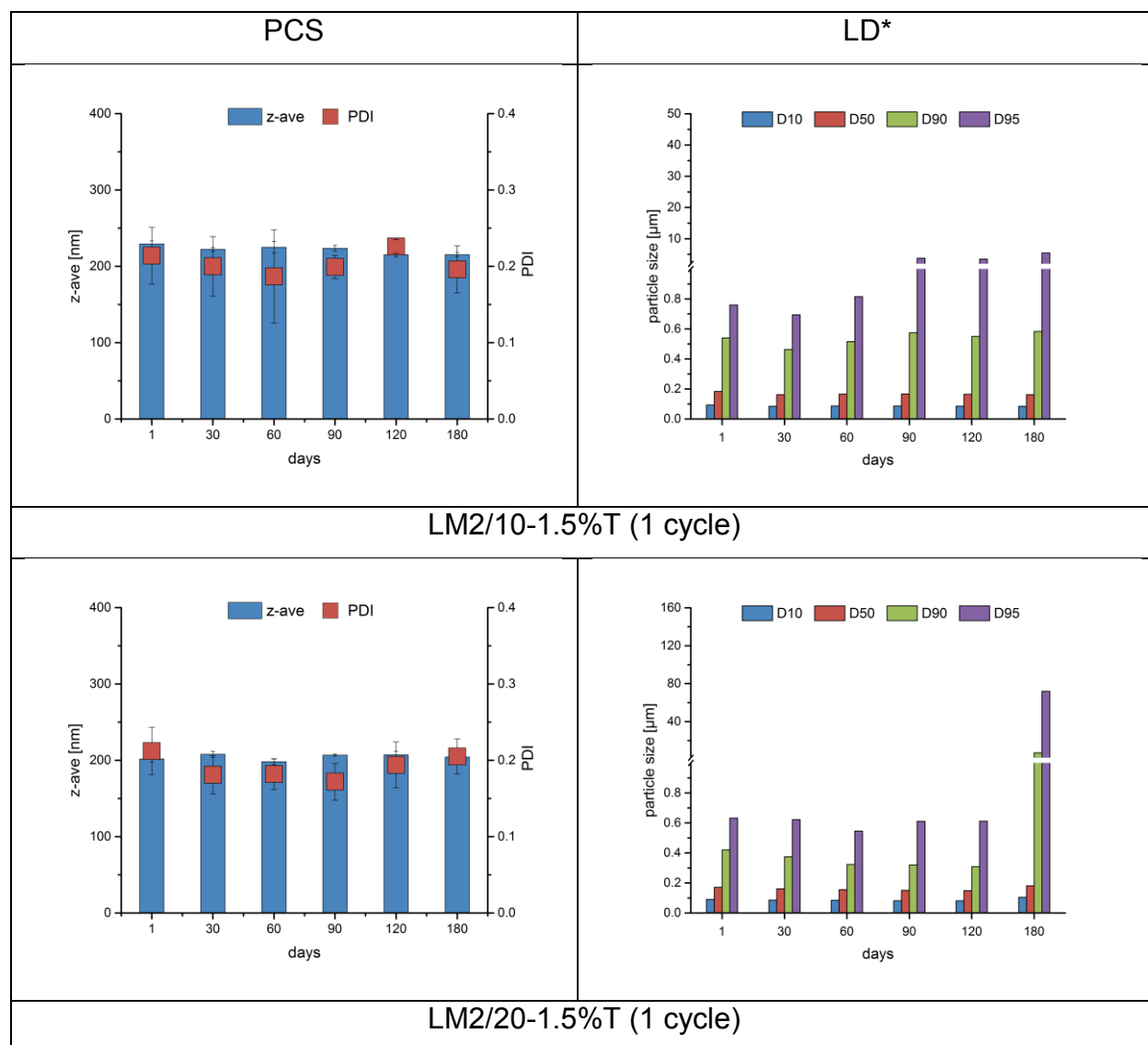
Fig. 5.4. upper part

LM4/0-3.0%T (1 cycle)
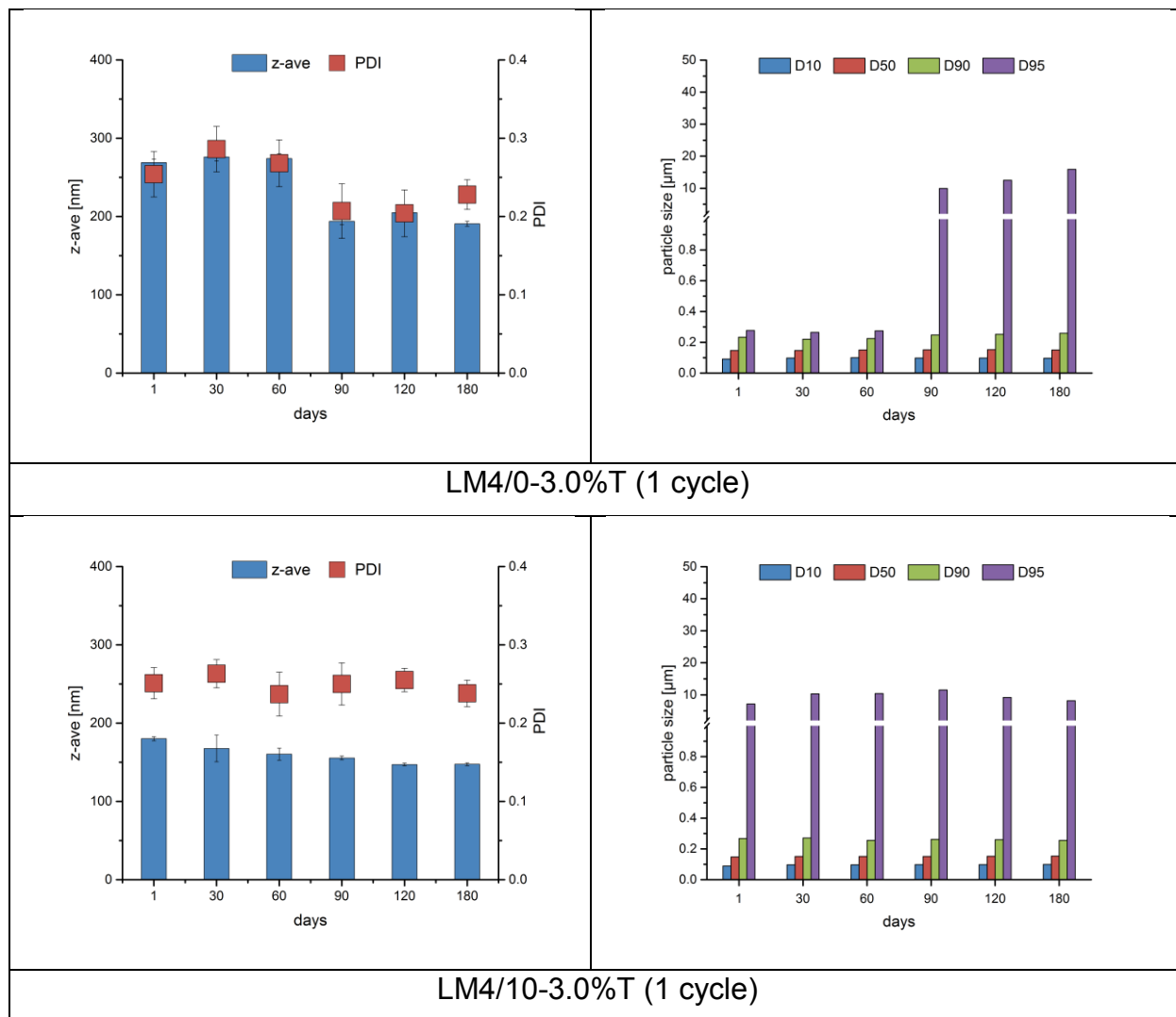
LM4/10-3.0%T (1 cycle)

Fig. 5.4. The PCS data (z-ave and PDI) and LD data (D10, D50, D90 and D95) of LM4/0-3.0%T (1 cycle), LM4/10-3.0%T (1 cycle), LM2/20-1.5%T (1 cycle) and LM2/10-1.5%T (1 cycle).

* the breaks in the y-axis are from 1 to 2 μm, and additionally mark a change in the scale.

5.4.6. The influence of production parameters

Aside from the lipid combination and surfactant, another important factor in producing stable smartLipids® is optimized production parameters. smartLipids® suspensions were produced using high pressure homogenization. In order to keep all lipid mixtures in a molten state during the homogenization process, lipid nanoparticles were produced at

85 °C. In general, homogenization favors the generation of small particles with a narrow particle size distribution, and enhances the physical stability of the suspension system. However, intermittent sampling after each homogenization cycle shows a decreasing physical stability with an increasing number of homogenization cycles for some formulations (Table 5.4). LM2/10-3.0%T after 1 homogenization cycle was stable for 180 days, but the stable lifetime decreased to 90 days after 2 cycles, and after 3 cycles the formulation gelated instantly following production. The z-ave and size distribution data during storage time are shown in Fig. 5.5. The z-ave values of LM2/10-3.0%T produced with 1 and 2 cycles were 188 and 166 nm, respectively. LM2/10-3.0%T after 1 cycle showed the best stability. After 180 days, 90% of the lipid nanoparticles were still smaller than 0.3 µm indicating good physical stability, even though the D95 value was around 5 µm by this time. As a contrast, LM2/10-3.0%T following 2 cycles aggregated after 120 days.

During homogenization, the high thermal energy and shear forces contribute to several effects: (1) reducing the size of the particles, (2) heating the lipid suspension and (3) increasing the kinetic energy of the particles. In the production process, the homogenization procedure first contributes to reducing the size of the lipid particles. Following a certain number of cycles, the lipid nanoparticles cannot be further reduced in size. The high energy is then mainly dispersed as heat and particle kinetic energy, both of which contribute to faster particle movement. This high kinetic energy causes more frequent and intense collisions between nanoparticles, and then potentially damages the surfactant film at the lipid nanoparticles' surface, causing aggregation (Freitas and Müller, 1999).

In order to develop an in-depth understanding on how the homogenization procedure affects the physical stability of lipid nanoparticles, LM4/0-3.0%T was selected for this study. This is because Table 5.4 shows that the number of homogenization cycles has a significant influence on the stability of this formulation. Thus, LM4/0-3.0%T was produced using various pressures (300, 400, 500, 600, 700, 800, 900 and 1000 bar), and with 1 to 5 homogenization cycles. The stability was monitored up to 90 days (Table 5.9). When

the pressure was increased from 300 up to 900 bar, no noticeable decrease in stability could be observed. However, the suspension produced at 1000 bar shows obvious instability, and the best formulation was stable for only 30 days. In addition, all formulations gelated immediately following a 5th homogenization cycle. This is in line with the expected frequent high-energy collisions between particles as discussed above. In addition, the data differs from the former results in Table 5.4 where the formulations show instabilities after 3 homogenization cycles. A possible cause for this discrepancy is that the total sample volume for each following homogenization cycle was different. In previous studies, 8 mL samples were collected for further analysis out of the 40 mL batch, but for LM4/0-3.0%T study only 3 mL of the suspension was collected following each cycle, leading to the different average energy among particles.

According to the stability investigations, for smartLipids® preparation 300-900 bar with two homogenization cycles are preferable and further increase of homogenization pressure/cycle should be avoided.
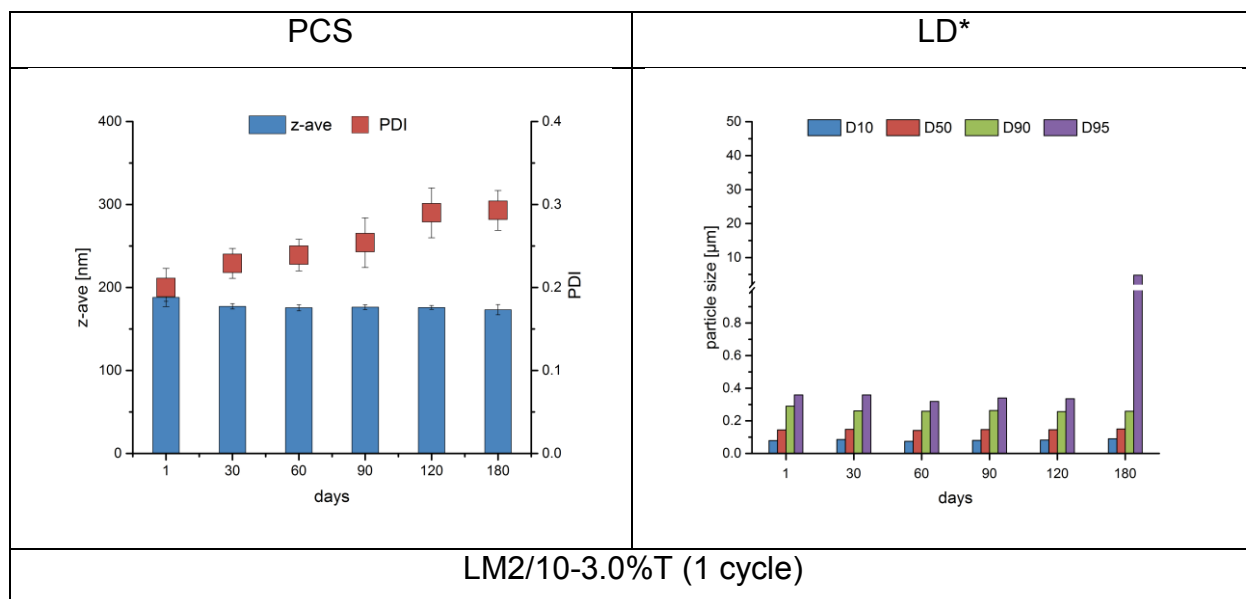
Fig. 5.5. upper part
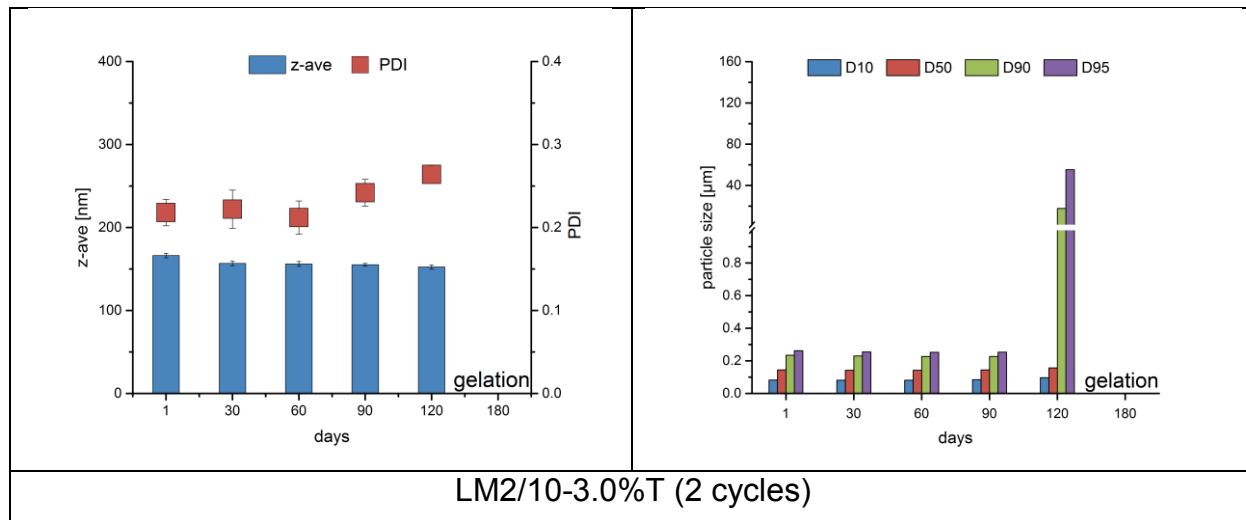
Fig. 5.5. The PCS data (z-ave and PDI) and LD data (D10, D50, D90 and D95) of LM2/10-3.0%T with 1 and 2 cycles.

* the breaks in the y-axis are from 1 to 2 µm, and additionally mark a change in the scale.

Table 5.9. The overview* of the storage stabilities of LM4/0-3.0%T smartLipids® suspensions applying various homogenization cycles. No day value is given for formulations aggregated or gelated shortly after production.

pressure [bar]	storage stability [day]				
	1 cycle	2 cycles	3 cycles	4 cycles	5 cycles
300	90	90	90	90	-
400	90	90	90	90	-
500	< 30	90	90	90	-
600	90	90	90	< 30	-
700	< 30	90	90	90	-
800	< 30	90	90	90	-
900	90	90	< 30	90	-
1000	< 30	30	< 30	< 30	-

* detailed results of the stability are shown in the Appendix Fig. A2.

5.4.7. The influence of the zeta potential

The zeta potential is a commonly used value aiding physical stability prediction in the case of electrostatic stabilization. The higher the zeta potential is, the higher is the electrostatic repulsion force among the particles, and therefore the physical stability of

the system. The zeta potential measured in conductivity water (50 μS/cm, adjusted by NaCl) represents the surface charge of the nanoparticles (Helmholtz potential). The zeta potential measured in original medium is a measure for the thickness of the diffuse layer. If the diffusive layer is thinner, the potential decays more strongly leading to a lower measured zeta potential. According to literature (Müller et al., 1996), zeta potential values higher than |30 mV| in the original medium indicate stable suspensions. Table 5.10 shows the overview of zeta potential values of smartLipids® suspensions. The zeta potential of LM2/10-1.5%T after 1 homogenization cycle in original medium was -37.9 mV, and the formulation was stable for 180 days, which is in accordance with the predicted stability based on electrostatic repulsion between the particles. Therefore, high zeta potential values appear to be a useful tool for the prediction of the long-term stability of smartLipids®.

However, the zeta potential value of the stable (180 days) smartLipids® suspension LM4/20-3.0%T with 2 cycles in original medium was only -12.0 mV. Despite this low absolute zeta potential value, the mean particle size remained perfectly unchanged (around 130 nm) for 180 days. The LD result confirms this observed stability, as the size distribution remains unchanged with a D95 value of around 0.3 μm throughout the storage timeframe. In this case, the stability does not solely originate from electrostatic repulsion, but additional steric stabilization may play a role as well (Mitri et al., 2011). Previously, Tween® 80 was already used as steric stabilizer for solid lipid nanoparticles in C. Olbrich's research, which exhibited a similarly low zeta potential value (Olbrich and Müller, 1999).

Table 5.10. Zeta potential (ZP) of smartLipids® formulations measured in conductivity water (CW) and original medium (OM), correlated to respective storage stabilities.

DG: decyl glucoside; LG: lauryl glucoside; T: Tween® 80; P: Plantacare® 2000 UP

lipid composition	surfactant		cycle number	ZP [mV]		storage stability [day]
	type	concentration		CW	OM	
LM2/0	P	1.5%	3	-56.5	-19.0	30
LM2/10	DG	1.5%	3	-68.0	-37.8	30
	T	1.5%	1	-60.3	-37.9	180
			2	-50.7	-29.5	90
			3	-52.9	-24.1	30
	T	3.0%	1	-52.6	-26.8	180
			2	-41.8	-19.6	90
	P	1.5%	1	-66.5	-26.8	60
			2	-69.8	-27.0	60
			3	-65.0	-20.0	30
	P	3.0%	1	-62.1	-14.7	90
			2	-60.4	-14.2	120
LM2/20	DG	1.5%	1	-68.8	-34.8	30
			2	-68.7	-39.1	60
			3	-62.9	-34.2	60
	T	1.5%	1	-59.7	-39.6	120
			2	-51.8	-30.5	120
			3	-46.5	-24.5	30
	T	3.0%	1	-55.5	-28.6	120
			2	-54.6	-20.5	90
			3	-38.4	-15.3	90
	P	1.5%	1	-74.8	-34.0	90
			2	-72.5	-29.1	60
			3	-75.3	-27.2	60
LM3/10	T	1.5%	1	-41.4	-6.97	30
			2	-33.8	-5.18	30
LM3/20	T	1.5%	1	-43.4	-9.17	30
LM4/0	T	3.0%	1	-43.9	-19.5	180
			2	-42.1	-18.2	180
			3	-40.6	-17.1	60
LM4/10	T	3.0%	1	-46.4	-16.2	180
			2	-41.2	-14.1	180
LM4/20	T	1.5%	1	-49.2	-28.3	180
			2	-41.5	-24.1	90
	T	3.0%	1	-41.2	-15.7	180
			2	-34.2	-12.0	180

5.5. Conclusions

smartLipids® suspensions with excellent physical stability were successfully developed in this study. Furthermore, the key factors in the development of stable lipid nanoparticle systems were thoroughly investigated. In summary, physically stable smartLipids® nanosuspensions can be obtained by using the low melting points lipids, surfactants with relative high HLB values as well as adding liquid lipid and applying only 1 or 2 homogenization cycles.

Identifying key parameters in both lipid selection and production parameters led to the successful development of stable smartLipids® suspensions. Future research efforts can be dedicated to further parameters (e.g. different storage temperature and packing material, etc.) as well as the incorporation of actives into smartLipids®. In the latter regard, this study has already shown preliminary success by demonstrating that adding liquid lipid improves the physical stability. Compared to the mixture of various solid lipids, the addition of liquid lipid further increases the amount of imperfections in the lipid matrix, which is indicative of possibly enhanced drug loading capacity. This improvement underlines the great potential of smartLipids® for practical application.

Nowadays, smartLipids® products are already on the market (e.g. BergaCare smartLipids® (Olechowski et al., 2016)), showing that further development causes the smartLipids® to have a good perspectives of fulfilling industrial requirements.

5.6. References

Adams, F., Walstra, P., Brooks, B., Richmond, H., Zerfa, M., Bibette, J., Hibberd, D., Robins, M., Weers, J., Kabalnov, A., 2007. Modern aspects of emulsion science. Royal Society of Chemistry.

Borgia, S.L., Regehly, M., Sivaramakrishnan, R., Mehnert, W., Korting, H., Danker, K., Röder, B., Kramer, K., Schäfer-Korting, M., 2005. Lipid nanoparticles for skin penetration

enhancement—correlation to drug localization within the particle matrix as determined by fluorescence and parelectric spectroscopy. Journal of controlled release 110, 151-163.

Capek, I., 2004. Degradation of kinetically-stable o/w emulsions. Advances in Colloid and Interface Science 107, 125-155.

Chen, X.-Q., Gudmundsson, O.S., Hageman, M.J., 2012. Application of lipid-based formulations in drug discovery. Journal of medicinal chemistry 55, 7945-7956.

Freitas, C., Müller, R., 1999. Correlation between long-term stability of solid lipid nanoparticles (SLN™) and crystallinity of the lipid phase. European Journal of Pharmaceutics and Biopharmaceutics 47, 125-132.

Göke, K., Bunjes, H., 2017. Drug solubility in lipid nanocarriers: Influence of lipid matrix and available interfacial area. Int J Pharmaceut 529, 617-628.

Greenhalgh, D.J., Williams, A.C., Timmins, P., York, P., 1999. Solubility parameters as predictors of miscibility in solid dispersions. Journal of pharmaceutical sciences 88, 1182-1190.

Helgason, T., Awad, T., Kristbergsson, K., McClements, D., Weiss, J., 2008. Influence of polymorphic transformations on gelation of tripalmitin solid lipid nanoparticle suspensions. Journal of the American Oil Chemists' Society 85, 501-511.

Helgason, T., Awad, T.S., Kristbergsson, K., McClements, D.J., Weiss, J., 2009. Effect of surfactant surface coverage on formation of solid lipid nanoparticles (SLN). J Colloid Interf Sci 334, 75-81.

Hernqvist, L., 1988. Crystal structures of fats and fatty acids. Crystallization and polymorphism of fats and fatty acids 31, 97-137.

Jenning, V., Gohla, S.H., 2001. Encapsulation of retinoids in solid lipid nanoparticles (SLN). J Microencapsul 18, 149-158.

Jenning, V., Thunemann, A.F., Gohla, S.H., 2000a. Characterisation of a novel solid lipid nanoparticle carrier system based on binary mixtures of liquid and solid lipids. Int J Pharmaceut 199, 167-177.

Jenning, V., Thünemann, A.F., Gohla, S.H., 2000b. Characterisation of a novel solid lipid nanoparticle carrier system based on binary mixtures of liquid and solid lipids. Int J Pharmaceut 199, 167-177.

Kovacevic, A., Savic, S., Vuleta, G., Muller, R.H., Keck, C.M., 2011. Polyhydroxy

surfactants for the formulation of lipid nanoparticles (SLN and NLC): Effects on size, physical stability and particle matrix structure. Int J Pharmaceut 406, 163-172.

Liu, Y., Wang, P., Sun, C., Zhao, J., Du, Y., Shi, F., Feng, N., 2011. Bioadhesion and enhanced bioavailability by wheat germ agglutinin-grafted lipid nanoparticles for oral delivery of poorly water-soluble drug bufalin. Int J Pharmaceut 419, 260-265.

Lucks, J.S., Müller, R.H., 1991. Medication vehicles made of solid lipid particles (solid lipid nanospheres SLN), EP0000605497.

McClements, D.J., 2015. Food emulsions: principles, practices, and techniques. CRC press.

Mitri, K., Shegokar, R., Gohla, S., Anselmi, C., Müller, R.H., 2011. Lipid nanocarriers for dermal delivery of lutein: preparation, characterization, stability and performance. Int J Pharmaceut 414, 267-275.

Müller, R.H., Hildebrand, G., Nitzsche, R., Paulke, B.-R., 1996. Zetapotential und Partikelladung in der Laborpraxis. PAPERBACK APV 37.

Müller, R.H., Mader, K., Gohla, S., 2000. Solid lipid nanoparticles (SLN) for controlled drug delivery - a review of the state of the art. Eur J Pharm Biopharm 50, 161-177.

Müller, R.H., Radtke, M., Wissing, S.A., 2002a. Nanostructured lipid matrices for improved microencapsulation of drugs. Int J Pharmaceut 242, 121-128.

Müller, R.H., Radtke, M., Wissing, S.A., 2002b. Solid lipid nanoparticles (SLN) and nanostructured lipid carriers (NLC) in cosmetic and dermatological preparations. Advanced drug delivery reviews 54, S131-S155.

Müller, R.H., Ruick, R., Keck, C.M., 2014. smartLipids® - the new generation of lipid nanoparticles after SLN and NLC, AAPS Annual Meeting, San Diego.

Myers, D., 2005. Surfactant science and technology. John Wiley & Sons.

Olbrich, C., Müller, R., 1999. Enzymatic degradation of SLN—effect of surfactant and surfactant mixtures. Int J Pharmaceut 180, 31-39.

Olechowski, F., Pyo, S.M., Keck, C.M., Müller, R.H., 2016. BergaCare smartLipids®-commercial lipid submicron particle concentrates for cosmetics, consumer care & pharma.

Pyo, S.M., Meinke, M., Klein, A.F., Fischer, T.C., Müller, R.H., 2016. A novel concept for the treatment of couperosis based on nanocrystals in combination with solid lipid nanoparticles (SLN). Int J Pharmaceut 510, 9-16.

Radomska-Soukharev, A., 2007. Stability of lipid excipients in solid lipid nanoparticles. Advanced drug delivery reviews 59, 411-418.

Saupe, A., Wissing, S.A., Lenk, A., Schmidt, C., Muller, R.H., 2005. Solid lipid nanoparticles (SLN) and nanostructured lipid carriers (NLC) - Structural investigations on two different carrier systems. Bio-Med Mater Eng 15, 393-402.

Siekmann, B., 1994. title., Technische Universität Carolo-Wilhelmina zu Braunschweig.

Siekmann, B., Westesen, K., 1994. Thermoanalysis of the recrystallization process of melt-homogenized glyceride nanoparticles. Colloids and surfaces B: Biointerfaces 3, 159-175.

Souto, E., Müller, R., 2006. Investigation of the factors influencing the incorporation of clotrimazole in SLN and NLC prepared by hot high-pressure homogenization. Journal of microencapsulation 23, 377-388.

Tadros, T., Izquierdo, P., Esquena, J., Solans, C., 2004. Formation and stability of nano-emulsions. Advances in colloid and interface science 108, 303-318.

Taylor, P., 1995. Ostwald ripening in emulsions. Colloids and Surfaces A: Physicochemical and Engineering Aspects 99, 175-185.

Vivek, K., Reddy, H., Murthy, R.S., 2007. Investigations of the effect of the lipid matrix on drug entrapment, in vitro release, and physical stability of olanzapine-loaded solid lipid nanoparticles. AAPS PharmSciTech 8, 16-24.

Weiss, J., Decker, E.A., McClements, D.J., Kristbergsson, K., Helgason, T., Awad, T., 2008. Solid lipid nanoparticles as delivery systems for bioactive food components. Food Biophysics 3, 146-154.

Yamaoka, Y., Roberts, R.D., Stella, V.J., 1983. Low-melting phenytoin prodrugs as alternative oral delivery modes for phenytoin: A model for other high-melting sparingly water-soluble drugs. Journal of pharmaceutical sciences 72, 400-405.

Zhuang, C.-Y., Li, N., Wang, M., Zhang, X.-N., Pan, W.-S., Peng, J.-J., Pan, Y.-S., Tang, X., 2010. Preparation and characterization of vinpocetine loaded nanostructured lipid carriers (NLC) for improved oral bioavailability. Int J Pharmaceut 394, 179-185.

Zur Mühlen, A., Zur Mühlen, E., Niehus, H., Mehnert, W., 1996. Atomic force microscopy studies of solid lipid nanoparticles. Pharmaceutical research 13, 1411-1416.

6. Solid lipid nanoparticles (SLN®) for the delivery of α-tocopherol – an efficient method for improving the drug loading capability

6.1. Abstract

α-tocopherol, an antioxidant possessing the highest biological activity in vitamin E subfamilies, finds widespread application in protecting the human skin against environmental damage. Incorporating α-tocopherol into lipid nanoparticles enhances its chemical stability as well as skin penetration rate, making this method highly suitable for dermal application. In this study, solid lipid nanoparticles (SLN®) produced using two different lipids, carnauba wax and cetyl palmitate, were selected for α-tocopherol loading. The lipid nanoparticles were loaded with 5% and 10% α-tocopherol (w/w, compared to the suspension). The mean particle sizes of all formulations were in the nano-range one day after production, and zeta potential values measured in the original medium were higher than |40 mV|. Among all the produced lipid suspensions, SLN® loaded with 10% α-tocopherol, produced with carnauba wax and undergoing three homogenization cycles showed the highest drug loading capability as well as best short-time stability. The thermal behavior of the SLN® suspension shows great potential for dermal application.

6.2. Introduction

As life expectancy increases around the globe, skin aging has been receiving an ever-growing amount of attention. Skin aging can be attributed to several factors, including environmental exposure to ultraviolet (UV) radiation, hormonal changes and metabolic processes (Rittié and Fisher, 2002). Unlike most other organs, the human skin is directly exposed to the environment, continuously coming into contact with free radicals. Therefore, environmental damage is of considerable significance for skin aging (Fisher et al., 2002). One of the primary environmental causes of skin aging is UV (UVA and UVB) irradiation from sunlight, and the effects of UVA (320-400 nm) and UVB (290-320 nm) in skin are different (Gange et al., 1985). UVA elicits premature ageing, whereas UVB causes erythema and skin cancer induced by DNA damage (McVean and Liebler, 1997; Wissing and Müller, 2001).

There is strong evidence indicating that Vitamin E can be used as an antioxidant for pharmaceutical and cosmetic products (Schmidt, 1993), and the antioxidants were shown to reduce skin aging by exposure to UV radiation (Trombino et al., 2009). Vitamin E, consists of two subfamilies: tocotrienols and tocopherols, and each of them was designated as four forms: α, β, γ and δ. Although the structures of the eight molecules are similar, their biological activities are different owing to the presence of three double bonds in the isoprenoid side chain (Musalmah et al., 2005; Serbinova et al., 1991). Among the eight forms, α-tocopherol has the highest biological activity as a chain-breaking antioxidant for preventing cell damage from free radicals (Brigelius-Flohe and Traber, 1999; Zigoneanu et al., 2008). Some cellular macromolecules, such as proteins and DNA, can be attacked by highly reactive free radicals, resulting in impairment of the cell function. Upon contact with a peroxyl radical generated by UV light, α-tocopherol acts as a radical trap and becomes an α-tocopheroxyl radical by losing its phenolic hydrogen atom. This more stable radical can subsequently react with a second radical, or be reduced by for example ascorbic acid (vitamin C), thereby regenerating the α-tocopherol (Brantley et al., 2000). Due to the effective impact on quenching oxidative chain reactions, α-tocopheroxyl radical protects the normal cells against oxidative damage. Aside from understanding the mechanism on a molecular scale, the ability of α-tocopherol to minimize the skin damage caused by UV radiation is also proven (Wissing and Müller, 2001). Furthermore, as a skin care active, α-tocopherol increases cell proliferation and moisture content of the skin. This effect further aids in protecting the skin against photoaging (Fuchs, 1998). Based on the pronounced skin-protecting effects of a-tocopherol, the development of the α-tocopherol-loaded delivery system for dermal application is very desirable.

There are currently several methods for the delivery of α-tocopherol, including nanoemulsions (Sharif et al., 2017; Teixeira et al., 2017), liposomes (Sahari et al., 2017) and polymeric nanoparticles (Alqahtani et al., 2015). With the purpose of improving physical and chemical stabilities of the incorporated active, solid lipid nanoparticles (SLN®) were developed in 1991 as an alternative drug delivery system to nanoemulsions, liposomes and polymeric nanoparticles (Lucks and Müller, 1991; Pardeike et al., 2009). SLN® consist of a solid lipid instead of a liquid lipid, which is commonly used in emulsion,

and possess the following advantages over other conventional systems used for topical administration: (1) improved chemical stability of the incorporated active, e.g. retinol (Jenning and Gohla, 2001); (2) high compatibility with human skin and enhanced penetration of the incorporated active (Souto and Müller, 2008); (3) increased drug loading capability (Ding et al., 2018); (4) easy to scale up preparation, and low toxicity because of the avoidance of organic solvents (Pardeike et al., 2009); (5) an increase of the water content of human skin because of an occlusive effect of SLN® (Wissing et al., 2001); (6) a high UV-blocking potential (Wissing and Müller, 2001).

Several studies on the α-tocopherol-loaded SLN® delivery systems have been published (de Carvalho et al., 2013; Dingler et al., 1999; Trombino et al., 2009), and have made positive contributions to pharmaceutical and cosmetic applications of α-tocopherol. However, only limited researches focus on improving the drug loading capability of α-tocopherol. Therefore, the aim of the current study was to produce α-tocopherol-loaded SLN® formulations for topical application with increased drug loading. Both carnauba wax and cetyl palmitate were used for forming lipid matrixes of SLN®. In addition, the characteristics of the produced SLN® suspensions were comprehensively investigated, including particle size and particle size distribution, zeta potential and thermal behavior.

6.3. Materials and methods

6.3.1. Materials

Cetyl palmitate was a gift from Dr. Rimpler GmbH (Wedemark, Germany). Tego Care 450 (polyglycerol methylglucose distearate) was provided by Evonik Nutrition & Care GmbH (Essen, Germany). DL-α-tocopherol was purchased from Alfa Aesar (Kandel, Germany). Carnauba wax was obtained from Kahl (Trittau, Germany). Ultra-purified water from Milli-Q apparatus (Millipore GmbH, Darmstadt, Germany) was used. All other reagents used in this study are analytical grade quality.

6.3.2. Production of lipid nanoparticle suspensions

The solid lipid nanoparticle suspensions were produced using cetyl palmitate or carnauba wax, with 1.8% Tego Care 450 as stabilizer and loaded with two different amounts of tocopherol (5% and 10%, w/w). The compositions of the lipid and water phase contained in the SLN® formulations are shown in Table 6.1. Solid lipid nanoparticles were produced using a hot-homogenization technique with a high-pressure homogenizer Micron Lab 40 (APV Homogeniser GmbH, Germany). Briefly, the lipids were melted at 95 °C (carnauba wax) or 85 °C (cetyl palmitate) and then α-tocopherol was added. The aqueous phase was added into the lipid phase and dispersed using an Ultra-Turrax (Janke & Kunkel GmbH, Germany) at 8000 rpm for 1 min. This mixture was homogenized at 95 °C (carnauba wax) or 85 °C (cetyl palmitate) and 500 bar, undergoing a total of three homogenization cycles. 6 mL of the suspension was collected after each cycle for further analysis. Following production, the produced hot lipid nanoparticle suspensions were cooled down to room temperature.

Table 6.1. An overview of the compositions of α-tocopherol-loaded SLN® suspensions, produced using carnauba wax or cetyl palmitate and stabilized by Tego Care 450. CW: carnauba wax; C: cetyl palmitate.

name	lipid phase (w/w)			water phase (w/w)	
	lipid		active	surfactant	water
	carnauba wax	cetyl palmitate	α-tocopherol	Tego Care 450	Milli Q
5% tocopherol-CW-SLN	15.0%	-	5.0%	1.8%	78.2%
10% tocopherol-CW-SLN	10.0%	-	10.0%		
5% tocopherol-C-SLN	-	15.0%	5.0%		
10% tocopherol-C-SLN	-	10.0%	10.0%		

6.3.3. Characterization of the lipid nanoparticles

6.3.3.1. Photon correlation spectroscopy (PCS)

The mean particle size (z-ave) of the lipid nanoparticles was measured by photon

correlation spectroscopy (PCS, Zetasizer Nano ZS, Malvern Instruments, UK). PCS also yields the polydispersity index (PDI), which describes the width of the particle size distribution. All samples were diluted with double distilled water (10 µL into 5 mL) at room temperature and each z-ave and PDI was calculated from 10 measurements.

6.3.3.2. Laser diffractometry (LD)

In order to detect larger particles or aggregates, laser diffractometry (LD, Mastersizer 2000, Malvern Instruments, UK) with a measuring range of 20 nm to 2,000 µm was employed. The following measurement parameters were used: 1.456 for real refractive index and 0.01 for imaginary refractive index. The dispersion medium was distilled water and the stirring speed was 1,750 rpm. Results are expressed as volume weighted diameters 10%, 50%, 90% and 95% (D10, D50, D90 and D95). The D95 value represents 95% of the particle diameters are equal to or lower than the given size. The same illusion was applied to the D10, D50 and D90. Each value is given as the average of five measurements.

6.3.3.3. Zeta potential (ZP)

Zeta potential is a measure of the electrostatic charge on the nanoparticles' surface. The zeta potential measurement was performed using a Zetasizer Nano ZS (Malvern Instruments, UK) in conductivity water (50 µS/cm, pH 5.5) or original medium (water phase of SLN suspension). The electrophoretic mobility was converted into the zeta potential by the Helmholtz–Smoluchowski equation. All samples were diluted (10 µL into 5 mL) at room temperature and the mean values were calculated from three measurements.

6.3.3.4. Differential scanning calorimetry (DSC) measurements

Differential scanning calorimetry (DSC, Mettler Toledo, Germany) was used to investigate the thermal behavior of the SLN® suspensions. The lipid nanoparticle suspension

(approximately 1-2 mg of lipid) was weighed into a standard aluminum pan (40 µL, Mettler Toledo, Switzerland) and sealed. The samples were measured under nitrogen, using an empty pan as reference. The samples were heated from 20 °C to 95 °C at a heating rate of 10 K/min. The recrystallization indices (RI) were calculated as follows (Freitas and Muller, 1999):

$$\text{RI } [\%] = \frac{\Delta H_{\text{SLN}}}{\Delta H_{\text{bulk material}} \times \text{concentration}_{\text{lipid phase}}} \times 100$$

where ΔH_{SLN} and $\Delta H_{\text{bulk material}}$ are the melting enthalpies (J/g) of the lipid nanoparticles and bulk material, respectively. The concentration of the lipid phase for lipid nanoparticles was 20% w/w.

6.3.3.5. Physical stability

To determine the physical short-term stability of SLN® suspensions, each sample was stored at room temperature for 7 days. The physical stability was by measuring the particle size in regular intervals during the storage period (Vivek et al., 2007). Particle size analysis, including mean particle size and size distribution, was conducted using PCS and LD on the day following production (= day 1) and on the 7th day after production (= day 7).

6.4. Results and discussion

6.4.1. Particle size characterization determined by PCS

Fig. 6.1A shows the particle diameters (z-ave) and polydispersity indices (PDI) of the produced SLN® suspensions as measured by PCS, one day after production. The particle size clearly decreases with an increasing number of homogenization cycles for each formulation. Furthermore, homogenization narrows the size distribution. This effect is already established in literature, and is caused by the shear forces during the homogenization process, which break the lipid particles to nano size (Müller et al., 2000). After three homogenization cycles, all lipid nanoparticle suspensions measured had a

mean particle size lower than 350 nm and a PDI less than 0.25. The impact of homogenization cycle on reducing the particle size was more pronounced for SLN® suspensions produced with carnauba wax. In addition, the star which marks the 5% tocopherol-C-SLN formulation with 3 cycles shows the particle size (280 nm) of the same formulation from literature (Dingler et al., 1999). The small difference proves the reproducibility of the formulation which is significant for further industrialization.

Fig. 6.1B shows the mean particle size and PDI on the 7th day after production. Compared to Fig. 6.1A the particle size or size distribution did not change significantly. The lipid nanoparticle suspensions produced with different numbers of homogenization cycles all remained in nano-range with narrow size distributions. Thus, all lipid nanoparticle suspensions were physically stable during short-time storage as evidenced by the PCS measurements.

A.
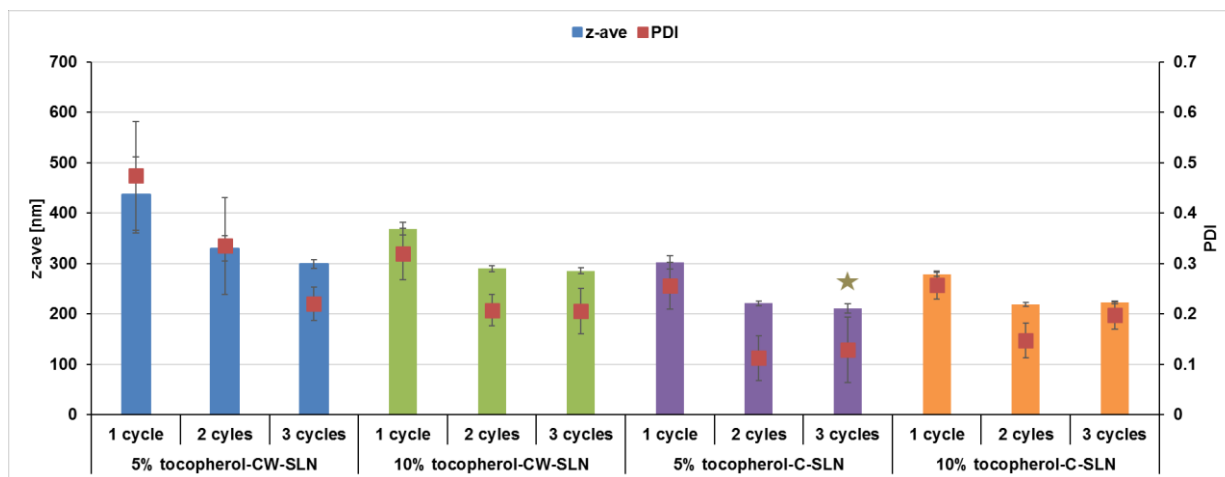
B.
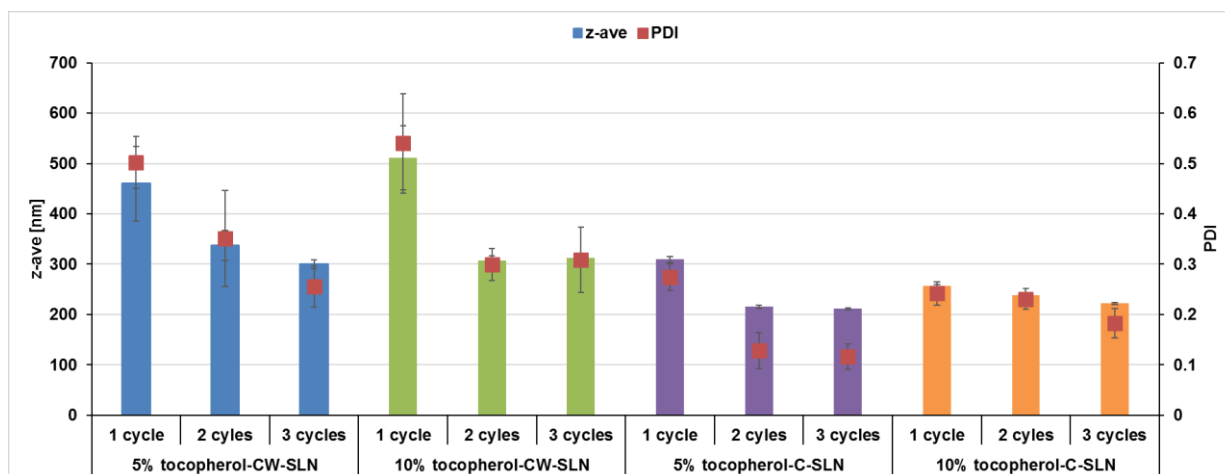
Fig. 6.1. Particle diameters (z-ave, bars) and polydispersity indices (PDI, dots) of α-tocopherol-loaded SLN suspensions measured on (A) day 1 and (B) day 7 after production.

The star in A represents the particle size of the same formulation from literature (Dingler et al., 1999).

6.4.2. Particle size characterization determined by LD

Fig. 6.2 shows the LD size of the SLN® suspensions on 1 and 7 days after production. In consistence with the PCS results shown in Fig. 6.2, increasing the number of homogenization cycles reduces the particle size, and yields a narrower size distribution.

Both 10% tocopherol-CW-SLN after 2 or 3 homogenization cycles as well as all tocopherol-C-SLN suspensions show nano-range particle sizes, with narrow size distributions one day after production. Although the z-ave values of 10% tocopherol-CW-SLN after 2 and 3 cycles were very similar, a wider size distribution was measured after 2 homogenization cycles. This phenomenon is mentioned in literature as well, and is explained as the "two-step diminution process" in the homogenization procedure. In the first step, most of the lipid particles reach their maximum dispersibility fast. In the second step, the effect on reducing the mean size of the particles is little, but the width of the size distribution can be reduced further. Thus, even though the mean sizes of the lipid nanoparticles after 2 and 3 cycles were similar, the additional homogenization cycle contributes to improve the homogeneity of the lipid nanoparticle suspension, which is in line with literature observations (Kovačević et al., 2014).

As seen in Fig. 6.2B, larger aggregates were detected in the 10% tocopherol-CW-SLN formulation with 2 homogenization cycles after 7 days of storage. On the contrary, the same suspension proved very stable after performing 3 homogenization cycles. 90% of the particles were less than 1 μm in diameter, and the D95 value – which is very sensitive to the presence of larger aggregates – shows no obvious change after 7 days of storage. Meanwhile, the SLN® suspensions produced with cetyl palmitate showed excellent physical stability after either 2 or 3 homogenization cycles. 95% of the particles in these two nanosuspensions were still smaller than 0.7 μm after 7 days of storage, indicating a good potential for topical application. It is important to note that although the storage timeframes investigated in this study are relatively short, in a final product the particles would be immobilized in a gel base shortly after production, further stabilizing them.

A.
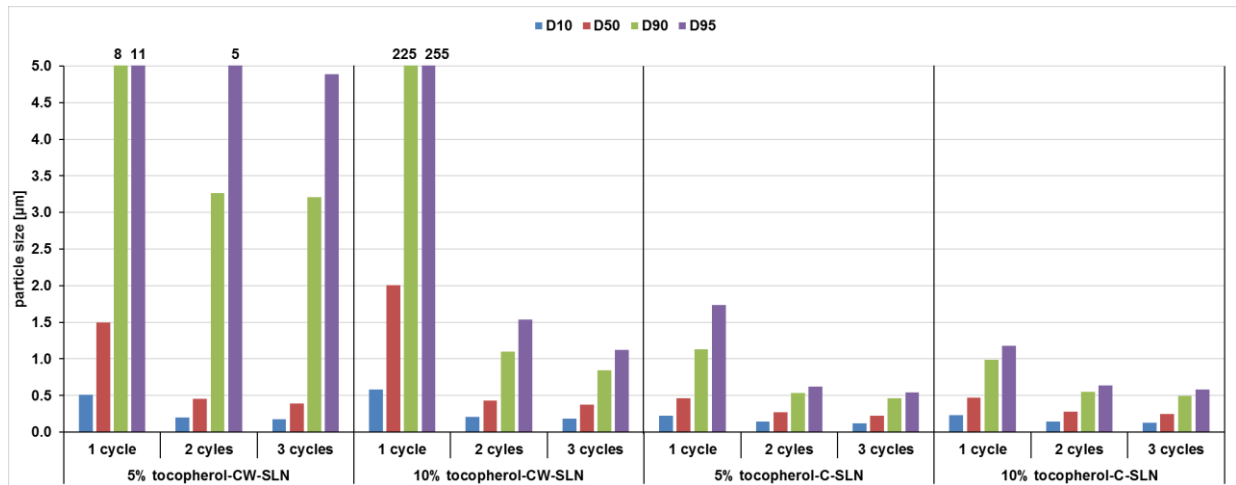
B.
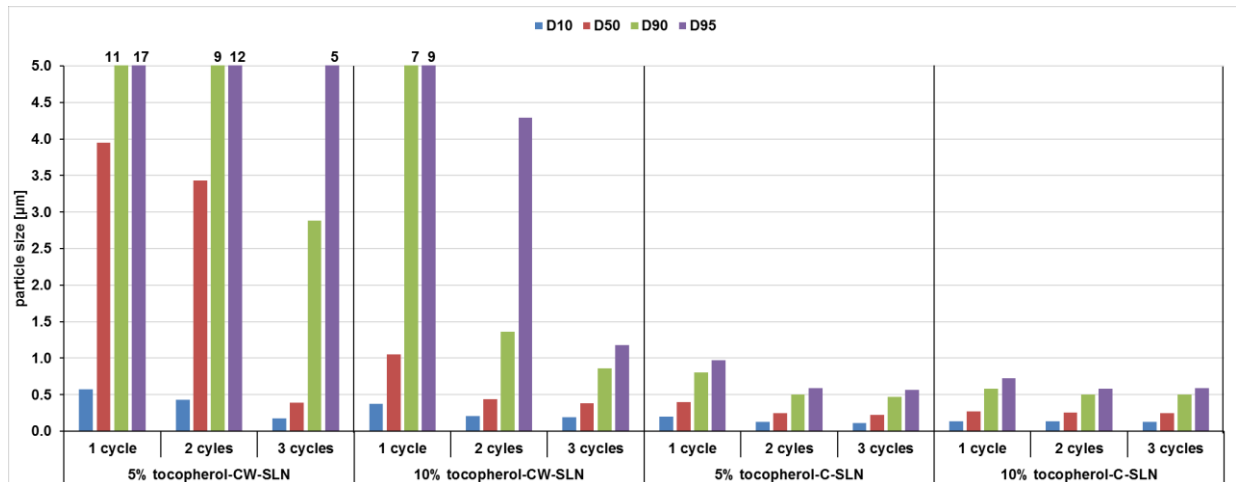
Fig. 6.2. Particle size distributions of α-tocopherol-loaded SLN® suspensions measured on (A) day 1 and (B) day 7 after production. D95 means that 95% of particles are equal to or lower than the given value. The same applies to D10, D50 and D90.

6.4.3. Particle charge (zeta potential)

The zeta potential (ZP) is commonly used for predicting the stability of nanoparticle suspensions (Souto et al., 2004). The ZP of the SLN® suspensions was measured in both conductivity water (50 µS/cm) as well as in the original medium (1.8% Tego Care 450). The ZP determined in conductivity water represents the Stern potential, a value depicting the surface charge of the particles (Nernst potential). The ZP measured in the original

medium is a measure for the thickness of the diffuse layer. The higher the both ZP values are, the higher the stability of the suspension is expected to be. The reason for this is that particles with a higher surface charge have a stronger electrostatic repulsion between them. ZP values measured in original medium higher than |30 mV| indicate good physical stability (Müller et al., 1996). Fig. 6.3 shows the ZP values of the α-tocopherol-loaded SLN® suspensions. All the particles were highly negatively charged. Zeta potential values measured in original medium were higher than |40 mV|. However, the LD measurements (Fig. 6.2) show a certain degree of aggregation for 5% tocopherol-CW-SLN despite of the high ZP values measured. Nonetheless, the 10% tocopherol-CW-SLN formulation with 3 homogenization cycles as well as all cetyl palmitate SLN® suspensions have both narrow size distributions and high ZP values. This shows that for most formulations, the ZP values accurately predict the physical stability.
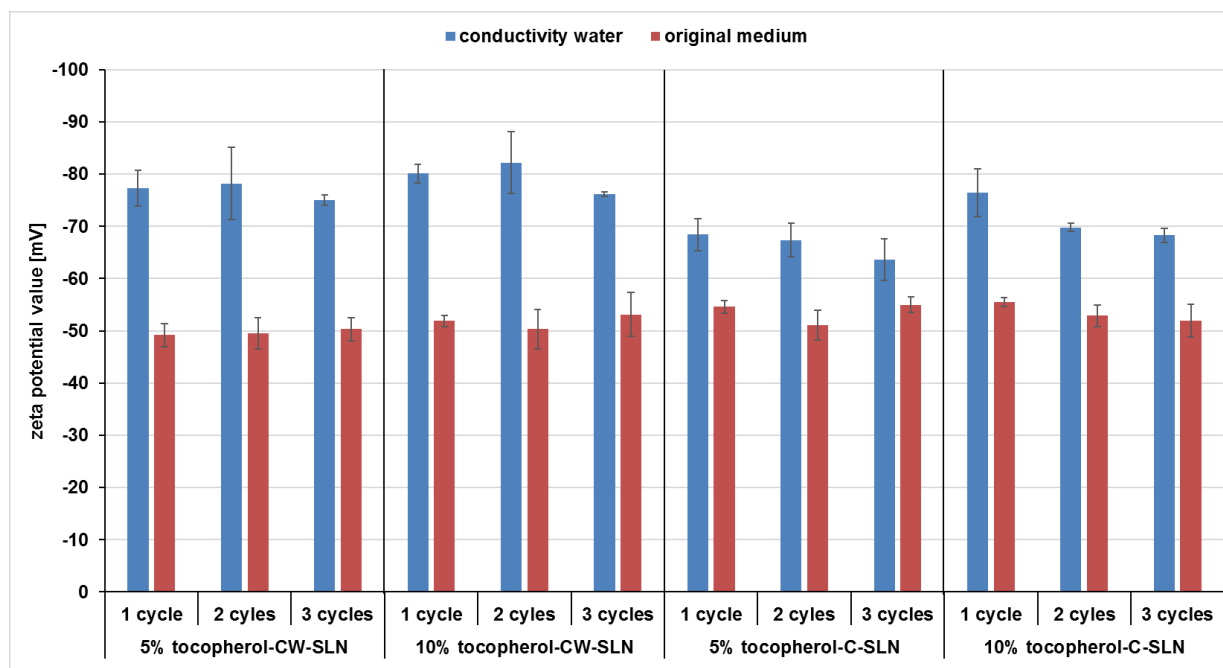
Fig. 6.3. Zeta potential (ZP) of α-tocopherol-loaded SLN suspensions measured in conductivity water and original medium on the following day after production.

6.4.4. Differential scanning calorimetry (DSC)

The thermal behavior of the produced SLN® suspensions and the bulk materials were analyzed by DSC (Fig. 6.4 and Table 6.2). Fig. 6.4 shows the melting curves of the lipid nanoparticle suspensions, and of the bulk materials from 20 °C to 95 °C at a heating rate of 10 K/min. Table 6.2 lists the corresponding DSC parameters as well as the calculated recrystallization index (RI). The SLN® suspensions produced with same lipid and same amount of drug loading show no obvious difference in melting curves. The melting peaks of SLN® produced with 10% α-tocopherol shift to lower temperature compared to 5% α-tocopherol. The same melting point depression also occurred in enthalpy values and RIs, indicating a less ordered structure. The reason for this is that an increasing amount of liquid α-tocopherol more strongly disrupts the ordered crystal lattice (Jenning et al., 2000; Kovacevic et al., 2011). The onset of melting temperature of all SLN® suspensions occurs above the human skin temperature (32 °C), indicating a potential for dermal application in the solid particle state.

10% α-tocopherol-loaded SLN® produced with cetyl palmitate show only very weak melting peaks (Fig. 6.4B), and the corresponding RIs are about 5%. This indicated that loading 10% of α-tocopherol is not suitable for cetyl palmitate SLN®. Thus, 10% tocopherol-CW-SLN with 3 homogenization cycles, loaded with 10% α-tocopherol is the most potential formulation for practical application, and showed perfect stability over the 7 days storage timeframe.

A.
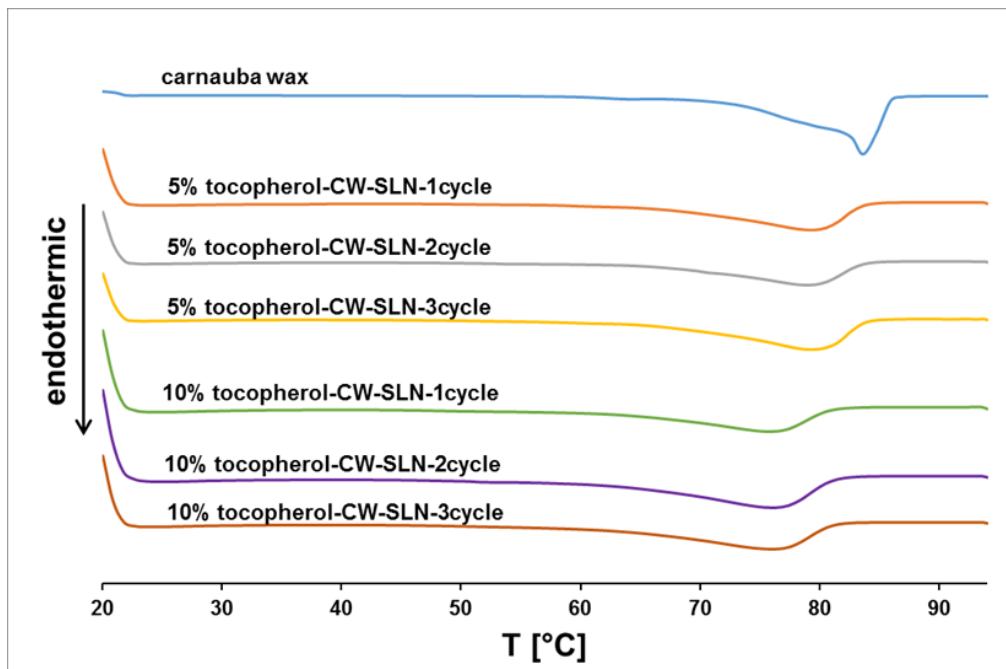
B.
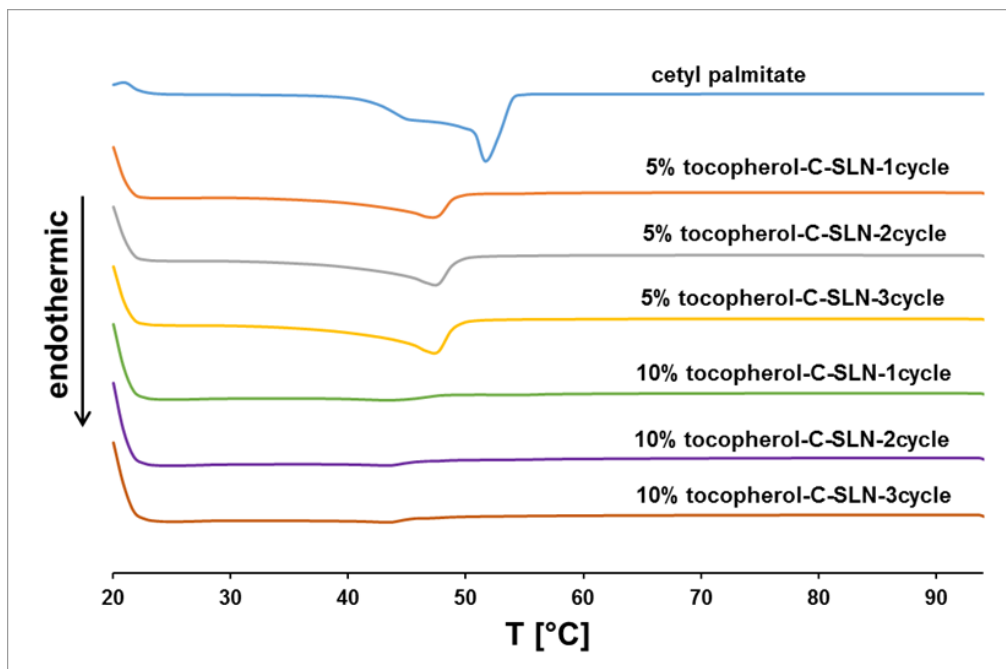
Fig. 6.4. Differential scanning calorimetry (DSC) thermograms (20-95 °C) of the pure lipids (carnauba wax (A) and cetyl palmitate(B)) and SLN® loaded with 5 and 10% α-tocopherol, following 1, 2, and 3 homogenization cycles. All samples were measured at a heating rate of 10 K/min.

Table 6.2. Melting peaks, enthalpy and recrystallization indices (RI) of the SLN® suspensions as well as the lipids (carnauba wax and cetyl palmitate) measured by DSC.

item	cycle	onset [°C]	peak 1 [°C]	peak 2 [°C]	enthalpy [J/g]	RI [%]
carnauba wax	-	81.07	83.97		-202.30	100
5% tocopherol-CW-SLN	1	67.14	79.43		-164.13	81.1
	2	67.03	78.96		-164.43	81.3
	3	69.02	79.45		-167.27	82.7
10% tocopherol-CW-SLN	1	63.11	76.01		-158.88	78.5
	2	63.89	76.27		-159.33	78.8
	3	64.06	76.37		-161.80	80.0
cetyl palmitate	-	42.19	45.04	51.97	-201.32	100
5% tocopherol-C-SLN	1	41.55	47.19		-106.84	53.1
	2	42.74	47.33		-106.87	53.1
	3	43.17	47.12		-107.08	53.2
10% tocopherol-C-SLN	1	39.34	43.70		-10.81	5.4
	2	38.06	43.51		-10.31	5.1
	3	38.43	43.52		-10.25	5.1

6.5. Conclusions

Solid lipid nanoparticles loaded with the antioxidant α-tocopherol were successfully prepared. The lipid nanoparticle suspensions could be increased to 10% α-tocopherol, and the formulations showed excellent short-term stability even at these high drug loadings. The nanoparticle diameters remained in the nano-range with narrow distributions, not changing significantly from 1 day till 7 days after production. It is important to note that although the stability timeframe measured is relatively short, the shelf life is more than enough considering such lipid nanoparticles would be rapidly incorporated into a semisolid base such as hydrogels or creams. The melting curves determined by DSC showed the lipid nanoparticles will remain solid during dermal application.

In addition, lipid nanoparticles are already on current market for dermal delivery owing to the ease of upscaling as well as lack of organic solvents required for production. Therefore, after further optimization on the selection of dermal bases, the α-tocopherol

loaded SLN® suspension shows a strong potential for pharmaceutical and cosmetic applications.

6.6. References

Alqahtani, S., Simon, L., Astete, C.E., Alayoubi, A., Sylvester, P.W., Nazzal, S., Shen, Y., Xu, Z., Kaddoumi, A., Sabliov, C.M., 2015. Cellular uptake, antioxidant and antiproliferative activity of entrapped α-tocopherol and γ-tocotrienol in poly (lactic-co-glycolic) acid (PLGA) and chitosan covered PLGA nanoparticles (PLGA-Chi). J Colloid Interf Sci 445, 243-251.

Brantley, P., Elmadfa, I., Kafatos, A., Kelly, F., Manios, Y., Roxborough, H., 2000. 539 Schuch, W.; Sheehy, PJA; Wagner, KH Vitamin E. J. Sci. Food Agric 80, 913-938.

Brigelius-Flohe, R., Traber, M.G., 1999. Vitamin E: function and metabolism. The FASEB Journal 13, 1145-1155.

de Carvalho, S.M., Noronha, C.M., Floriani, C.L., Lino, R.C., Rocha, G., Bellettini, I.C., Ogliari, P.J., Barreto, P.L.M., 2013. Optimization of α-tocopherol loaded solid lipid nanoparticles by central composite design. Industrial Crops and Products 49, 278-285.

Ding, Y., Nielsen, K.A., Nielsen, B.P., Bøje, N.W., Müller, R.H., Pyo, S.M., 2018. Lipid-drug-conjugate (LDC) solid lipid nanoparticles (SLN) for the delivery of nicotine to the oral cavity–optimization of nicotine loading efficiency. European Journal of Pharmaceutics and Biopharmaceutics.

Dingler, A., Blum, R., Niehus, H., Muller, R., Gohla, S., 1999. Solid lipid nanoparticles (SLNTM/LipopearlsTM) a pharmaceutical and cosmetic carrier for the application of vitamin E in dermal products. Journal of microencapsulation 16, 751-767.

Fisher, G.J., Kang, S., Varani, J., Bata-Csorgo, Z., Wan, Y., Datta, S., Voorhees, J.J., 2002. Mechanisms of photoaging and chronological skin aging. Archives of dermatology 138, 1462-1470.

Freitas, C., Muller, R.H., 1999. Correlation between long-term stability of solid lipid nanoparticles (SLN (TM)) and crystallinity of the lipid phase. European Journal of Pharmaceutics and Biopharmaceutics 47, 125-132.

Fuchs, J., 1998. Potentials and limitations of the natural antioxidants RRR-alpha-tocopherol, l-ascorbic acid and β-carotene in cutaneous photoprotection1. Free Radical Biology and Medicine 25, 848-873.

Gange, R.W., Blackett, A.D., Matzinger, E.A., Sutherland, B.M., Kochevar, I.E., 1985. Comparative protection efficiency of UVA-and UVB-induced tans against erythema and formation of endonuclease-sensitive sites in DNA by UVB in human skin. Journal of investigative dermatology 85, 362-364.

Jenning, V., Gohla, S.H., 2001. Encapsulation of retinoids in solid lipid nanoparticles (SLN). Journal of microencapsulation 18, 149-158.

Jenning, V., Thunemann, A.F., Gohla, S.H., 2000. Characterisation of a novel solid lipid nanoparticle carrier system based on binary mixtures of liquid and solid lipids. Int J Pharmaceut 199, 167-177.

Kovacevic, A., Savic, S., Vuleta, G., Muller, R.H., Keck, C.M., 2011. Polyhydroxy surfactants for the formulation of lipid nanoparticles (SLN and NLC): Effects on size, physical stability and particle matrix structure. Int J Pharmaceut 406, 163-172.

Kovačević, A.B., Müller, R.H., Savić, S.D., Vuleta, G.M., Keck, C.M., 2014. Solid lipid nanoparticles (SLN) stabilized with polyhydroxy surfactants: preparation, characterization and physical stability investigation. Colloids and Surfaces A: Physicochemical and Engineering Aspects 444, 15-25.

Lucks, J., Müller, R., 1991. Medication vehicles made of solid lipid particles (solid lipid nanospheres SLN). EP0000605497.

McVean, M., Liebler, D.C., 1997. Inhibition of UVB induced DNA photodamage in mouse epidermis by topically applied alpha-tocopherol. Carcinogenesis 18, 1617-1622.

Müller, R.H., Hildebrand, G., Nitzsche, R., Paulke, B.-R., 1996. Zetapotential und Partikelladung in der Laborpraxis. PAPERBACK APV 37.

Müller, R.H., MaÈder, K., Gohla, S., 2000. Solid lipid nanoparticles (SLN) for controlled drug delivery–a review of the state of the art. European journal of pharmaceutics and biopharmaceutics 50, 161-177.

Musalmah, M., Nizrana, M., Fairuz, A., NoorAini, A., Azian, A., Gapor, M., Ngah, W.W., 2005. Comparative effects of palm vitamin E and α-tocopherol on healing and wound tissue antioxidant enzyme levels in diabetic rats. Lipids 40, 575-580.

Pardeike, J., Hommoss, A., Müller, R.H., 2009. Lipid nanoparticles (SLN, NLC) in cosmetic and pharmaceutical dermal products. Int J Pharmaceut 366, 170-184.

Rittié, L., Fisher, G.J., 2002. UV-light-induced signal cascades and skin aging. Ageing Res Rev 1, 705-720.

Sahari, M.A., Moghimi, H.R., Hadian, Z., Barzegar, M., Mohammadi, A., 2017. Physicochemical properties and antioxidant activity of α-tocopherol loaded nanoliposome's containing DHA and EPA. Food Chem 215, 157-164.

Schmidt, K., 1993. Durch freie Radikale verursachte Krankheiten-Ätiologie und Prävention. Vitamin E in der modernen Medizin. Schriftenreihe der Nordrheinischen Akademie für ärztliche Fort-und Weiterbildung, MKM Verlagsgesellschaft Lenggries/Obb 8, 67-76.

Serbinova, E., Kagan, V., Han, D., Packer, L., 1991. Free radical recycling and intramembrane mobility in the antioxidant properties of alpha-tocopherol and alpha-tocotrienol. Free Radical Biology and Medicine 10, 263-275.

Sharif, H.R., Goff, H.D., Majeed, H., Liu, F., Nsor-Atindana, J., Haider, J., Liang, R., Zhong, F., 2017. Physicochemical stability of β-carotene and α-tocopherol enriched nanoemulsions: Influence of carrier oil, emulsifier and antioxidant. Colloids and Surfaces A: Physicochemical and Engineering Aspects 529, 550-559.

Souto, E., Müller, R., 2008. Cosmetic features and applications of lipid nanoparticles (SLN®, NLC®). International Journal of Cosmetic Science 30, 157-165.

Souto, E., Wissing, S., Barbosa, C., Müller, R., 2004. Evaluation of the physical stability of SLN and NLC before and after incorporation into hydrogel formulations. European journal of pharmaceutics and biopharmaceutics 58, 83-90.

Teixeira, M., Severino, P., Andreani, T., Boonme, P., Santini, A., Silva, A., Souto, E., 2017. d-α-tocopherol nanoemulsions: Size properties, rheological behavior, surface tension, osmolarity and cytotoxicity. Saudi Pharmaceutical Journal 25, 231-235.

Trombino, S., Cassano, R., Muzzalupo, R., Pingitore, A., Cione, E., Picci, N., 2009. Stearyl ferulate-based solid lipid nanoparticles for the encapsulation and stabilization of β-carotene and α-tocopherol. Colloids and Surfaces B: Biointerfaces 72, 181-187.

Vivek, K., Reddy, H., Murthy, R.S., 2007. Investigations of the effect of the lipid matrix on drug entrapment, in vitro release, and physical stability of olanzapine-loaded solid lipid

nanoparticles. AAPS PharmSciTech 8, 16-24.

Wissing, S., Lippacher, A., Müller, R., 2001. Investigations on the occlusive properties of solid lipid nanoparticles (SLN). Journal of cosmetic science 52, 313-324.

Wissing, S., Müller, R., 2001. A novel sunscreen system based on tocopherol acetate incorporated into solid lipid nanoparticles. International journal of cosmetic science 23, 233-243.

Zigoneanu, I.G., Astete, C.E., Sabliov, C.M., 2008. Nanoparticles with entrapped α-tocopherol: synthesis, characterization, and controlled release. Nanotechnology 19, 105606.

7. Summary

1. Lipid-drug-conjugate (LDC) solid lipid nanoparticles (SLN®) for the delivery of nicotine to the oral cavity – optimization of nicotine loading efficiency.

Nicotine lipid-drug-conjugates (LDC) were prepared by mixing nicotine with a fatty acid (Kolliwax® S or stearic acid). Hydrogenated sunflower oil (HSO) combined with the LDC were used as the lipid matrix in the LDC-containing SLN® system, whereas non-LDC SLN® were produced as a reference using HSO and pure nicotine. Both LDC-containing SLN® and non-LDC SLN® were successfully produced using a hot high-pressure homogenization method. Following production, photon correlation spectroscopy (PCS) confirmed all formulations were in the submicron size range (150 to 350 nm diameter) with narrow size distributions (PDI around 0.25). The laser diffractometry (LD) results showed 90% of the particles had a diameter lower than 1,000 nm. Light microscopy images show no aggregation of the particles, which is good agreement with the LD result. Differential scanning calorimetry (DSC) was used to investigate the thermal behavior of the system, and showed the thermal response of the four formulations was dominated by the HSO. The onset temperature of the melting process (> 39 °C) was higher than mouth temperature (37 °C), showing good applicability for buccal delivery. The nicotine-loaded particles could be successfully separated from the water phase using Amicon® Ultra-4 centrifugal filter devices, and the encapsulation efficiency of nicotine in LDC-containing SLN® was about 50% w/w. This is an almost fivefold increase compared to the conventional nicotine loaded SLN® (around 10% w/w). The high degree of encapsulation makes the LDC-containing SLN® a promising system for buccal delivery of nicotine with low side effects, and incorporating the SLN® into nicotine chewing gum or lozenges has the potential to be an innovative nicotine replacement therapy.

2. smartLipids® as third solid lipid nanoparticle generation – stabilization of retinol for dermal application.

Following a screening of several stabilizers, Tween® 20 proved most suitable for smartLipids® production. smartLipids® were successfully produced by a hot high-pressure homogenization method, and loaded with different amounts of retinol (5%, 15%, 20%

w/w). The mean diameter of smartLipids® formulations was about 200 nm, and remained unchanged during a storage period of two months as determined by PCS. DSC results showed an absence of polymorphic transitions, an indication of good physical stability. Furthermore, the onset temperatures of melting peaks were above 38 °C, ensuring the particles maintain their solid state during the skin penetration process (skin temperature is 32 °C). Results showed that after 60 days of storage, 37%, 59% and 75% w/w of retinol remained in the particle suspensions loaded with 5%, 15% and 20% retinol, respectively. Thus, the degradation of loaded retinol was reduced significantly by incorporating it into smartLipids® when compared to other studies. Since the loading capacity was superior to other studies as well, two major advantages characteristic for smartLipids® were combined. Dispersing the smartLipids® suspension into a gel base as a dermal formulation did not change the particle size, and the same chemical stability was observed as for the lipid nanoparticle suspension. Thus, the concept of smartLipids® worked efficiently for retinol, improving not only the encapsulation efficiency but also physical and chemical stability, as well as showing good performance in a gel base.

3. The influencing factors of producing stable smartLipids®: lipids, surfactants and production parameters.

Although smartLipids® provide a more universal delivery approach owing to the possibility of stabilizing a wide spectrum of different actives, the stability of the lipid nanoparticle suspensions strongly depends on a variety of influencing factors, and developing stable formulations is generally a resource- and time-intensive process. This study investigated in more detail the influences of the lipid compositions, the type and concentration of the surfactants and the production parameters on the stability. Most of the produced formulations instantly gelated after production, or showed macroscopic particle growth. The investigated lipid composition 2 and 4 - combinations of low melting range lipids - showed nano-ranged particle sizes, narrow particle size distributions and were stable for 180 days. The addition of a liquid lipid increased the stability in lipid composition 2, 3 and 4, due to the enhanced miscibility of the lipid matrix. Formulations stabilized by surfactants with a high hydrophilic-lipophilic balance (HLB) showed better physical

stability. On the contrary, increasing the concentration of surfactants did not successfully suppress aggregation when surfactants with a lower HLB value are used, likely owing to increased Ostwald ripening. Furthermore, the zeta potential value did not reliably predict the long-term stability of smartLipids®. Both stable lipid nanoparticle suspensions with low zeta potential were encountered as well as unstable formulations with a high zeta potential were encountered, showing that steric effects are important. Additionally, the most stable formulations were achieved by performing only 1 or 2 homogenization cycles.

4. Solid lipid nanoparticles (SLN®) for the delivery of α-tocopherol – an efficient method for improving the drug loading capability.

Solid lipid nanoparticle suspensions loaded with 5% and 10% α-tocopherol (w/w) were successfully developed. The mean particle sizes of these lipid nanoparticle suspensions remained in the nano-range following production, and their size distributions narrowed with an increasing number of homogenization cycles. After storing all suspensions at room temperature for 7 days, the SLN® suspensions produced with carnauba wax did not remain stable, except for the formulation produced with 10% α-tocopherol and 3 homogenization cycles. On the contrary, all SLN® suspensions produced with cetyl palmitate showed great physical stability. Zeta potential values of the produced lipid nanoparticle suspensions measured in original medium were higher than |40 mV|, and in conductivity water were higher than |60 mV|, a sign of potentially good physical stability. The thermal analysis of SLN® suspensions showed very weak peaks in 10% α-tocopherol-loaded SLN® produced with cetyl palmitate, indicative of an only slightly ordered matrix. Therefore, 10% α-tocopherol-loaded SLN® produced with carnauba wax and 3 homogenization cycles were recommended for further practical usage. Furthermore, the onset of the melting behavior of this SLN® suspension occurs above skin temperature, making it suitable for dermal application. Using carnauba wax and producing the formulation with 3 homogenization cycles, the loading of α-tocopherol could be increased to 10% w/w. Aside from increased drug loading, this formulation has a suitable particle size, narrow size distribution, good physical stability as well as a desirable thermal profile, making it highly promising for dermal application.

8. Zusammenfassung

1. Feste Lipid Nanopartikel (SLN) mit Lipid-Arzneistoff-Konjugat (LDC) für die Freisetzung von Nicotin in der Mundhöhle – Optimierung der Nicotin-Beladungseffizienz.

Nicotin-Lipid-Konjugate (LDC) wurden durch eine Mischung von Nicotin und einer Fettsäure (Kolliwax® S bzw. Stearinsäure) hergestellt. Hydriertes Sonnenblumenkernöl (HSO) und das LDC wurden als Matrix für die LDC-SLN®-System verwendet. Zusätzlich wurden LDC-freie SLN® unter Verwendung von HSO und reinem Nicotin als Referenz hergestellt. Sowohl die LDC-SLN® als auch die Referenz wurden erfolgreich mittels Hochdruckhomogenisation hergestellt. Alle produzierten Formulierungen wiesen eine mittels Photonen-Korelations-Spektroskopie (PCS) bestimmte mittele Teilchengröße zwischen 150 und 350 nm, sowie eine enge Partikelgrößenverteilung (PDI bei etwa 0,25) auf. Mittels Laserdiffraktometrie (LD) wurden nachgewiesen, dass 90% aller Partikel einen Durchmesser < 1000 nm aufwiesen. Die Abwesenheit von Aggregaten wurde mittels Lichtmikroskopie nachgewiesen. Darüber hinaus wurde das thermische Verhalten der LDC-SLN® mittels Dynamischer Differenzkalorimetrie (DSC) bestimmt, wobei sich zeigte, dass das Schmelzverhalten in erster Linie durch HSO bestimmt wird. Die Lipidmatrix begann erst bei 39 °C zu schmelzen, was über der üblichen Temperatur in der Mundhöhle (37 °C) liegt und die buccale Anwendbarkeit bestätigt. Die Nicotin beladenen Partikel wurden mit Hilfe eines Amicon® Ultra-4 Zentrifugenfilter von der wässrigen Phase abgetrennt, wodurch die Einschlusseffizienz des Wirkstoffs mit etwa 50% (w/w) bestimmt werden konnte. Dieser Wert übersteigt die Effizienz des konventionell mit Nicotin beladenen SLN® (etwa 10%) um das Fünffache. Diese hohe Einschlusseffizienz der LDC-beladenen SLN® ist vielversprechend für die Anwendung von Nicotin in der Mundhöhle und zeichnet sich wahrscheinlich durch weniger Nebenwirkungen aus. Werden die SLN® in Kaugummi oder Lutschpastillen eingearbeitet, haben sie das Potential, eine innovative Nicotin-Ersatz-Therapie darzustellen.

2. smartLipids® als dritte Generation der Lipidnanopartikel – Stabilisierung von Retinol zur dermalen Anwendung.

In einem Tensidscreening zeigte sich Tween® 20 als am besten geeignet für die

Herstellung der smartLipids®. smartLipids® wurden mittels Hochdruckhomogenisation hergestellt und mit verschiedenen Konzentrationen Retinol (5%, 15%, 20% w/w) beladen. Der mittlere Durchmesser der smartLipids®-Formulierung betrug etwa 200 nm (PCS) und zeigte auch nach zwei Monaten Lagerung keine Veränderung, Mittels DSC wurde nachgewiesen, dass keinerlei Polymorphie auftrat, was eine gute physikalische Stabilität der Formulierung beweist. Darüber hinaus wurde der Onset des Schmelzens oberhalb von 38 °C bestimmt, so dass die Partikel während der Penetration auf der Haut im festen Zustand verbleiben (die Temperatur der Haut beträgt 32 °C). Die Ergebnisse zeigen, dass nach 60 Tagen Lagerung 37%, 59% und 75% (w/w) des Retinols in den Partikelsuspensionen mit 5%, 15% bzw. 20% verblieben. Demnach konnte die chemische Zersetzung von Retinol durch smartLipids® im Vergleich zu anderen Studien erheblich verringert werden. Da auch die Retinol-Beladung anderen Studien überlegen ist, vereinigen smartLipids® zwei charakteristische Vorteile. Darüber hinaus kann die smartLipids®-Suspension in eine Gelformulierung eingearbeitet werden. Die Partikelgröße und chemische Stabilität der Lipid Nanopartikel Suspension wurden dadurch nicht beeinflusst. Demnach funktioniert das smartLipids®-Konzept sehr effektiv für Retinol, wodurch nicht nur die Einschlusseffizienz, die physikalische und chemische Stabilität werden konnten, auch die Einarbeitung in ein Gel funktioniert problemlos.

3. Einflussfaktoren auf die Stabilität von smartLipids®: Lipide, Tenside und Produktionsparameter.

Obwohl smartLipids® durch die Stabilisierung eines breiten Spektrums verschiedener Wirkstoffe einen universellen carrier darstellen, hängt die Stabilität der Lipid Nanopartikel Suspensionen von einer Vielzahl von Einflussfaktoren ab. Diese Studie untersuche detailliert den Einfluss der Lipidkomponenten, der Art und Konzentration des Tensids und der Produktionsparameter auf die Stabilität. Die Mehrzahl der getesteten Formulierungen bildete sofort nach der Produktion ein Gel aus oder zeigte bereits makroskopisch Partikelwachstum. Die Untersuchten Lipidmischungen 2 und 4 – Kombinationen von niedrig schmelzenden Lipiden – zeigten Partikelgrößen im Nanometer-Bereich, eine enge Partikelgrößenverteilung und waren für 180 Tage stabil. Das Beimischen eines flüssigen

Lipides verbesserte die Stabilität der Lipid-Zusammensetzungen 2, 3 und 4, was durch diene verbesserte Mischbarkeit der Einzelkomponenten in der Lipidmatrix erklärt werden kann. Formulierungen, die mit einem Tensid mit einem hohen HLB-Wert stabilisiert wurden, zeigten verbessere physikalische Stabilität. Im Gegensatz dazu konnte eine höhere Konzentration eines Tensids mit einem höheren HLB-Wert die Aggregation der Partikel nicht immer verhindern, wobei die Ostwald-Reifung eine Rolle spielt. Das Zeta-Potential konnte nicht zuverlässig die Langzeitstabilität der smartLipids® voraussagen. Sowohl stabile Lipid Nanopartikel Suspensionen mit niedrigem Zeta-Potential als auch instabile Formulierungen mit hohem Zeta-Potential wurden beobachtete, da die Stabilisierung in erster Linie durch sterische Effekte der Tenside zustande kommt. Darüber hinaus wurden die stabilsten Formulierungen nach lediglich 1-2 Homogenisier-Zyklen gefunden.

4. Feste Lipid Nanopartikel (SLN®) für die Freisetzung von α-Tocopherol – eine Effiziente Methode zur Steigerung der Wirkstoff-Beladung.

Feste Lipid Nanopartikel-Suspensionen mit 5% und 10% α-Tocopherol (w/w) wurden entwickelt. Die mittlere Partikelgröße dieser Suspensionen wurde im Nanometer-Bereich bestimmt, und die Partikelgrößenverteilung wurde mit steigender Anzahl an Homogenisierzyklen enger. Bei einer Lagerung bei Raumtemperatur über 7 Tage waren alle Karnaubawachs-haltigen SLN instabil. Die einzige Ausnahme stellte die Formulierung mit 10% α-Tocopherol nach 3 Homogenisierzyklen dar. Im Gegensatz dazu zeigten alle mit Cetylpalmitat produzierten Formulierungen ausgezeichnete physikalische Stabilität. Die Beträge der Zeta Potentiale aller Formulierungen waren größer als |40 mV| im Original-Medium und |60 mV| in Wasser. Daraus lässt sich eine gute physikalische Stabilität ableiten. Die thermografische Analyse zeigte sehr schwache Peaks der mit 10% α-Tocopherol beladenen SLN® mit Cetylpalmitat. Dies zeigt eine Matrix an, die einen geringen Ordnungsgrad aufweist. Aus diesem Grund wird empfohlen, die 10%-beladene Karnaubawachs Formulierung nach dem 3. Homogenisierzyklus zu verwenden. Der Schmelzpunkt dieser Formulierung liegt oberhalb der Hauttemperatur, wodurch sie problemlos dermal angewendet werden kann. Mithilfe von Karnaubawachs und 3

Homogenisierzyklen konnte die Beladungskapazität von α-Tocopherol auf 10% (w/w) gesteigert werden. Neben der hohen Beladung zeigt die Formulierung Partikel im Nanometer-Bereich, eine Partikelgrößenverteilung, gute physikalische Stabilität sowie das erforderliche Schmelzverhalten für eine dermale Anwendung.

Abbreviations

|	
API	active pharmaceutical ingredient
CMC	critical micelle concentrations
DSC	differential scanning calorimetry
FDA	US Food and Drug Administration
HLB	hydrophilic-lipophilic balance
HPC	hydroxypropyl cellulose
HPLC	high performance liquid chromatography
HPH	high pressure homogenization
LD	laser diffractometry
LDC	lipid-drug-conjugate
LM	light microscopy
NLC	nanostructured lipid carriers
PCS	photo correlation spectroscopy
PDI	polydispersity index
PEG	polyethylene glycol
RI	recrystallization indices
RT	room temperature
SLN	solid lipid nanoparticles
ZP	zeta potential

Appendix

Chapter 5. The influence of lipids, surfactants and homogenization cycles in physical stability of smartLipids®

A. Formulations stable for 120 days.

LM2/10-3.0%P (2 cycles)

LM2/20-1.5%T (2 cycles)
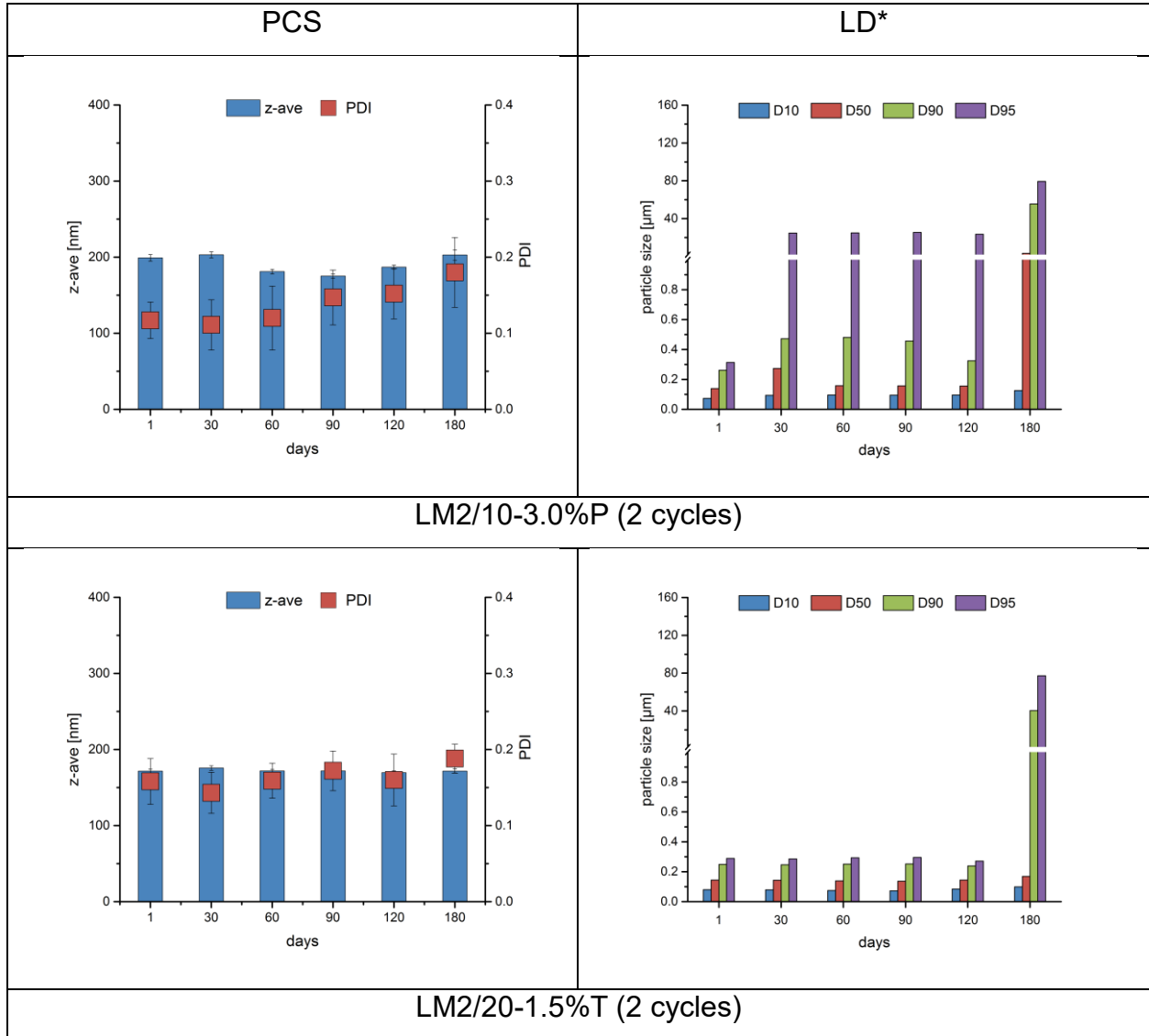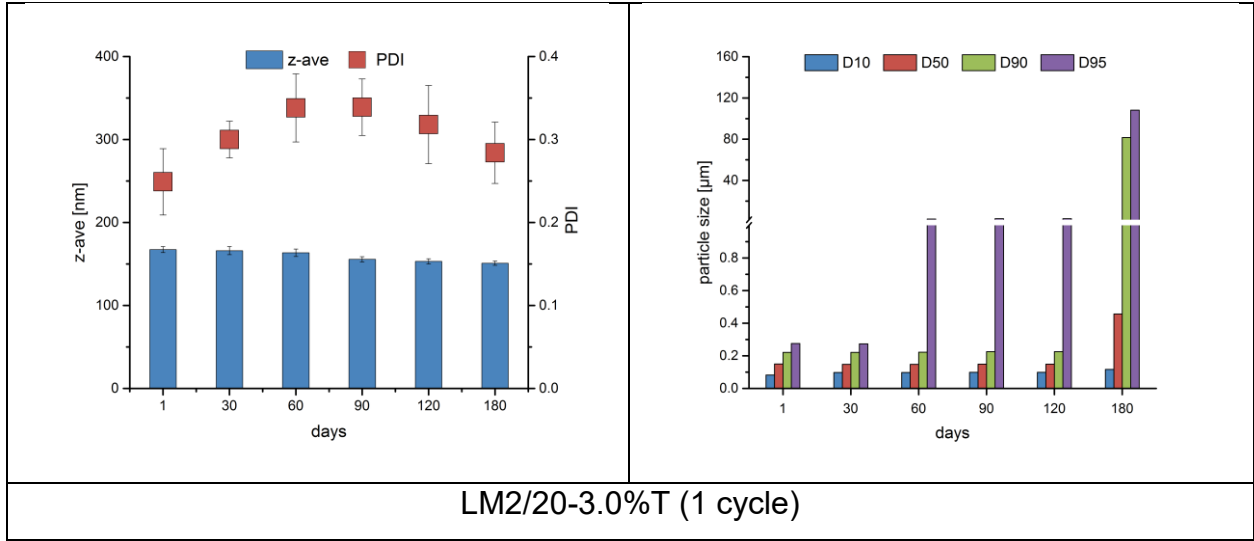
LM2/20-3.0%T (1 cycle)

B. Formulations stable for 90 days.

PCS	LD
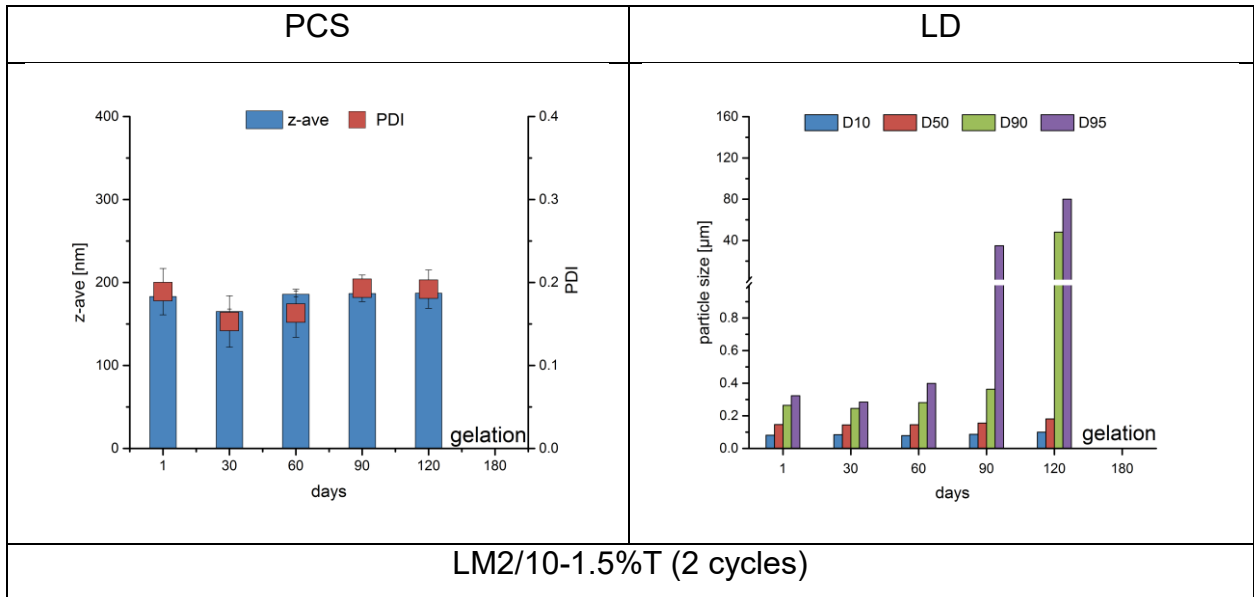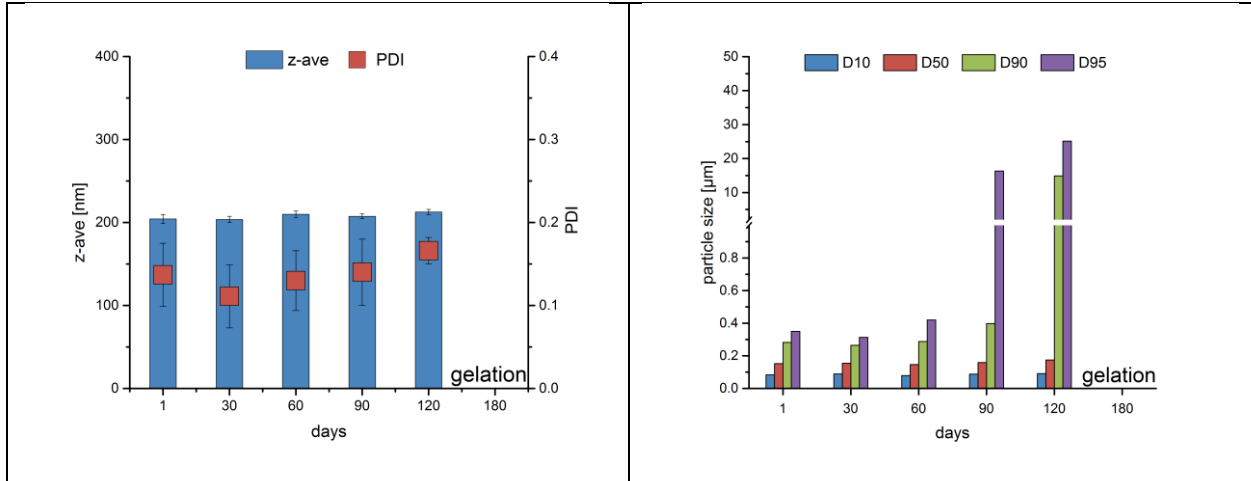
LM2/10-1.5%T (2 cycles)

LM2/10-3.0%P (1 cycle)
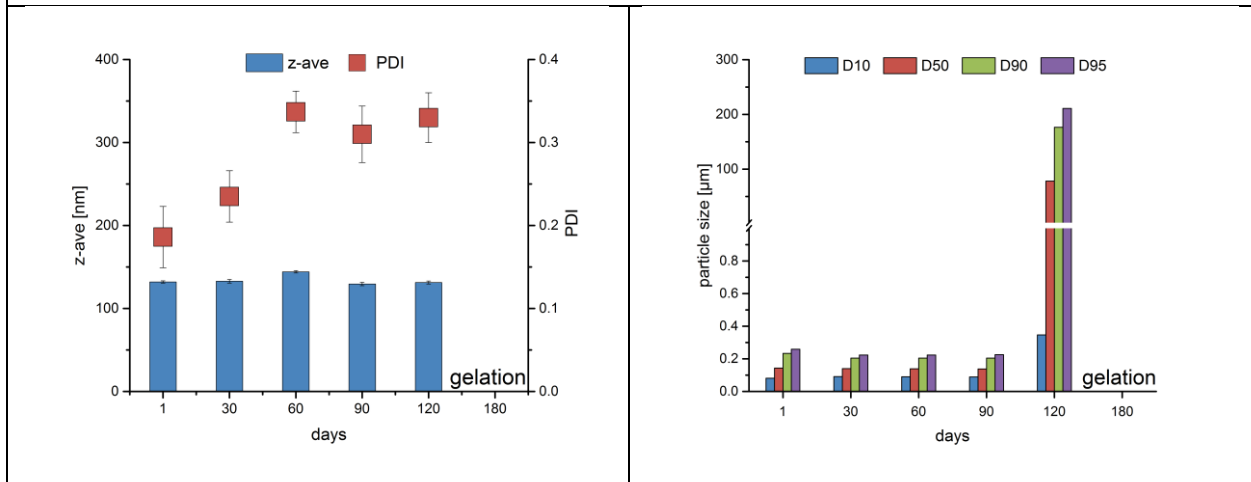
LM2/20-3.0%T (2 cycles)
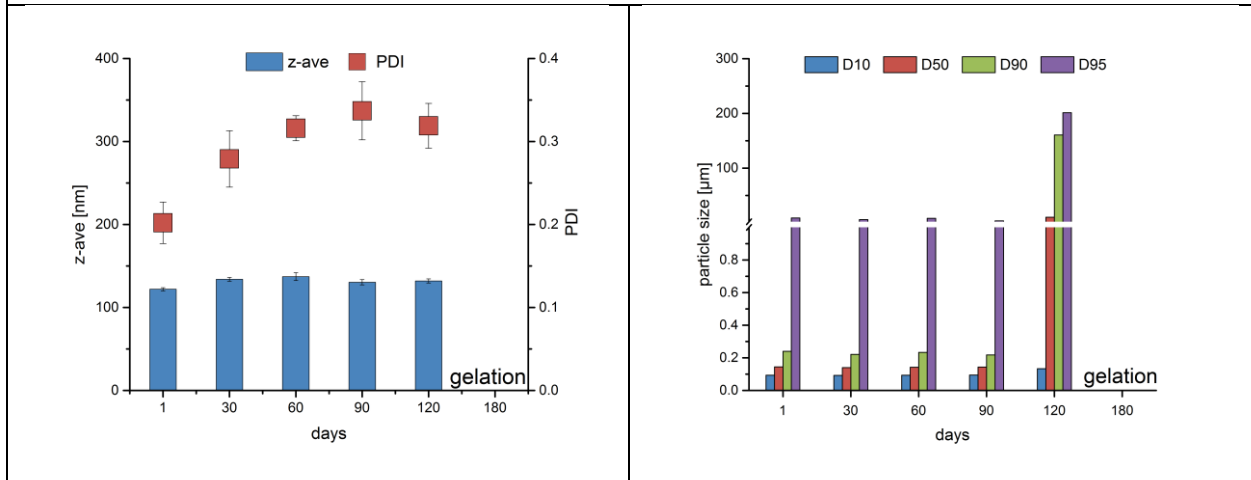
LM2/20-3.0%T (3 cycles)
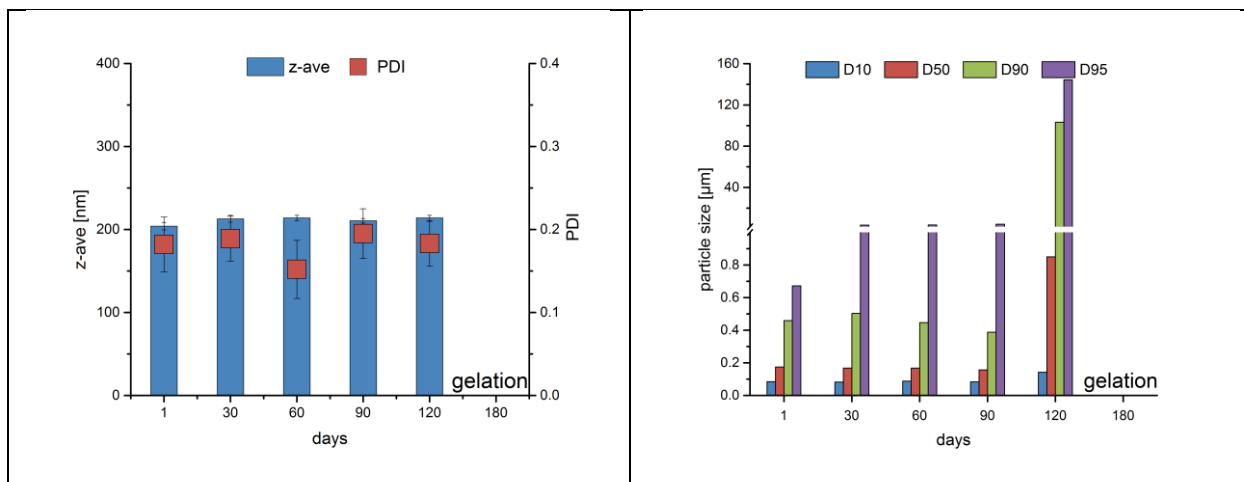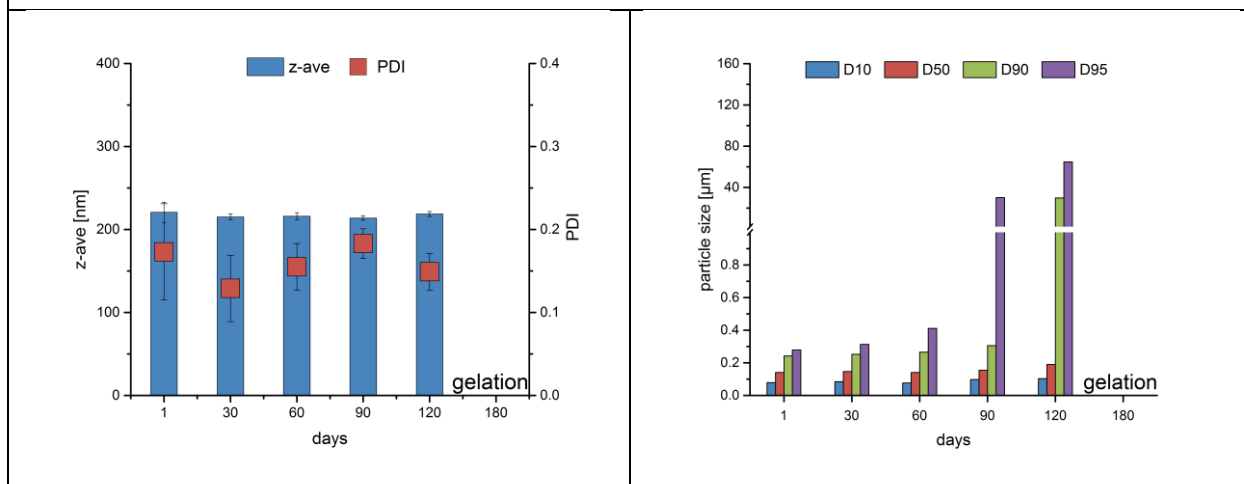
LM2/20-1.5%P (1 cycle)

LM4/20-1.5%T (2 cycles)

C. Formulations stable for 60 days.

LM2/10-1.5%P (1 cycle)

LM2/10-1.5%P (2 cycles)
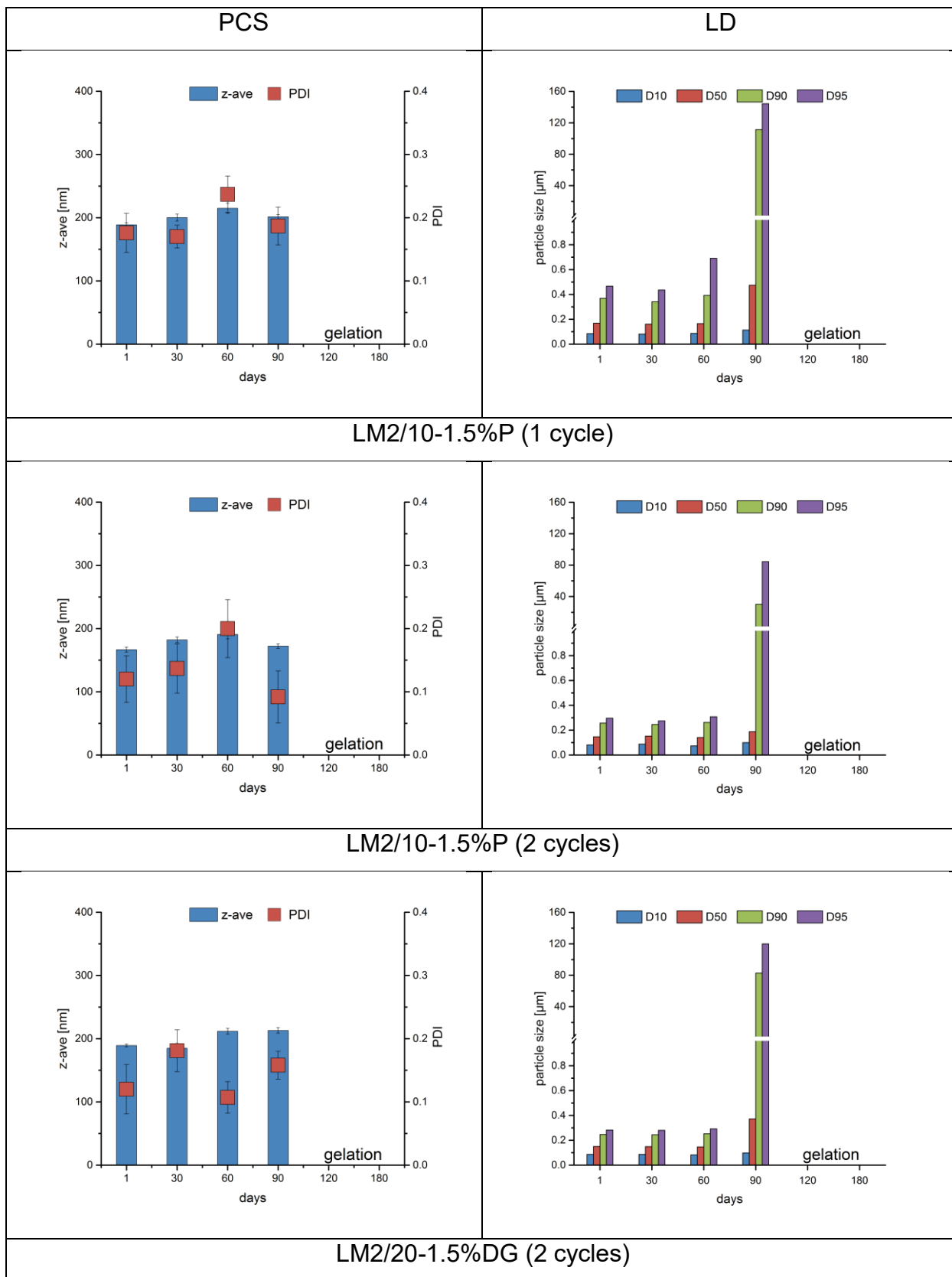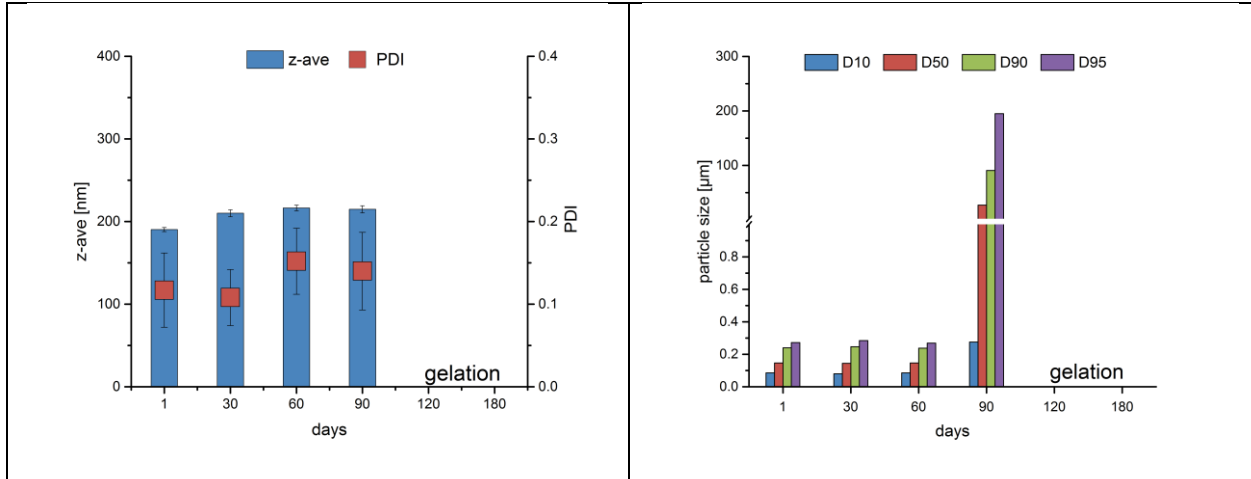
LM2/20-1.5%DG (2 cycles)
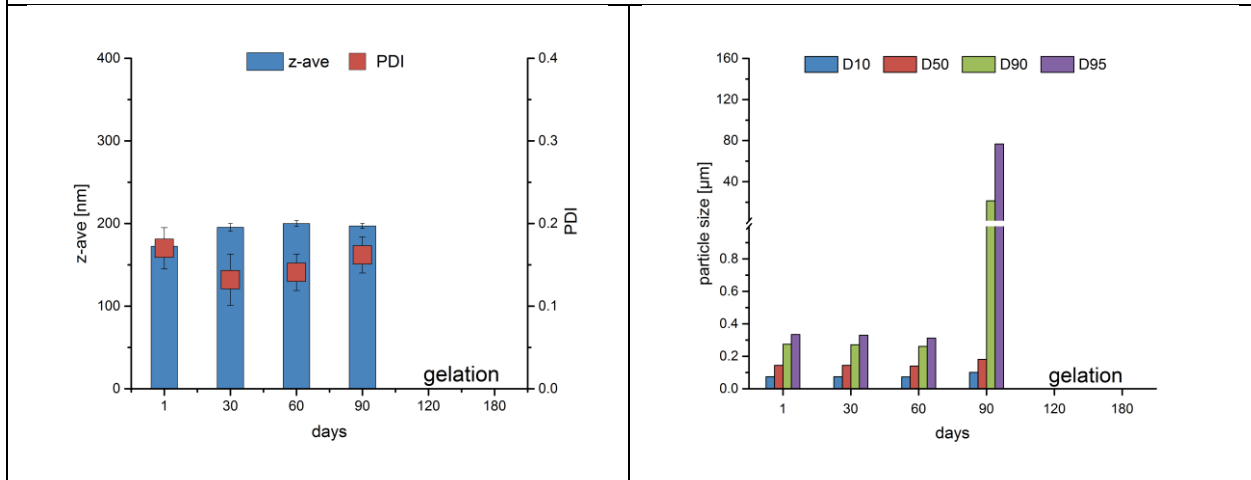
LM2/20-1.5%DG (3 cycles)

LM2/20-1.5%P (2 cycles)

LM2/20-1.5%P (3 cycles)

LM4/0-3.0%T (3 cycles)
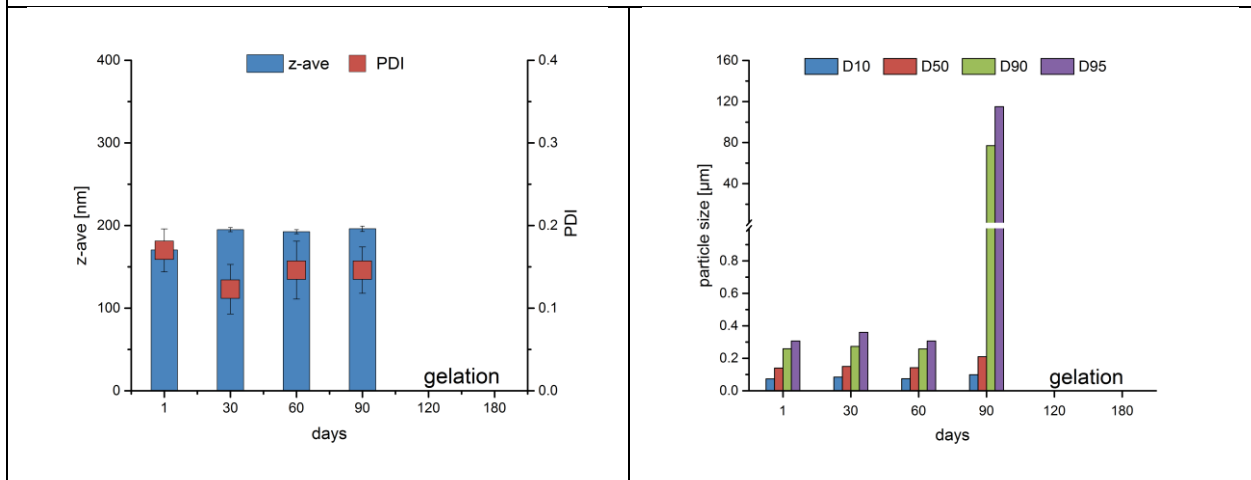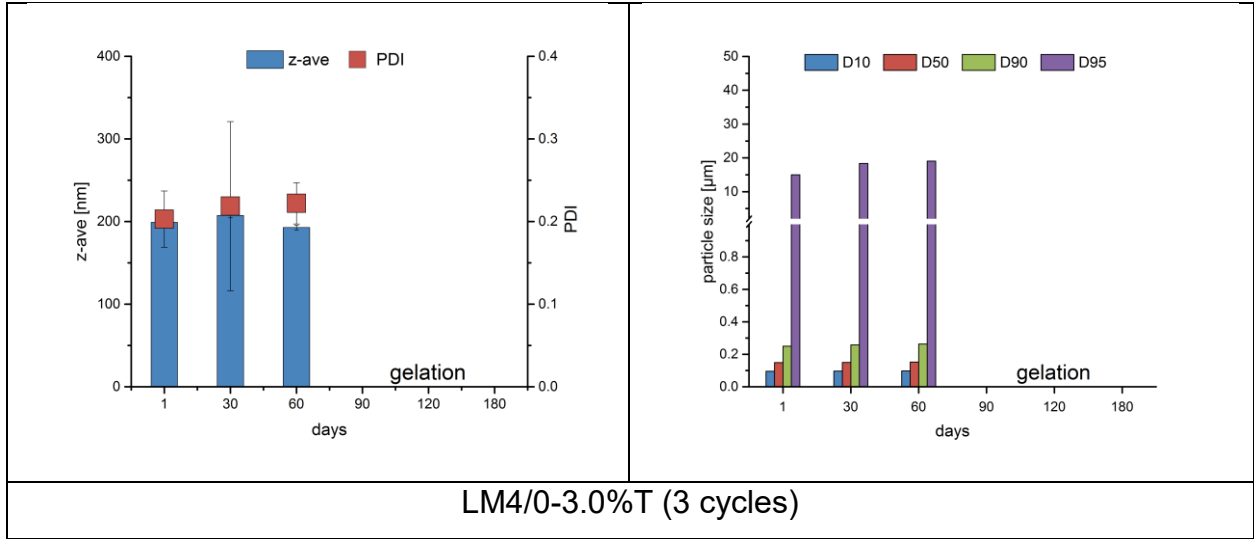
D. stable for 30 days
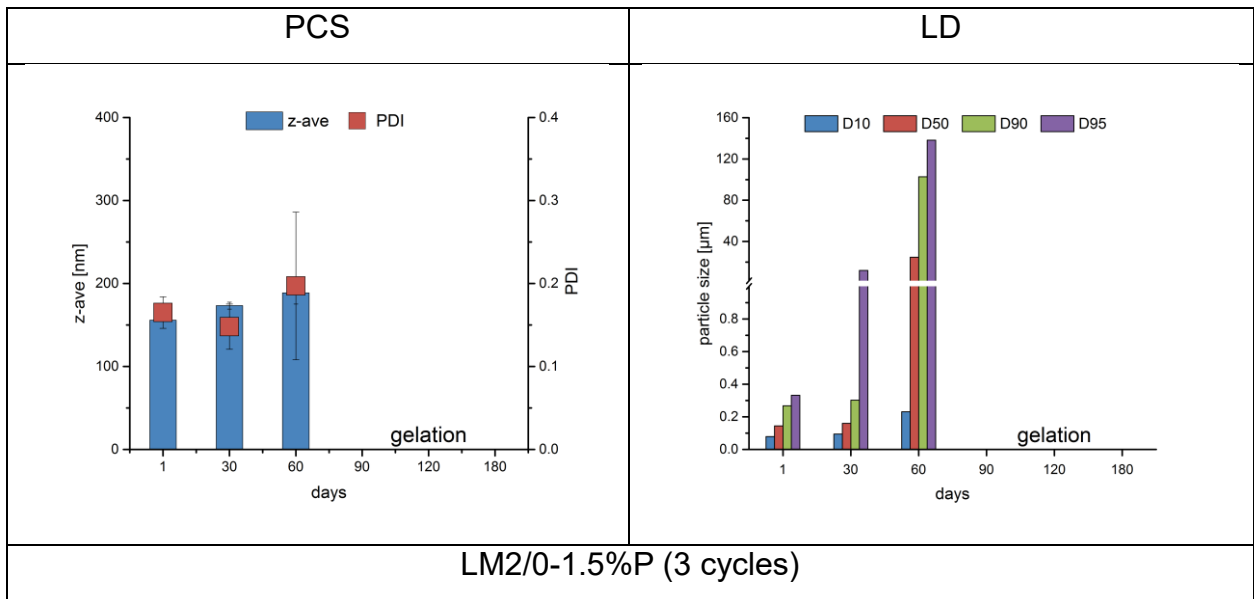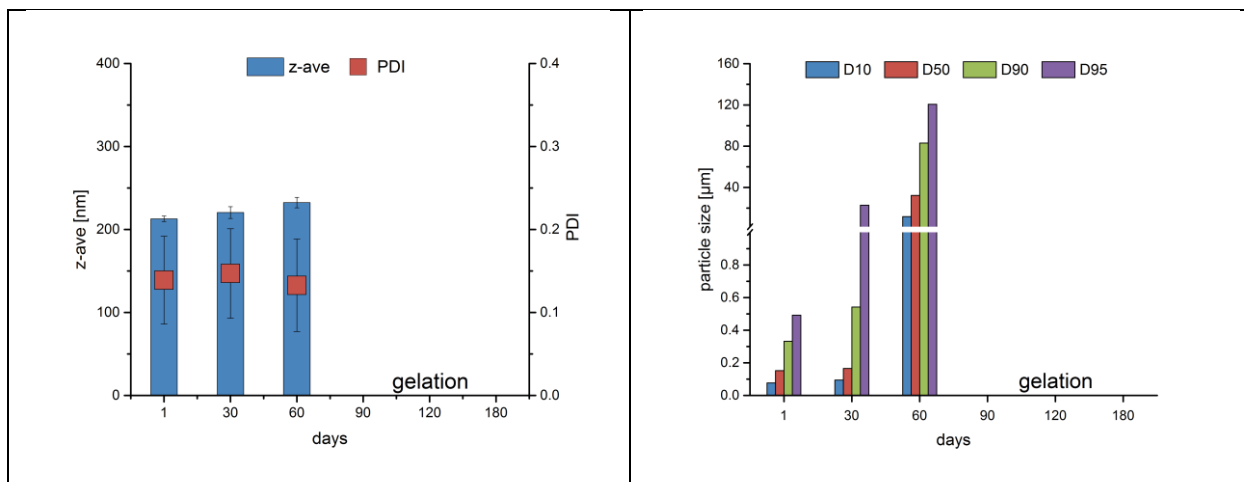
LM2/0-1.5%P (3 cycles)

LM2/10-1.5%DG (3 cycles)
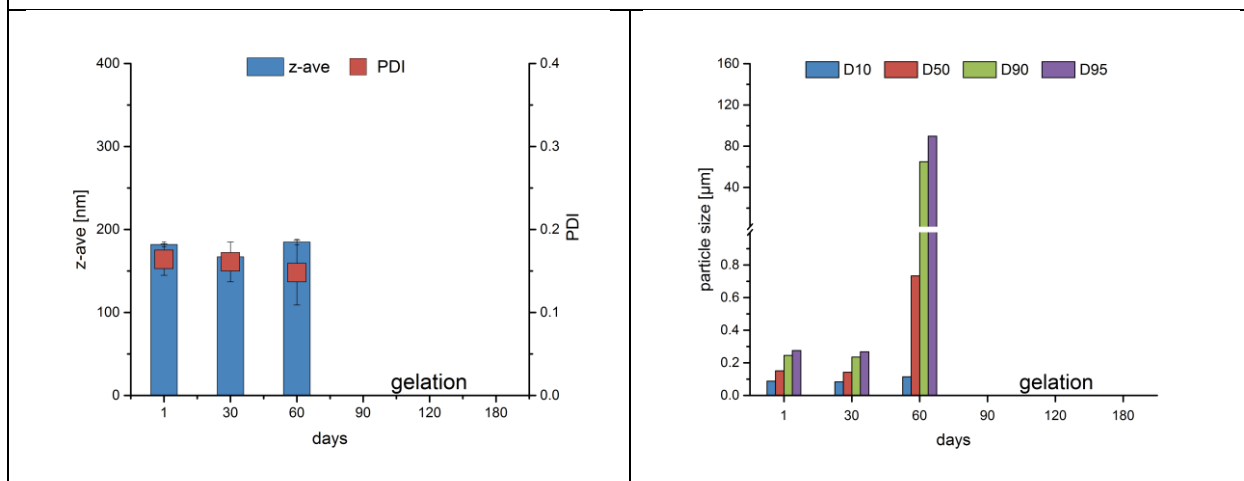
LM2/10-1.5%T (3 cycles)
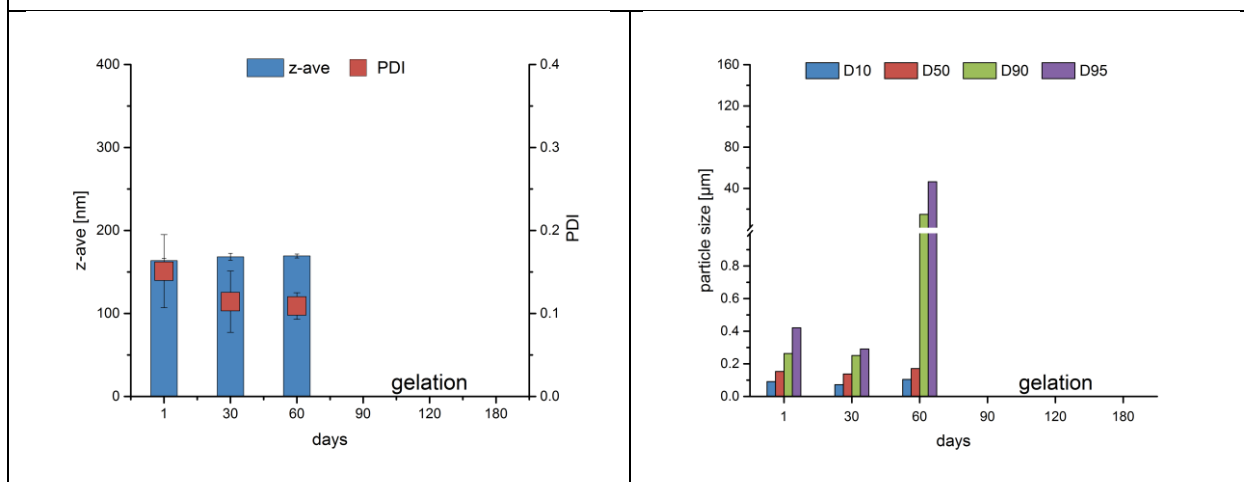
LM2/10-1.5%P (3 cycles)
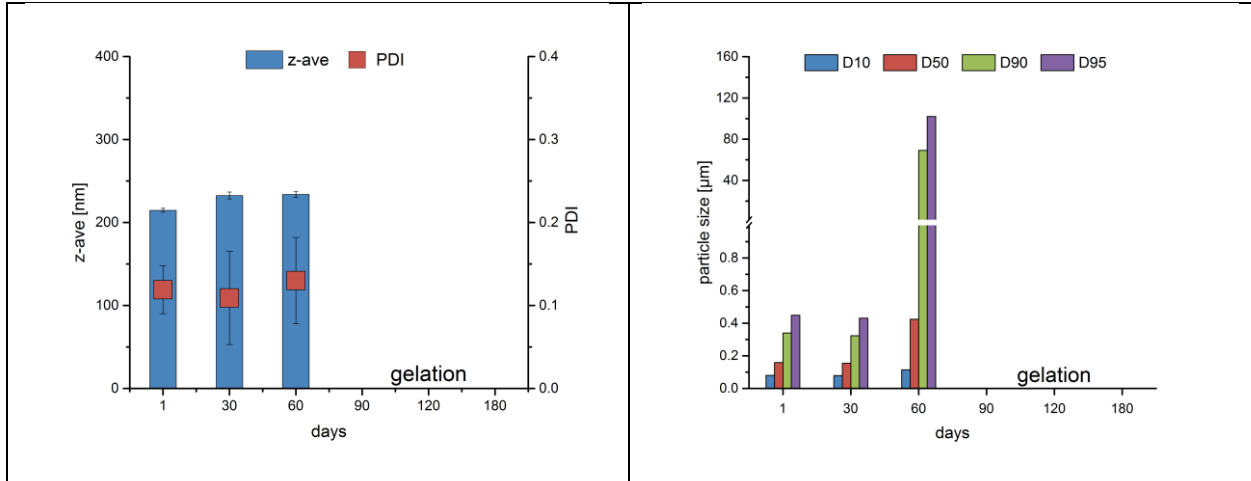
LM2/20-1.5%DG (1 cycle)
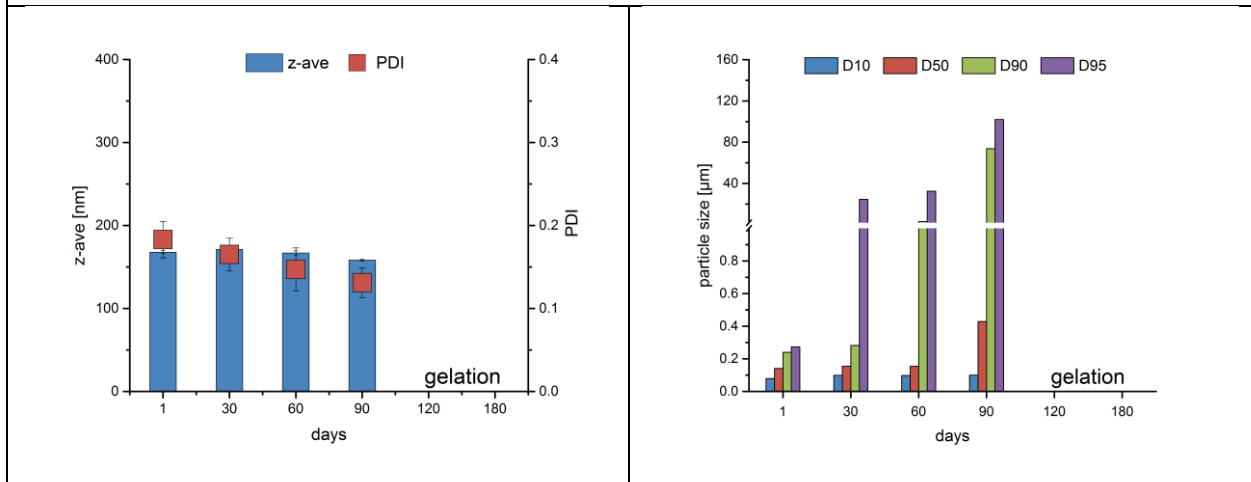
LM2/20-1.5%T (3 cycles)

LM3/10-3.0%T (1 cycle)

LM3/10-3.0%T (2 cycles)
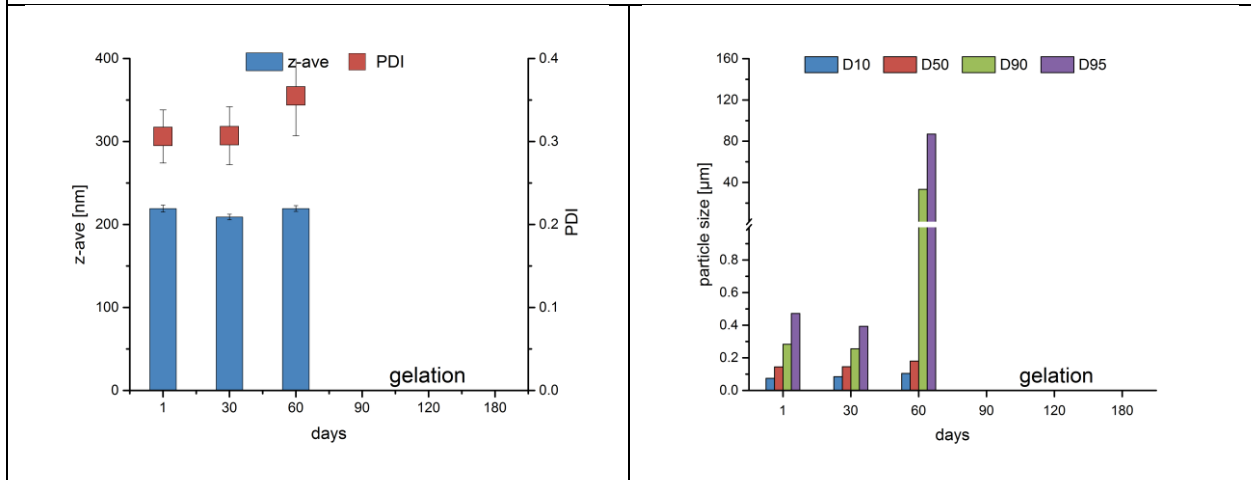
LM3/20-3.0%T (1 cycle)
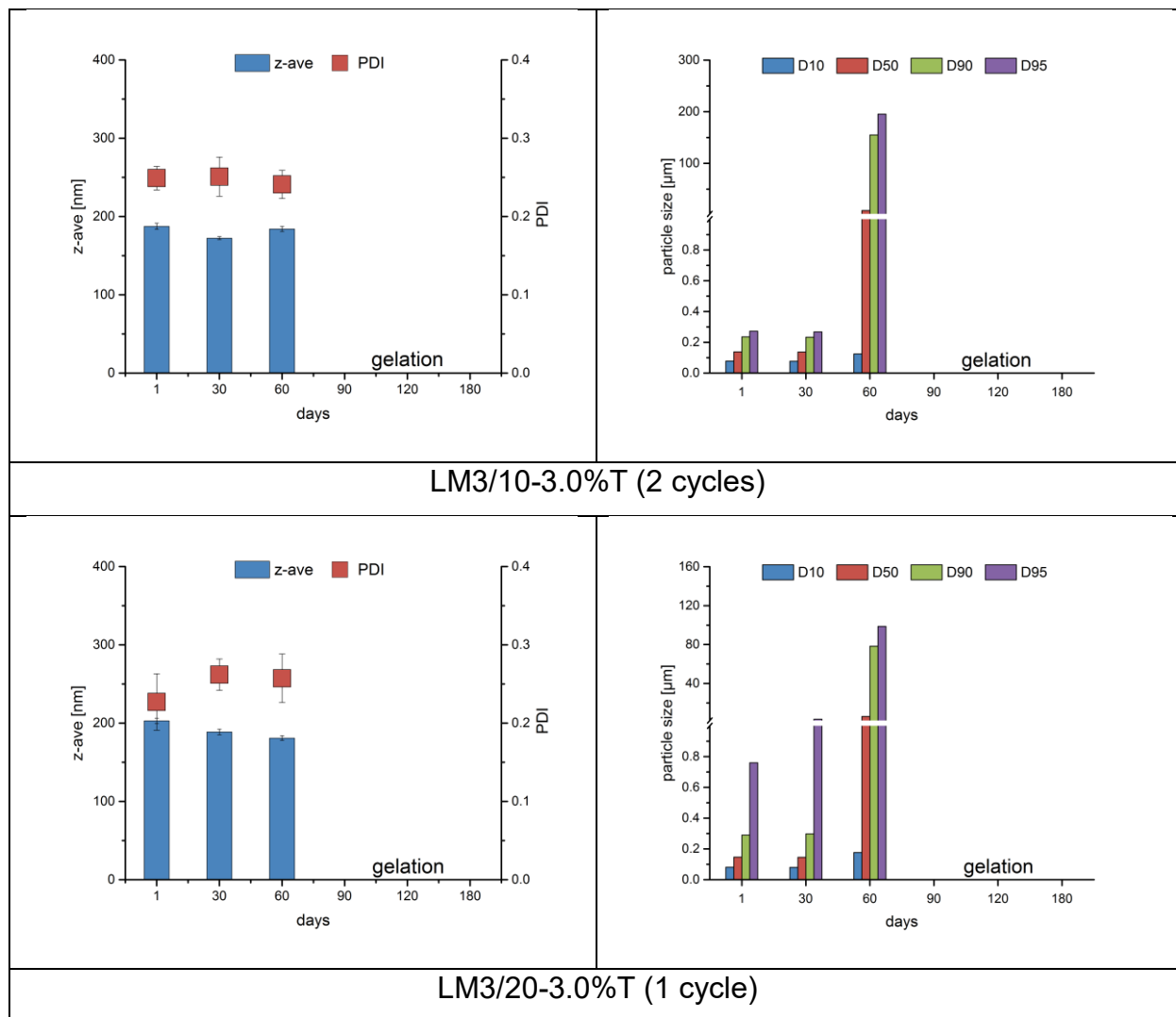
Fig. A1. The PCS data (z-ave and PDI) and LD data (D10, D50, D90 and D95) of the smartLipids® suspensions with different stability properties: A. stable for 120 days, B. stable for 90 days, C. stable for 60 days and D. stable for 30 days.

 DG: decyl glucoside; LG: lauryl glucoside; T: Tween® 80; P: Plantacare® 2000 UP

* the breaks in the y-axis are from 1 to 2 µm, and the scale changes above the break.

Chapter 5. The influence of lipids, surfactants and homogenization cycles in physical stability of smartLipids®

Table A1. Zeta potential (ZP) values of LM4/0 smartLipids® formulations measured in conductivity water (CW) and original medium (OM), correlated to respective storage stabilities.

pressure [bar]	homogenization cycle	zeta potential [mV]		storage stability [day]
		CW	OM	
300	1	-45.9	-17.8	90
	2	-43.2	-15.9	90
	3	-41.7	-15.0	90
	4	-41.9	-15.5	90
400	1	-45.0	-17.3	90
	2	-39.2	-13.9	90
	3	-37.9	-13.8	90
	4	-37.7	-12.8	90
500	1	-44.9	-16.9	< 30
	2	-39.6	-16.1	90
	3	-39.9	-13.1	90
	4	-40.8	-15.5	90
600	1	-42.1	-17.2	90
	2	-41.1	-13.6	90
	3	-38.4	-13.8	90
	4	-39.9	-16.8	< 30
700	1	-45.5	-17.9	< 30
	2	-40.5	-14.9	90
	3	-40.9	-15.0	90
	4	-40.5	-15.3	90

	1	-47.3	-17.1	< 30
800	2	-44.6	-14.8	90
	3	-42.9	-15.2	90
	4	-40.5	-15.0	90
	1	-44.4	-16.0	90
900	2	-43.8	-14.7	90
	3	-39.2	-15.7	< 30
	4	-41.9	-15.7	90
	1	-47.6	-19.3	< 30
1000	2	-44.0	-14.9	30
	3	-40.5	-14.7	< 30
	4	-41.7	-15.4	< 30

Chapter 5. The influence of lipids, surfactants and homogenization cycles in physical stability of smartLipids®
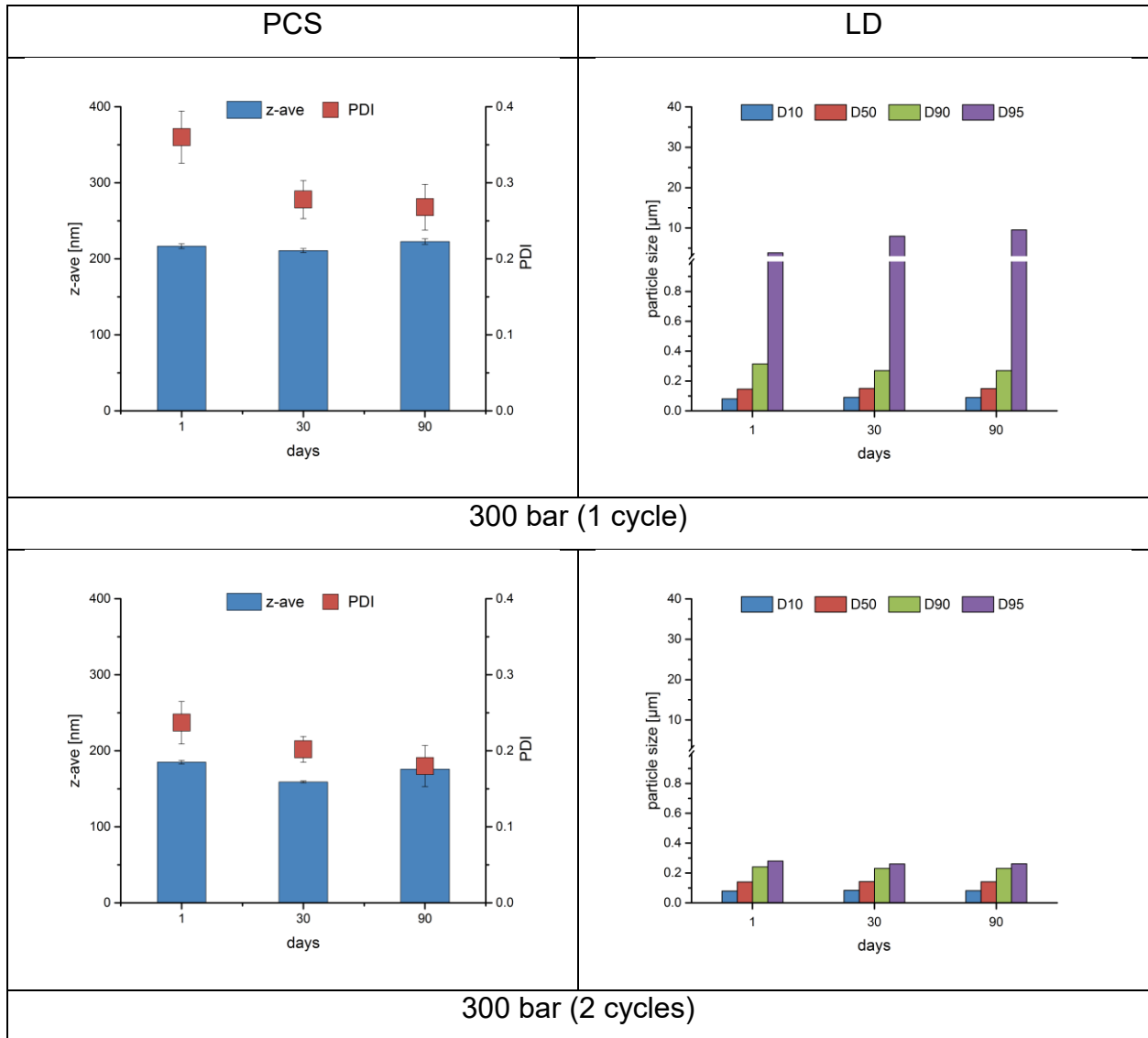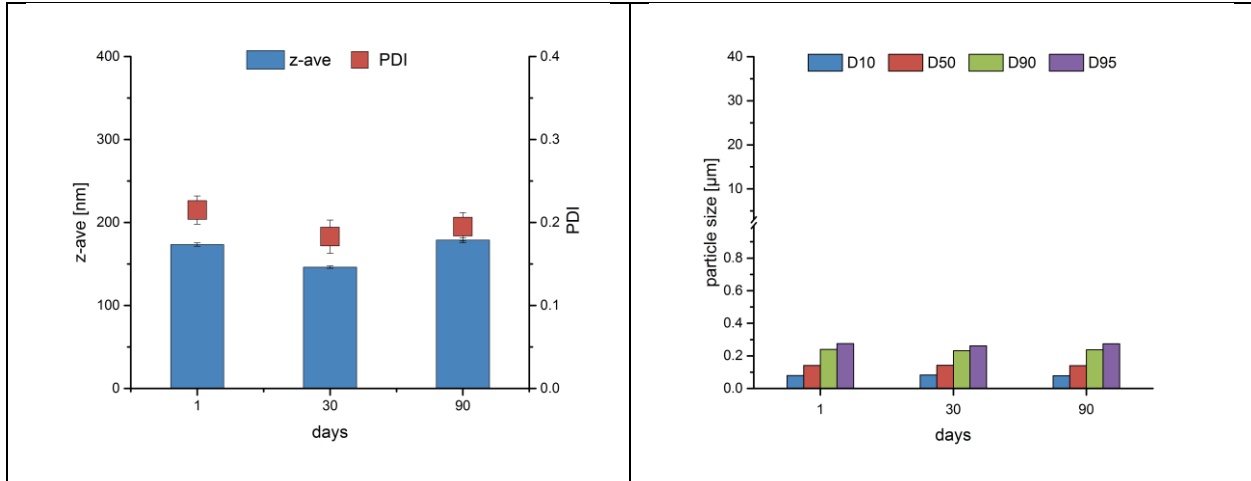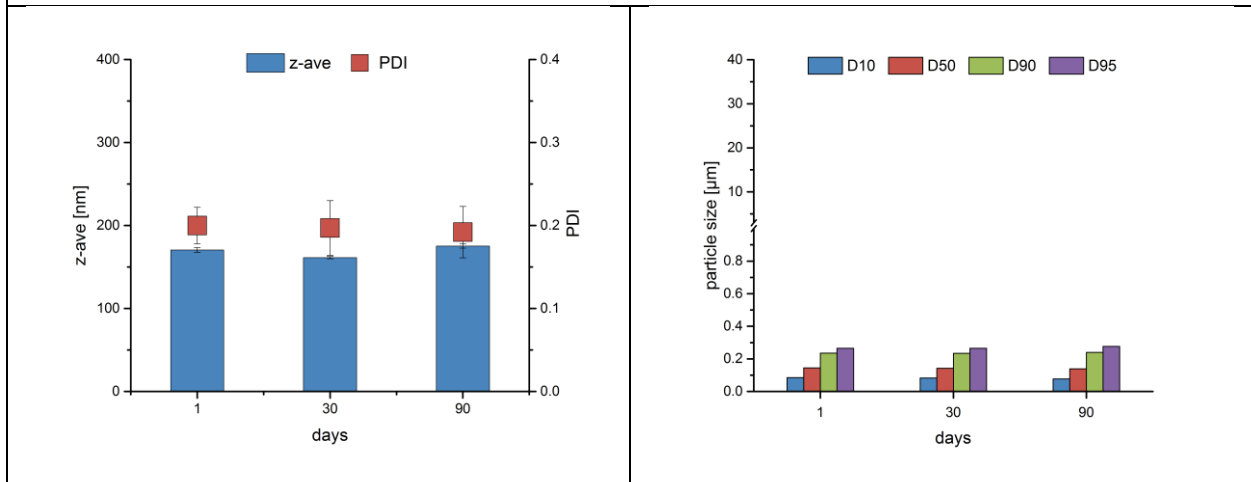
300 bar (3 cycles)

300 bar (4 cycles)
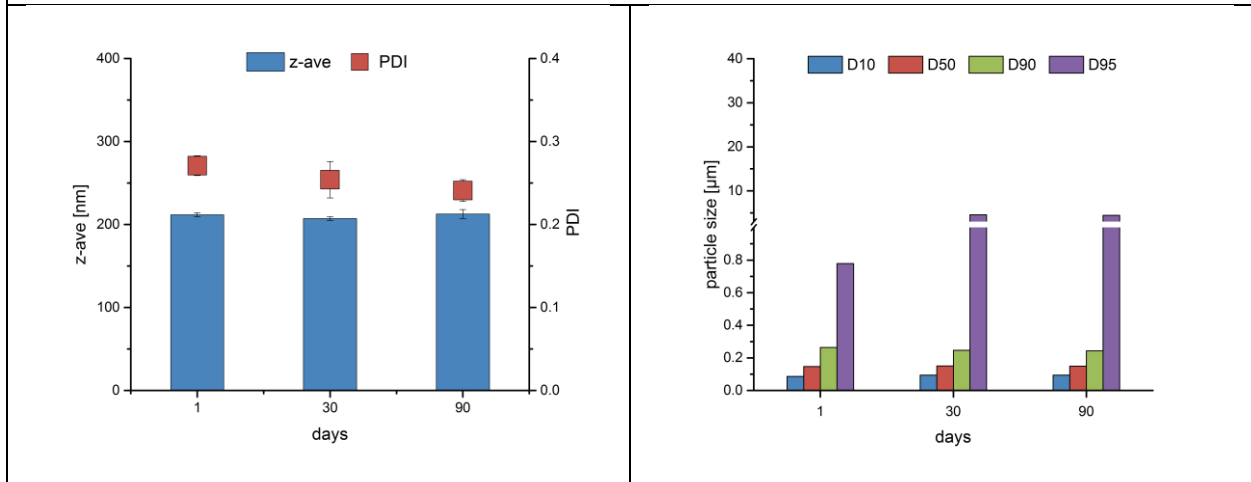
400 bar (1 cycle)
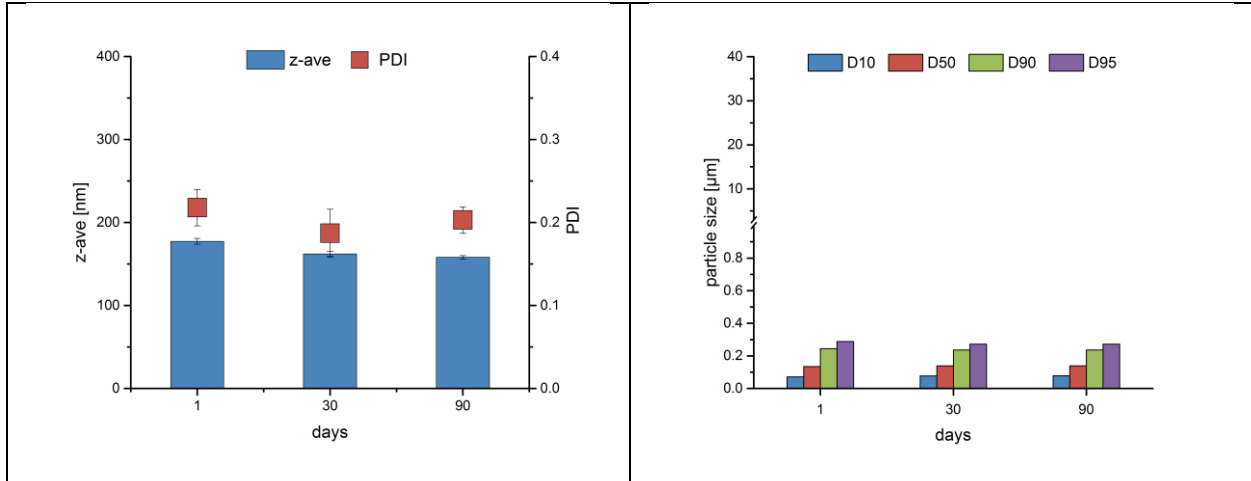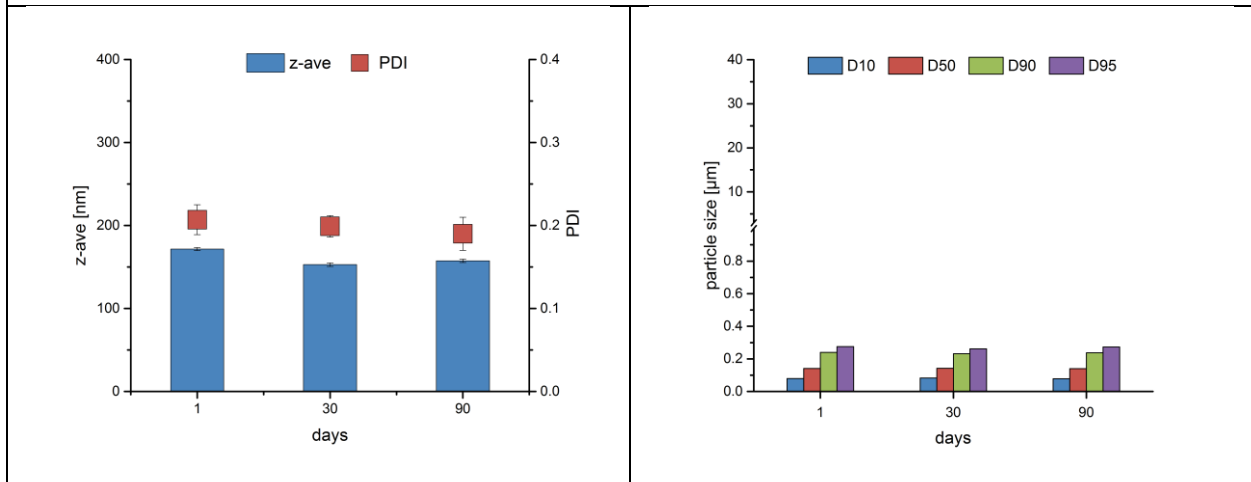
400 bar (2 cycles)

400 bar (3 cycles)
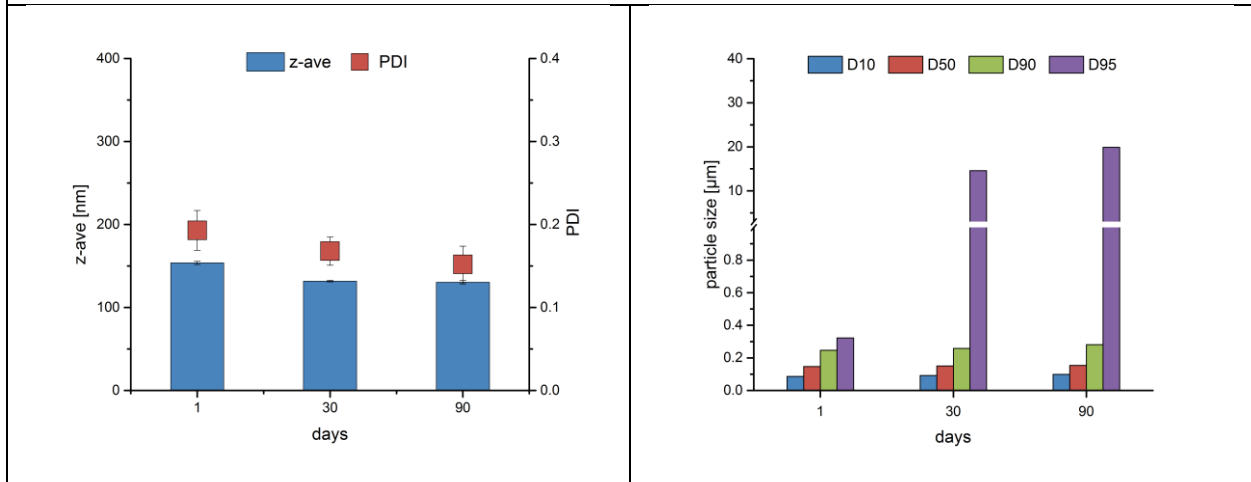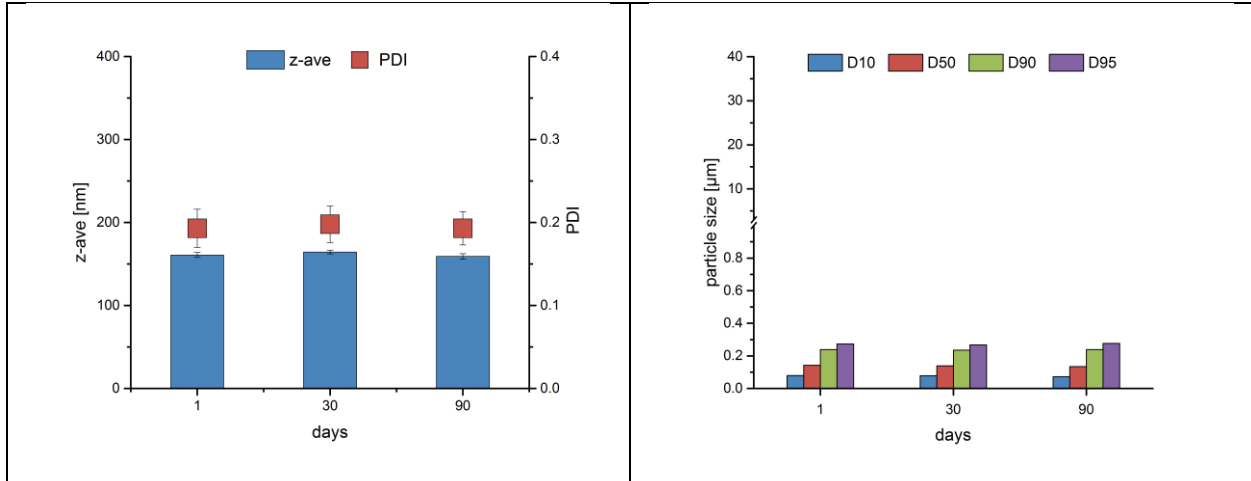

400 bar (4 cycles)
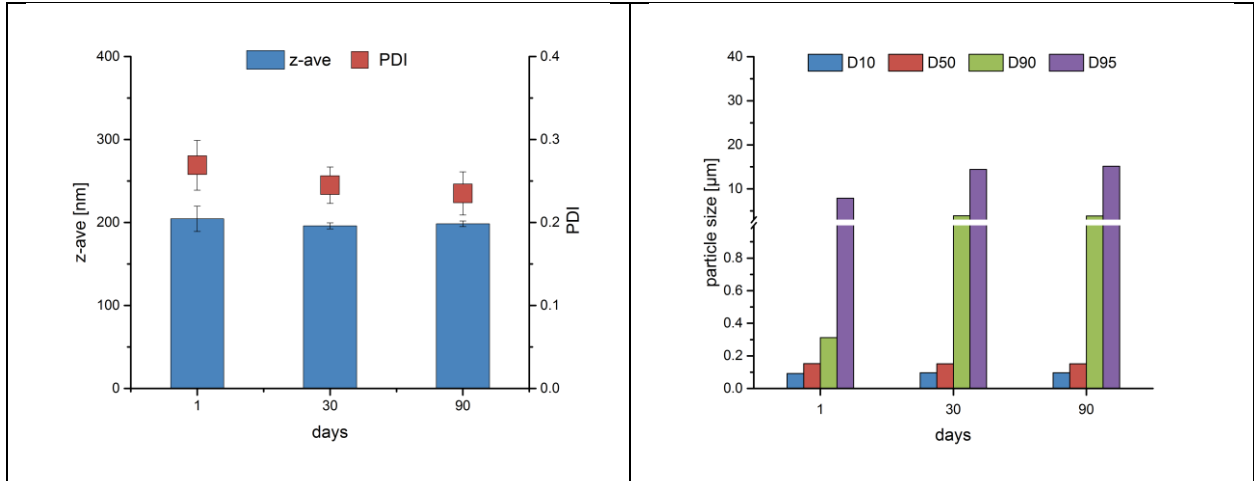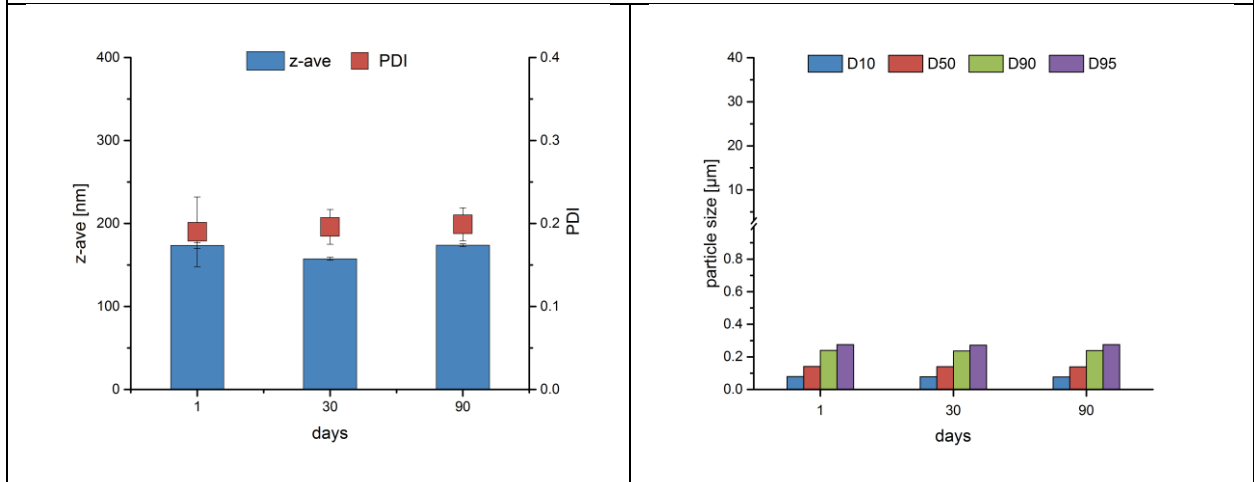
500 bar (1 cycle)

500 bar (2 cycles)
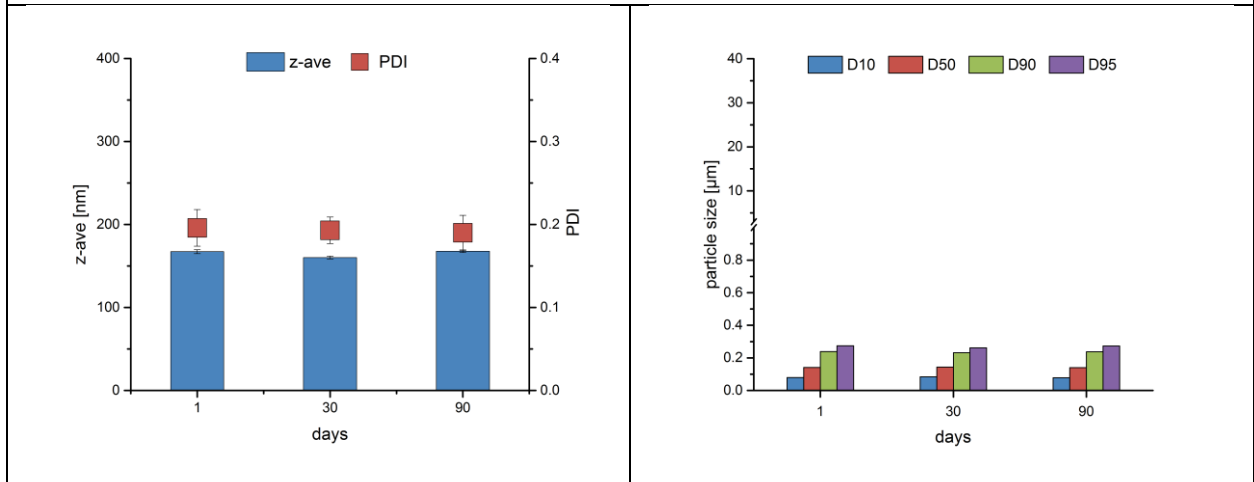
500 bar (3 cycles)

500 bar (4 cycles)

600 bar (1 cycle)

600 bar (2 cycles)

600 bar (3 cycles)

600 bar (4 cycles)

700 bar (1 cycle)

700 bar (2 cycles)

700 bar (3 cycles)
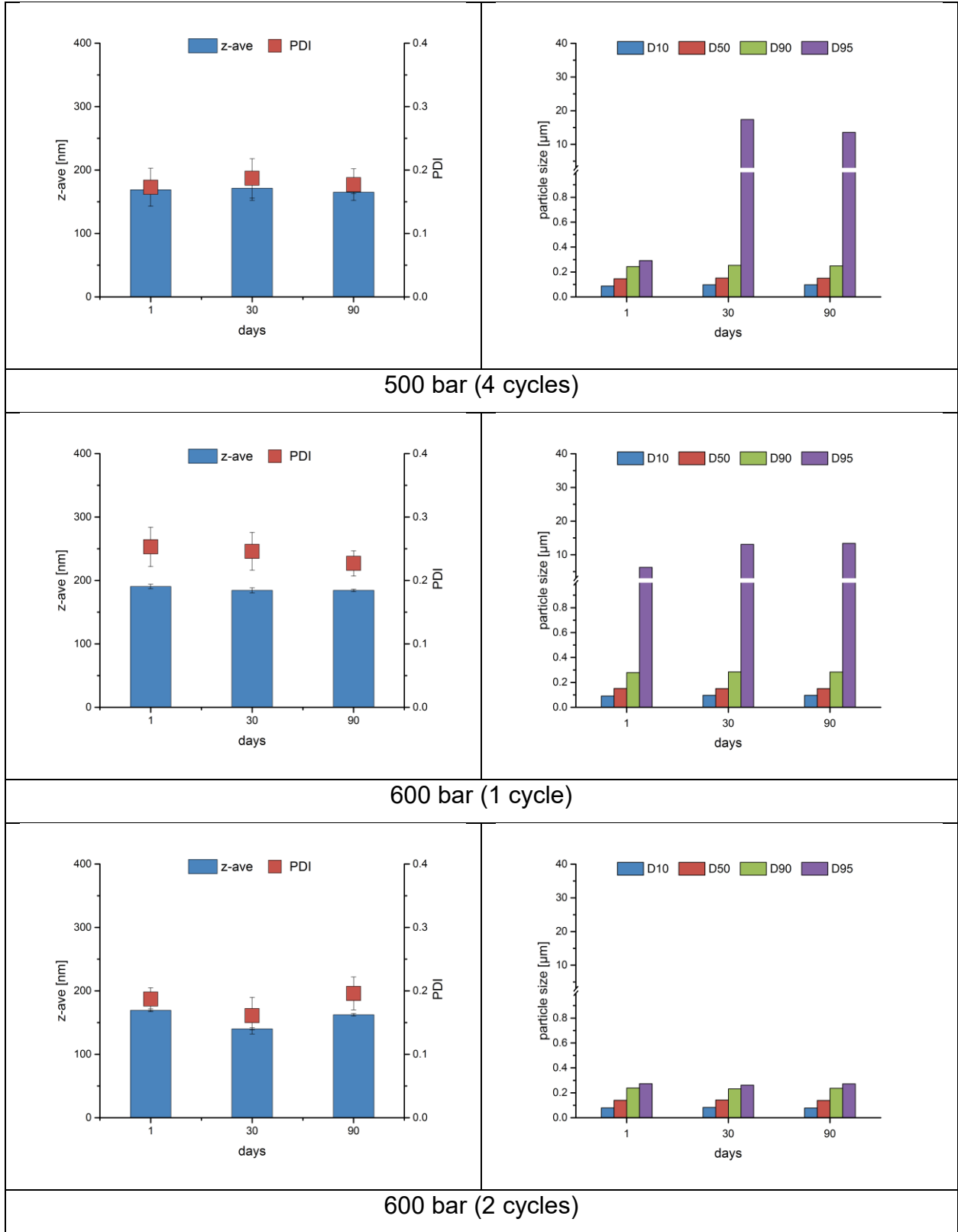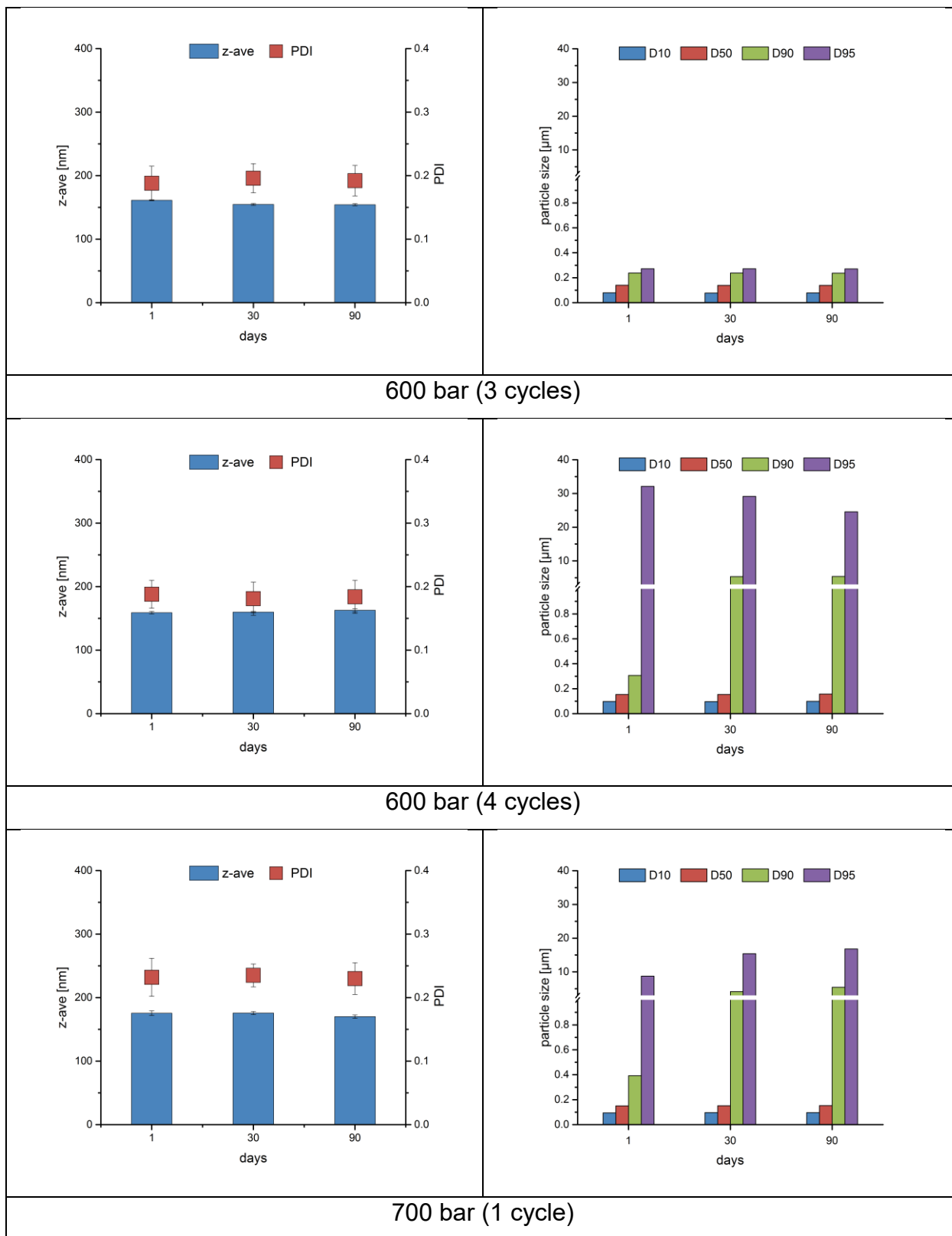
700 bar (4 cycles)
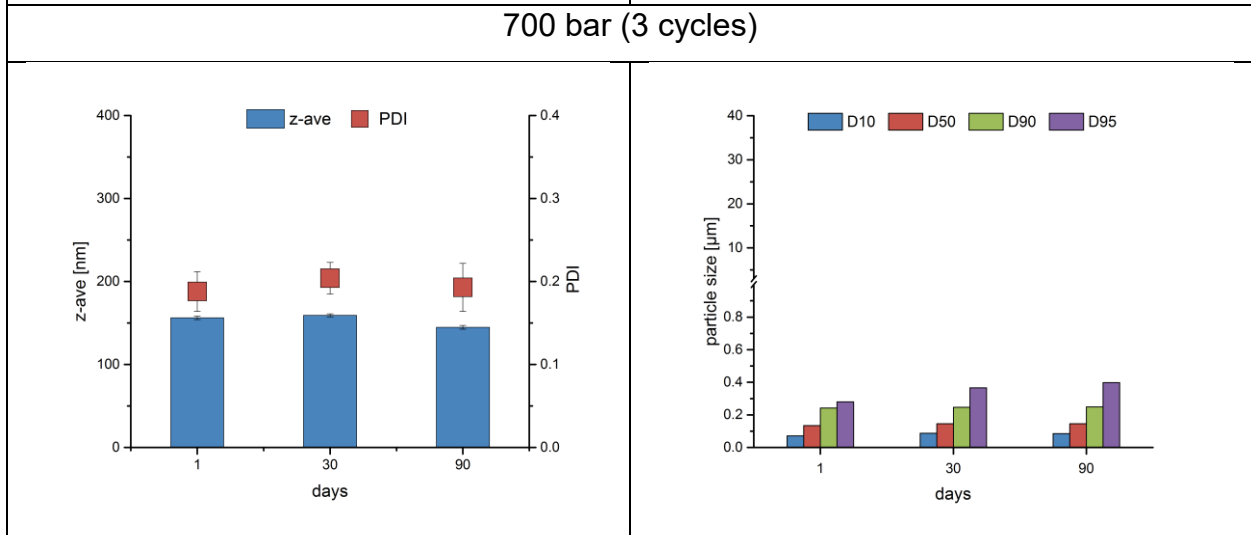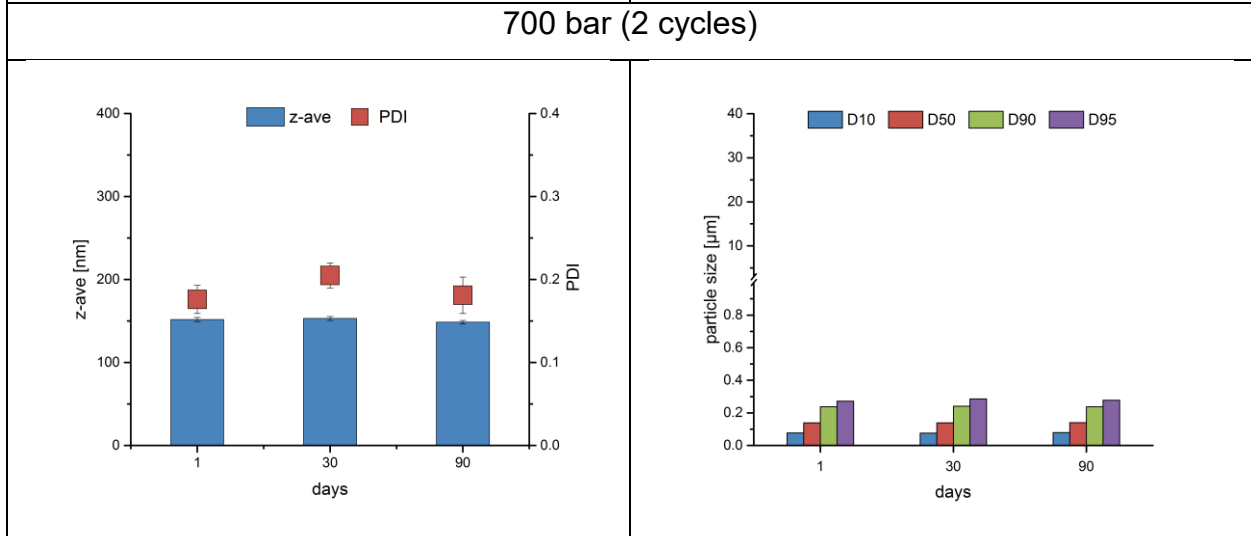
800 bar (1 cycle)

800 bar (2 cycles)
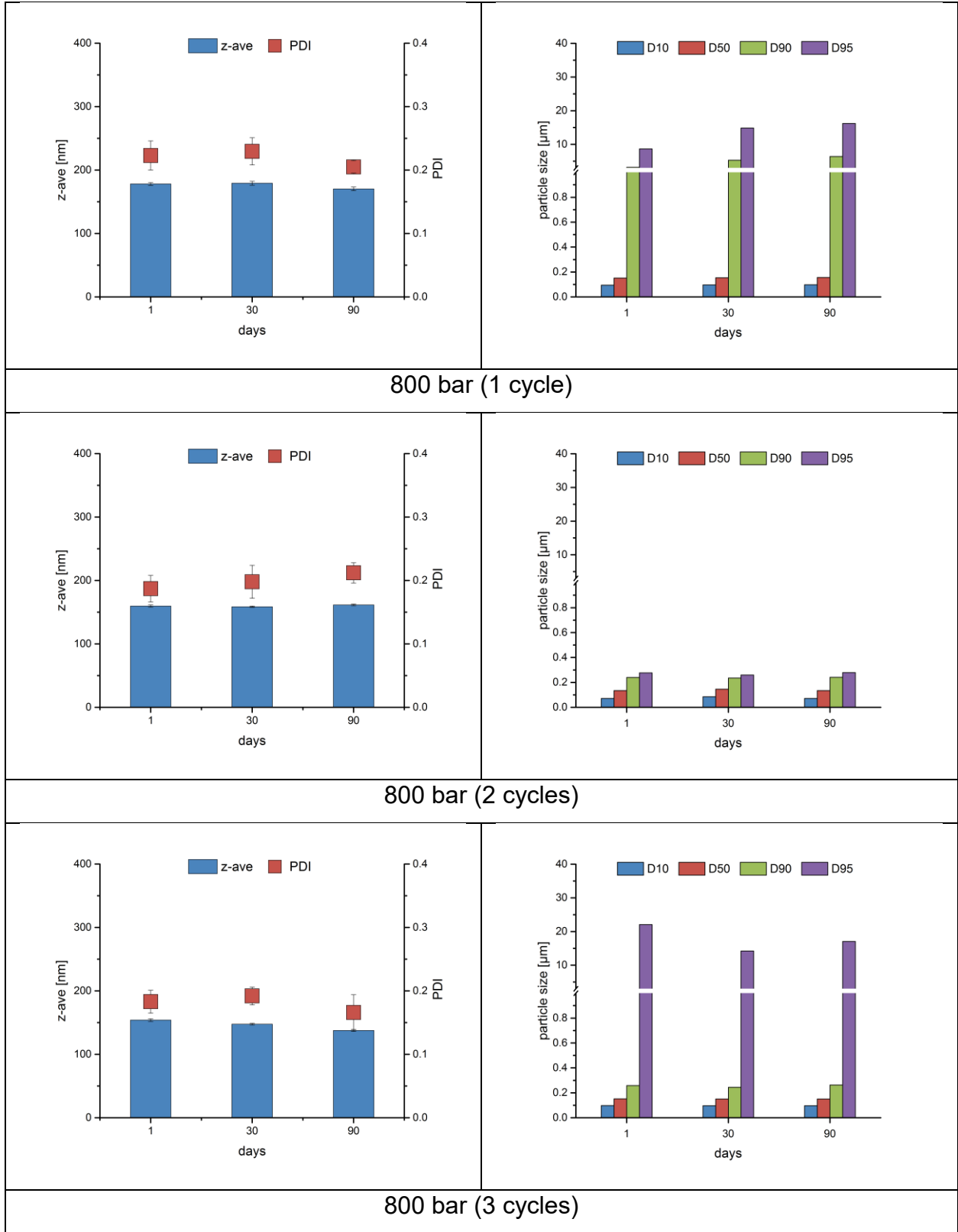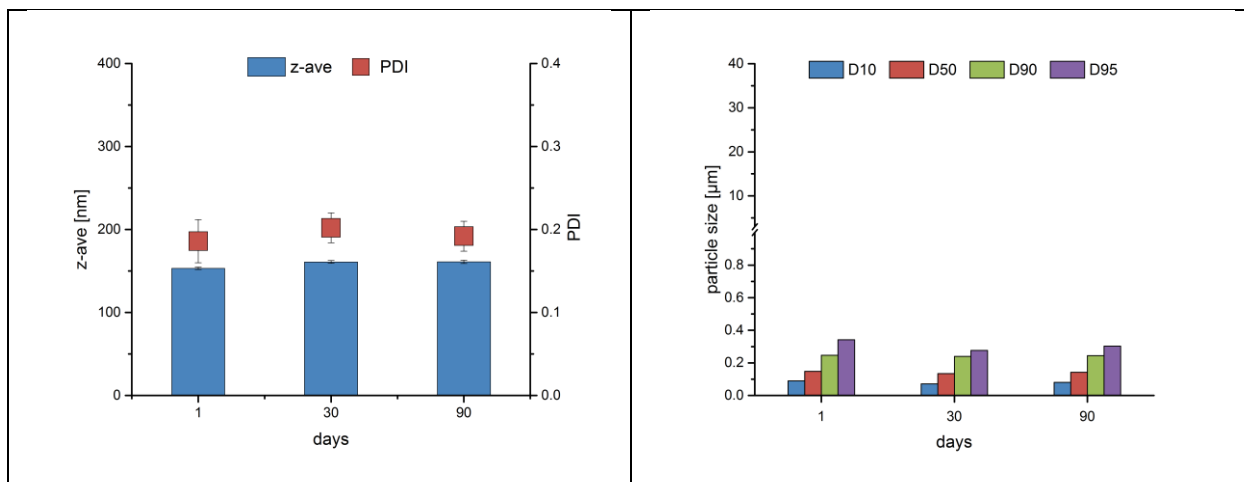
800 bar (3 cycles)

800 bar (4 cycles)
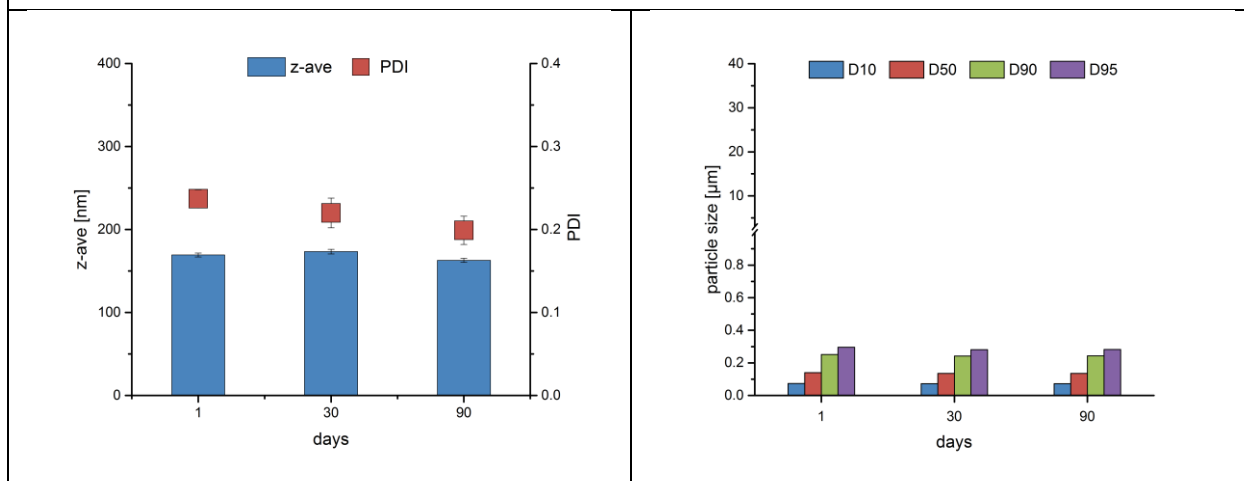
900 bar (1 cycle)

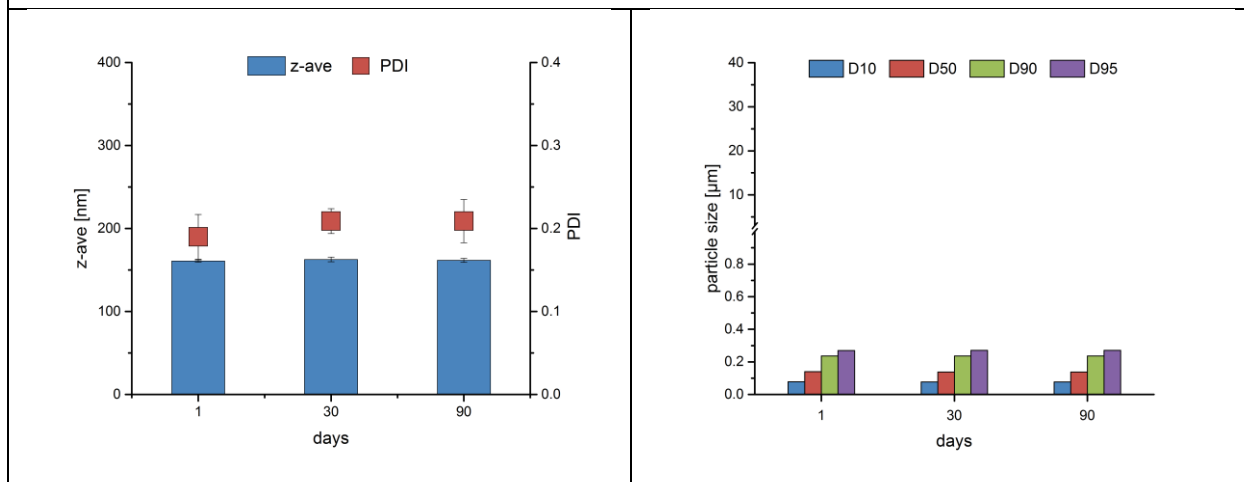900 bar (2 cycles)

900 bar (3 cycles)

900 bar (4 cycles)

1000 bar (1 cycle)

1000 bar (2 cycles)

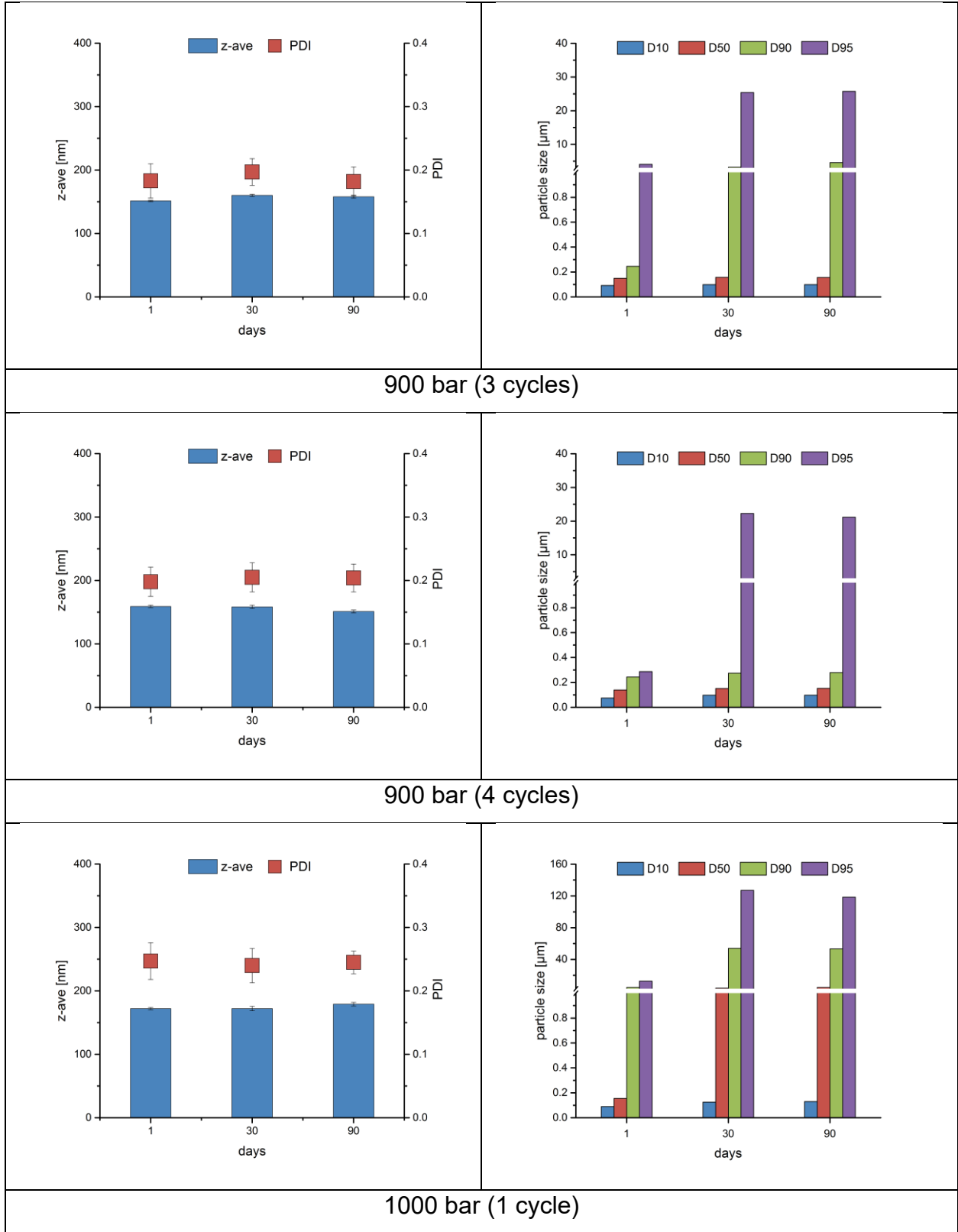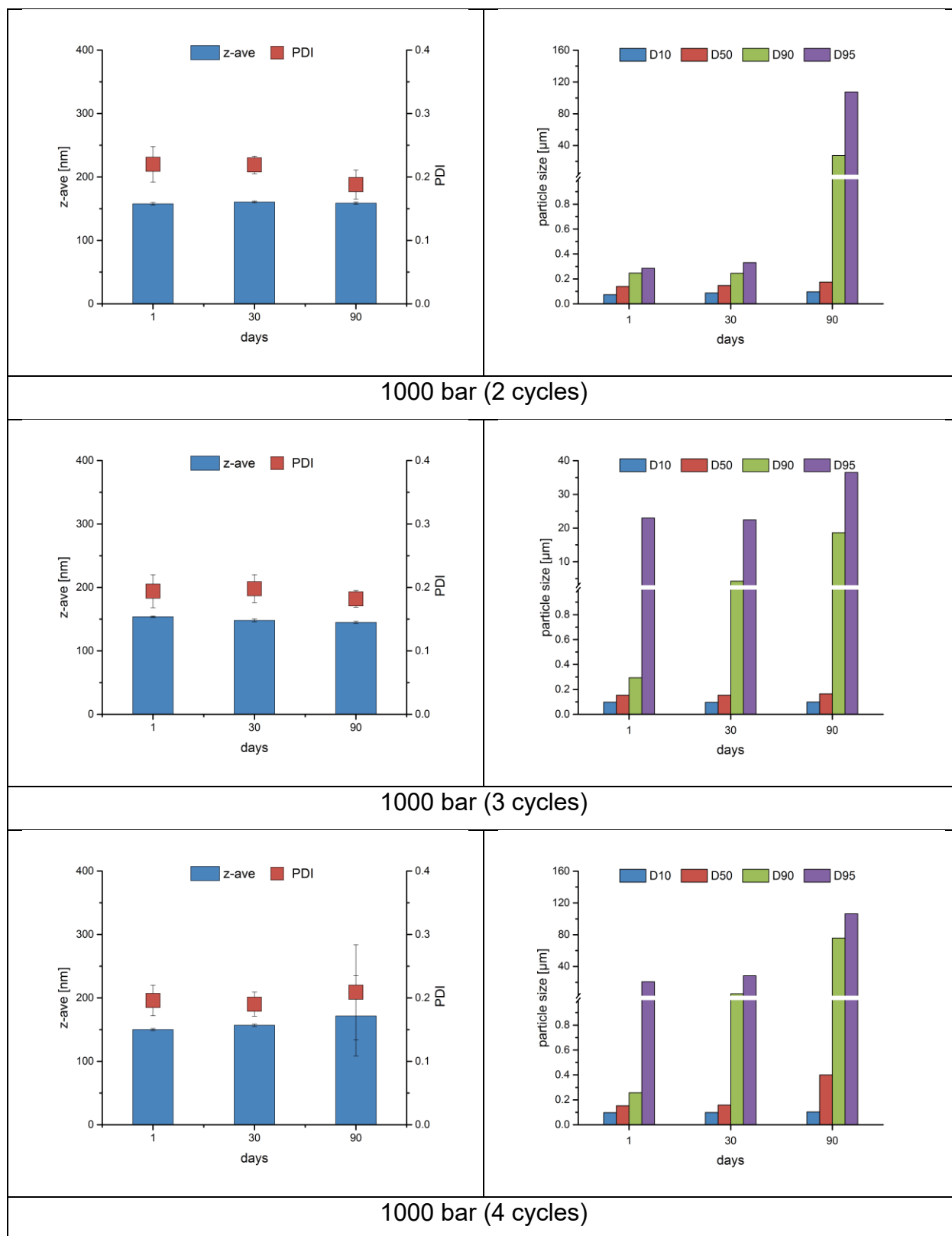1000 bar (3 cycles)

1000 bar (4 cycles)

Fig. A2. The PCS data (z-ave and PDI) and LD data (D10, D50, D90 and D95) of the LM4/0 smartLipids® produced with various pressure (300, 400, 500, 600, 700, 800, 900

and 1000 bar) and homogenization cycle numbers (1, 2, 3 and 4) measured on day 1, 30 and 90.

* the breaks in the y-axis are from 1 to 2 µm, and the scale changes above the break.

List of publications

Articles

1. **Ding, Y.**, Pyo, S. M., Müller, R. H., smartLipids® as third solid lipid nanoparticle generation–stabilization of retinol for dermal application. Die Pharmazie-An International Journal of Pharmaceutical Sciences, 2017, 72(12): 728-735.

2. **Ding, Y.**, Nielsen, K. A., Nielsen, B. P., Bøje, N. W., Müller, R. H., Pyo, S. M., Lipid-drug-conjugate (LDC) solid lipid nanoparticles (SLN) for the delivery of nicotine to the oral cavity–optimization of nicotine loading efficiency. European Journal of Pharmaceutics and Biopharmaceutics, 2018, 128: 10-17.

Abstracts

1. **Ding, Y.**, Staufenbiel, S., Keck, C. M., Müller, R. H., The smartLipids – new lipid nanoparticle generation for vitamin A delivery, PT-03, 8th Polish-German Symposium on Pharmaceutical Sciences: Retrospects, Insights and Prospects, Kiel, Germany, 29-30 May 2015

2. **Ding, Y.**, Staufenbiel, S., Keck, C. M., Müller, R. H., smartLipids – 3rd solid lipid nanoparticle generation for dermal delivery of retinol, M1130, AAPS Annual Meeting, Orlando, USA, 25-29 October 2015

3. **Ding, Y.**, Müller, R. H., smartLipids® - new lipid nanoparticle generation for dermal delivery of retinol, Tag der Pharmazie, Berlin, Germany, 01 July 2016

Proceeding

1. **Ding, Y.**, Pyo, S. M., Müller, R. H., Key factors influencing the stability of smartLipids®, CRS Local Chapter Germany, Halle, 01-02 March 2018

Acknowledgements

First of all, I would like to extend my sincere gratitude to my supervisor, Prof. Rainer H. Müller, for offering me the opportunity to perform my PhD study. I sincerely appreciate his supervision, guidance, instructive advice and useful suggestions in my research work during the past four years. His constant encouragement and patience accompanied me to walk through all the stages of my academic studies. In preparation of this thesis, he spent a lot of time reading each draft and provided me with inspiring advice. I will keep this precious experience always in mind and this will encourage me in every moment of my future life.

Many thanks go to Prof. Cornelia M. Keck. Even though we did not spend too much time together, I was always surprised by her professional skills and comprehensive academic theories.

Special thanks go to Dr. Sung Min Pyo for her expert guidance and daily support. She was always patient to answer my questions about scientific theories. I will never forget she prepared a birthday surprise for me.

I would like to thank all my colleagues in my research group: Ms. Corinna Schmidt, Ms. Inge Voltz, Ms. Gabriela Karsubke, Ms. Birthe Herziger, Mr. Daniel Köpke, Mr. David Hespeler. Without their help my study would be tough to proceed. Each day we spent together was really great time and I appreciate all the valuable memories.

I would like to express my heartfelt gratitude to Dr. Xiaoying Hu, Dr. Xiangyu Li and Dr. Nan Jin for daily encouragement and personal help.

I express my deepest thanks to my family and friends for their endless support and generous help in everyday life. Special thanks go to my boyfriend, Mr. Guido Creusen, for his careful proofreading of this thesis.

Last but not least, I would like to appreciate China Scholarship Council (CSC) for the financial support to my four year PhD study.